UNIVERSITÀ POLITECNICA DELLE MARCHE

FACOLTÀ DI INGEGNERIA

Dipartimento di Ingegneria Industriale e Scienze Matematiche

Corso di Laurea Magistrale in Ingegneria Meccanica

OTTIMIZZAZIONE DELLE STRUTTURE DI SUPPORTO IN INCONEL 718 PER IL PROCESSO ADDITIVO A LETTO DI POLVERE

Optimization of Inconel 718 support structures for powder bed additive process

Relatore:

Prof. Ing. Michele Germani

Correlatore:

Ing. Paolo Calefati

Tesi di Laurea di:

Fiorenza de Iudicibus

Anno Accademico 2018/2019

INDEX

Acronyms & Abbreviations

Contraction	Definition
AM	Additive Manufacturing
CAD	Computer Aided Design
CAM	Computer Aided Manufacturing
DED	Direct Energy Deposition
DoE	Design of Experiment/Experimental Design
EBM	Electron Beam Melting
EDM	Electrical Discharge Machining
FDM	Fused Deposition Modelling
LED	Linear Energy Density
PBF	Powder Bed Fusion
RP	Rapid Prototyping
SED	Surface Energy Density
SLA	Stereolithography
SLM/LPBF	Selective Laser Melting/Laser Powder Bed Fusion
STL	Standard Triangle Language
TGM	Temperature Gradient Mechanism
VED	Volume Energy Density

Abstract

Additive technology as a production technique has received increasing attention in recent years. What makes this process interesting are the many advantages it has, such as the geometric complexity of the piece, the reduction of components and the number of assemblies. Among the disadvantages, on the other hand, the one that inspired the work exposed in this thesis is the need to introduce support structures in the SLM (Selective Laser Melting) process. The main reasons why they are provided is the structural support of the part under construction and the capacity of thermal dissipation. The aim is to find geometrical and process parameters for which the block supports perform their functions. Three experiments were carried out for this purpose, for which different parts requiring support structures were printed. Between the first two experiments the geometry of the reference sample changes, as in the first one there is a part with a protrusion (L-shape) and in the second one there is a bridge structure. Both were conducted with the same process parameters, so as to evaluate only the influence of the geometric parameters of the supports. The third experiment is divided into four cases and aims to analyse the process parameters on the realization of supports that sustain a bridge structure, so as to compare the results with the standard parameters used for the second experiment. After all evaluations were carried out, the supports were removed manually, so as to assign a level of removability to each of them. This attribute is crucial because it affects the final cost. The results obtained at the end of the entire work were finally used in a case study in which supports with parameters optimized for a bracket used in the automotive sector were generated.

Riassunto

La tecnologia additiva come tecnica di produzione ha ricevuto sempre più attenzione negli ultimi anni. Ciò che rende questo processo interessante sono i numerosi vantaggi che esso presenta, come la complessità geometrica del pezzo, la riduzione dei componenti e quella del numero di assemblaggi. Tra gli svantaggi, invece, quello da cui prende spunto il lavoro esposto in questo elaborato è la necessità di introdurre strutture di supporto nel processo SLM (Selective Laser Melting). I motivi principali per cui esse vengono previste è il sostegno strutturale della parte in costruzione e la capacità di dissipazione termica. L'obiettivo è quello di trovare dei parametri geometrici e di processo per i quali i supporti a blocco assolvono le proprie funzioni. A tal proposito sono stati condotti tre esperimenti per i quali sono state stampate parti diverse che necessitassero di strutture di supporto. Tra i primi due esperimenti cambia la geometria del campione di riferimento, in quanto nel primo si ha una parte con una sporgenza (L-shape) e nel secondo si ha una struttura a ponte. Entrambi sono stati condotti con gli stessi parametri di processo, così da valutare solo l'influenza dei parametri geometrici dei supporti. Il terzo esperimento si suddivide in quattro casi ed ha come scopo l'analisi dei parametri di processo sulla realizzazione di supporti che sorreggono una struttura a ponte, così da confrontare i risultati con i parametri standard utilizzati per il secondo esperimento. Dopo aver effettuato tutte le valutazioni, i supporti sono stati rimossi manualmente, così da assegnare ad ognuno di essi un livello di rimovibilità. Questo attributo è fondamentale perché influisce sul costo finale. I risultati ottenuti al termine dell'intero lavoro sono stati infine utilizzati in un caso di studio nel quale sono stati generati supporti con i parametri ottimizzati per una staffa utilizzata nel settore automotive.

Introduction

Additive Manufacturing (AM) is a production technology that opposes subtractive manufacturing since it involves the addition of material, usually layer by layer, to create the product. This technique consists in transforming a 3D model into a concrete object: it is based on the subdivision of a virtual 3D shape into a number of thin 2D layers. These layers are then physically deposited, one by one, by a printer (the additive production machine), fixing each layer on the previous one and reconstituting a real three-dimensional object [1].
Initially, at the end of the 1980s, additive manufacturing was known as Rapid Prototyping because 3D printing was used to obtain prototypes that allowed some product features, such as functionality and shape, to be tested before they were sent into production. The limited mechanical properties and high porosity obtained did not allow this process to be used to produce the designed part. With the development of technology, the primary purpose of additive manufacturing has become the production of components, semi-finished or finished. Furthermore, over time, 3D printing of metals has reduced processing times, becoming compatible with mass production. To date, there are different types of additive processes among which some factors may change such as the energy source, the processing material, its form and method of construction.

An important aspect to consider both in the design phase and in the printing phase of a part to be produced in AM is the use of the support structures. These are created in order to support it during the printing phases. In fact, it can happen that with the advance of the layers there can be areas that do not rest on anything, causing as a consequence the failure of the first layers that compose them. In addition to a structural function, the supports are also a solution to dissipate heat, which could cause distortions that alter the shape of the desired part.

This study was carried out in collaboration with Prima Industrie SpA, a leading company in the production of laser systems for industrial applications, and is focused on the study of supports and the influence of various parameters. In this case the treated type of process is the SLM or LPBF (Selective Laser Melting or Laser Powder Bed

Fusion), that involves the use of the laser as an energy source and the material is metallic in the form of powder.
This thesis is divided into seven chapters that start with an overview of Additive Manufacturing and end with the results obtained.

In the first chapter, the history and evolution of the AM since its beginning is retraced. In addition, the process steps are illustrated and explained. Finally, some of the main types of AM are presented.

The second chapter deals with the main theme of this work, as it introduces the support structures of which the importance is explained. Through a comparison of scientific research, a table has been created in which the types of supports present and the cases for which they are suitable are collected.

The third chapter follows, in which the process parameters and the main technological systems of the machine used for the SLM process are presented.

The fourth chapter describes the material used, the Inconel 718, and reports the results obtained from studies already existing in the literature from which it was possible to extract useful information on what has already been scientifically verified.

The experimental phase begins in the fifth chapter. It describes in detail the experiments carried out and all the phases to perform them, from the use of the software, to the variation of the process parameters, to the printing of the samples used as a study element.

Chapter 6 contains the results obtained and the relative assessments carried out after analyses conducted with visual inspection, measurements and removal of the support structures. For a more immediate understanding, graphs and tables have been created for all the data collected. Thanks to the results of the experiments, it was possible to identify the optimal set of parameters based on the requirements of the supports.

The seventh and last chapter concerns a case study on an application made by Prima Additive, a division of the Prima Industrie Group. The objective of this implementation is to use the results obtained from experiments on a real case and compare the different solutions.

A summary of what was obtained from the entire experimental work closes the thesis.

Chapter 1: What is Additive Manufacturing

This chapter aims to introduce additive manufacturing technology by describing its process and reporting its advantages and disadvantages. In order to have a complete vision of the treated topic, the several types of additive manufacturing are briefly described, distinguishing each other based on the systems and the parameters used.

1.1 Additive Manufacturing

The necessity to find an alternative production process to conventional processes, such as machining, foundry or forging, derives from the need to produce components with a more complex shape and reduce the processing phases. These two requirements are met by additive technology because with the laying of the layers it is easy to create complex geometries in a single job of the machine. In this way, in addition to the machining phases, the AM sometimes allows the assembly phases to be reduced as well. The competitiveness of the AM is reinforced by the fact that it fits perfectly into the numerical design and production chain.

The way in which the parts are realized represents a profound change, which soon showed its potential. For this reason, there has been a growing interest over the years that has led to a high level of technological development over time.

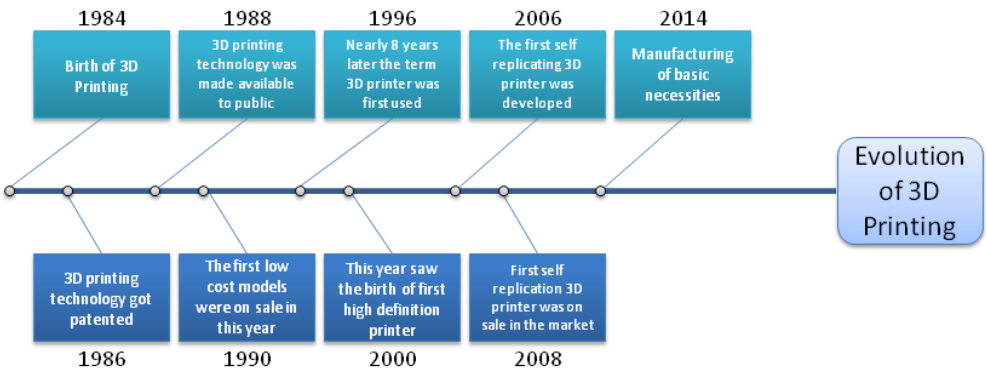

Figure 1.1.1 [44] – **Timeline of 3D printing.**

As mentioned above, Additive Manufacturing was born as a technique used to make prototypes. Thanks to this possibility, the representation and conceptualization of the projects has been facilitated.

With Rapid Prototyping (RP) and the use of the 3D printer, for the first time, three-dimensional objects were created starting from a CAD (Computer Aided Design) model.

The first equipment for additive manufacturing techniques was developed in the 1980s. In 1981, Hideo Kodama of the Nagoya Municipal Industrial Research Institute invented two rapid prototyping systems for AM photopolymers, in which the area subject to UV exposure was controlled by a mask model or by a scanning fiber transmitter [45].

In particular, Additive Manufacturing is associated with the birth of stereolithography, a technique introduced in 1983 by Chuck Hull, used for the additive production of polymers. Three years later, in 1986, he founded company 3D Systems. Before stereolithography was developed, rapid prototyping did not exist. Making prototypes or a functional model that represented a real object was a very time-consuming and costly operation. In addition, designers and engineers used CAD/CAM software, which did not allow communication with SLA 1, the first system used for Rapid Prototyping. For this reason, Chuck Hull and 3d Systems have developed the STL format, the same one used today, which allows to transfer the CAD model directly to the 3D printer [45].

The process at the base of stereolithography involves the thermosetting reaction of a liquid photopolymer subjected to a laser source, which acts selectively in a coherent way with the geometry to be created layer by layer. The principle behind this process is the same as that used for machines developed later on and is still valid today.

In 1986 Carl Deckard, Joe Beaman and Paul Forderhase, with other researchers, at the University of Texas at Austin's Department of Mechanical Engineering, introduced the Selective Lase Sintering, a technique that differs from stereolithography in that the photopolymer is in the form of dust and not liquid.

Scott Crump patented FDM (Fused Deposition Modelling) in 1988, a technology by which layers are made by depositing a filament of thermoplastic material contained in

a reel that is then extruded. An advantage of these last two techniques is that they can produce definitive parts and also facilitate post-processing operations.

In 1993 Emanuel Sachs, a professor at the MIT (Massachusetts Institute of Technology), developed a printing technique for coloured elements, Three Dimensional Printing. However, this technology is more suitable for prototyping because no definitive parts are obtained.

It was only in 1995 that the possibility of melting metal powders came about. From then on, the development of technology has always aimed at obtaining objects with characteristics comparable to those achieved with traditional processes. This was made possible by the introduction of Selective Laser Melting (SLM).

In 1999 scientists at the Wake Forest Institute used additive 3D printing technology to create objects with medical applications, printing the synthetic scaffolds that are necessary to grow a human bladder [46].

Only at the beginning of the 2000's did AM start to be used in the production of ready-to-use products. While accuracy and resolution have continued to improve, prices have fallen drastically when compared to the genesis of the technology. This has made it possible to increase the competitiveness of this process on the market.

Today, AM is still a sector in evolution, which aims to improve of the results. The various possibilities offered by additive technologies make AM part of Industry 4.0 projects. The latter is the fourth industrial revolution that is encouraging the integration of intelligent production systems and advanced information technologies. According to the thinking behind industry 4.0 it is necessary to develop unconventional production methods to meet the need for mass customization. Though there is still some concern about the use of AM as a technology for mass production, the use of additive techniques is increasing due to continuous technological advances [47].

In fact, as the following figure shows, according to the market outlook report published by SmarTech, the growth prospects of the process are very positive. The report is based on a database that includes fundamental terms of market sizing and forecasting, tracing the entire value chain and the activity of additive production. In fact, different aspects such as hardware, materials, software and production services are analysed.

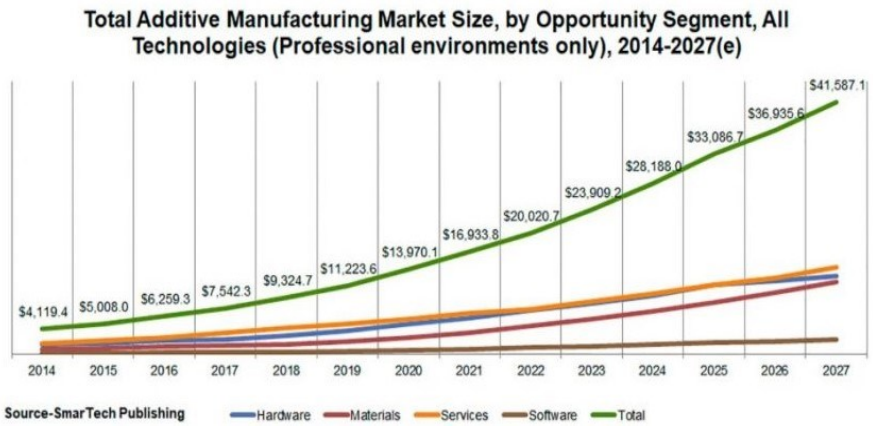

Figure 1.1.2 [48]- **Trend of Additive Manufacturing.**

AM is changing the way engineers think and design a product because features that are impossible to be obtained with traditional subtractive machining can be achieved. Using this type of processing, a 3D printer is used, which allows different materials to be processed, such as plastic, resin, ceramics, metal and bio-materials. In general, the term AM refers to metals, while the term 3D printing refers to polymers [2].

The fields of application in which this technology is growing are mainly biomedical automotive, aeronautics and aerospace.

Figure 1.1.3 [34] – **Biomedical application.**

Figure 1.1.4 [35] – **Water connectors for AUDI W12 engine.**

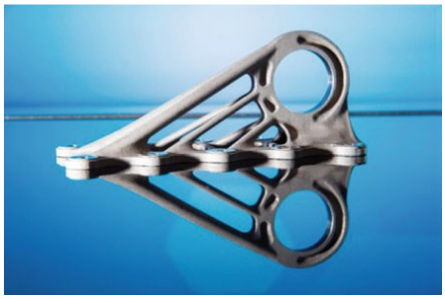

Figure 1.1.5 [36] – **Cabin bracket for the Airbus A350 XWB.**

In these fields of application its main advantages are exploited, such as the absence of constraints in the manufacturing design, the freedom of form, the high complexity of the components, the combination of several parts in a single piece and the production of functionally classified materials, the reduction of the need of tools and the possibility of production on demand. [2].

An example of the complexity achievable by using additive technology is the creation of internal channels (figure 1.1.6), impossible to produce with other types of machining.

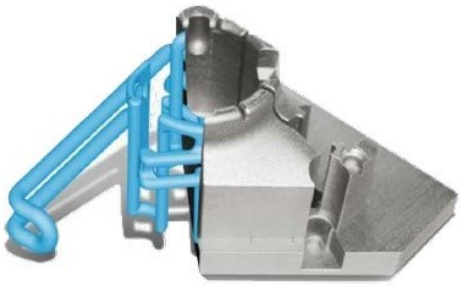

Figure 1.1.6 – **Example of internal channels.**

Thanks to the possibility to obtain elaborate geometries, the AM lends itself very well to the concept of topological optimization of the structures.

Topology optimization is a mathematical approach that allows to optimize the use of the material in space. This operation is possible for a given set of loads and boundary conditions, so that the resulting object satisfies the functionalities for which it was designed. The part is remodelled by means of the optimisation, because once the stressed areas have been identified, the material that is not functional to the resistance of the component is eliminated. Figure 1.1.7 shows the comparison between the same part before and after being optimized:

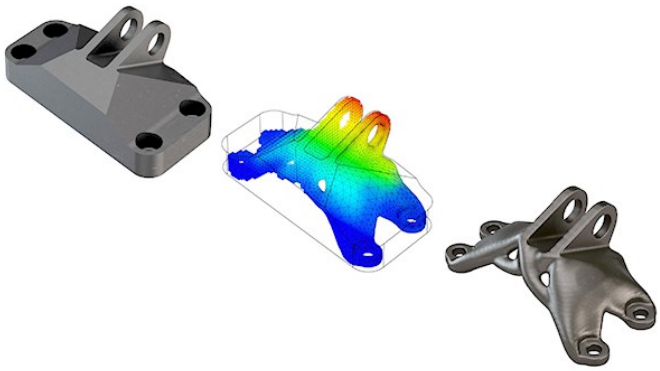

Figure 1.1.7 [39] – **Optimizing of GE Aviation Engine Bracket.**

Further advantages of additive manufacturing are:

- the optimisation of the construction structure for less use of raw materials, a greater performance and the possibility to use different materials from those currently in use [3];
- a drastic reduction of the costs of making variants compared to a basic model [3];
- the elimination of production waste [3];
- the possibility to print components and mechanisms already assembled [3].

On the other hand, there are the following disadvantages compared to conventional techniques:

- the productivity of the machines is generally low [1];
- the quality of the products varies considerably, since it needs finishing operations [1];
- relatively high cost of equipment and materials [1];
- this technology is not always suitable for very simple or large workpieces, or for high volume production series [1].

Due to the way in which the part is made, terms specific to this production system are introduced that were not used with traditional technologies. These include the build direction and layer thickness. The build direction is always that of the z axis and does

not always coincide with the longitudinal axis of the piece, because this could be positioned at different angles to the platform. The layer thickness is a very important quantity to be evaluated because it determines the mechanical characteristics and the resolution of the product. To divide the entire part into layers, it is necessary to use software that performs a slicing operation on the CAD model prepared previously.

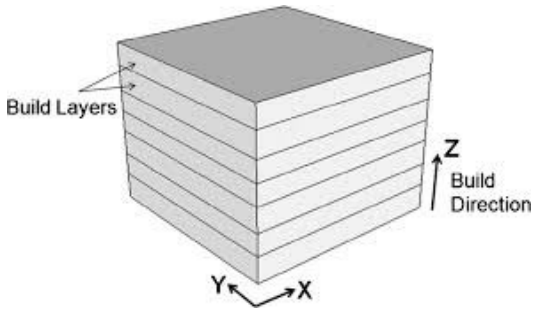

Figure 1.1.8 [29]- Representation of the build direction and layers.

1.2 Additive manufacturing: process sequence

The process of Additive Manufacturing can be divided into several steps that start from the CAD model up to the part realized. In figure 1.2.1 the identified phases are eight:

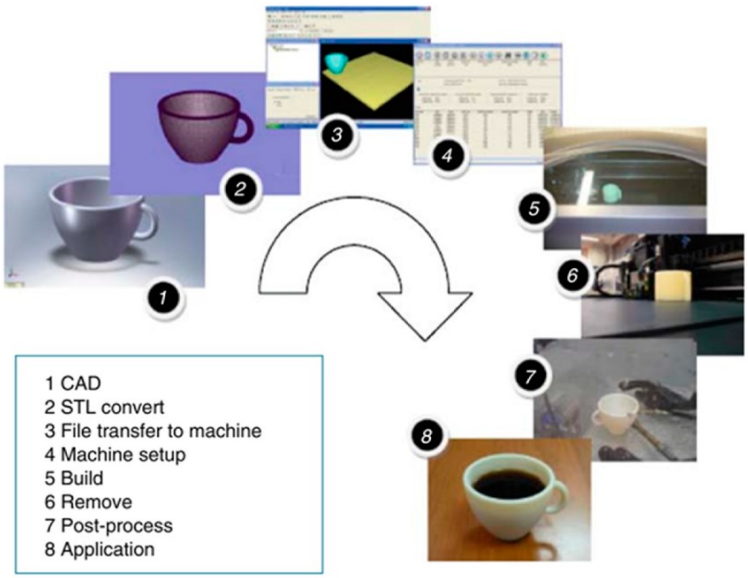

Figure 1.2.1 [37]- **Generic process of CAD to part, showing all 8 stages.**

Starting from the first to the last there are:

1) *CAD model*: it represents the initial input of the entire process of Additive Manufacturing. The CAD model can be built with one of the many professional solid modelling software available.

2) *STL convert*: the name of this format (Standard Triangle Language) derives from "stereolithography" and represents a way to describe only the surface geometry of a three-dimensional object through triangles. The triangles are defined by the unit normal and vertices.

3) *File transfer to machine*: once the file in STL format is obtained, it can be transferred to the machine. However, sometimes it is not enough to realize only the CAD model, but it is necessary to have some precautions such as the prevision of the support structures and this is possible thanks to the use of software.

4) *Machine setup*: this step is carried out with a post-processing software by which terms such as energy, layer thickness and material parameters are defined.

5) *Build*: this is the moment when the part begins to take shape. Once the machine is started up, the operator only carries out a monitoring activity to check if there are problems or not and once the process passes the initial phase, the machine does not need any intervention.

6) *Remove*: this phase follows the construction process and is carried out by the operator with the appropriate safety precautions. Then the parts are extracted from the working chamber in different ways depending on the type of machine and the type of process used.

7) *Post-process*: once the piece is extracted from the machine, this could involve additional post-processing operations. Some of these include separation from

the platform, removal of support structures where required, or surface finishing.

8) *Application*: after the previous phases, the piece can be considered finished and ready to use.

1.2.1 Exchange format

Paying particular attention to the second step of the process, the need to convert the file format is explained. As mentioned in paragraph 1.1, the STL format was introduced by 3D Systems in 1987 to allow the transfer of CAD model data to the 3D printer.

It offers the advantage of being easily generated by all CAD software and became the standard format for additive manufacturing applications. The process that processes the STL format converts the continuous geometry of the CAD file into small triangles or a triplet of x, y and z coordinates defined by the normal vector to triangles.

Triangles define facets that identify the surface of the 3D object. Each facet is located on the boundary between the inside and outside of the object and each of it must share two vertices with each of its adjacent triangles (vertex rule). To understand if a facet is internal or external, it is necessary to see the direction of the vector normal to the triangle and in what order the three vertices are ordered, following the rule of the right hand.

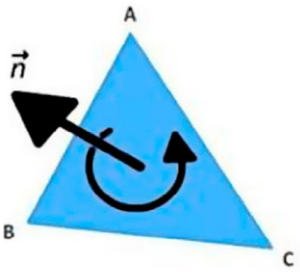

Figure 1.2.1.1 [50] – **Vertices and normal vector.**

With the STL file format there are two different ways to store information about the triangular facets that reproduce the surface of the object. These ways are ASCII encoding and binary encoding.

The first method involves writing all the coordinates of the vertices of the triangles and their normal vectors, but if you need many triangles to reproduce the model, the code could become very long. For this reason, a more compact form is needed to store the information and binary code is used [49].

Sometimes errors such as holes or intersections between triangles can be generated during the creation of the surface. When this happens, the STL model needs to be repaired.

With computers available today, calculation data and mesh generation are no longer an obstacle. The available computing power is sufficient to generate a high resolution STL file. The latter is given by the number of triangles used to reproduce the model: if there are more triangles, higher is the resolution and greater is the size of the file.

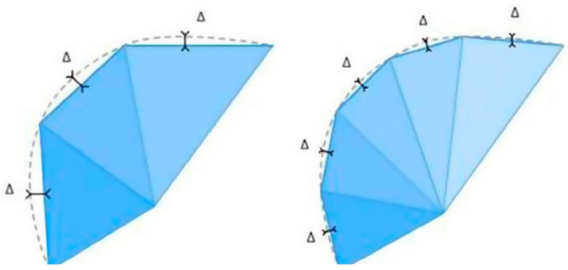

Figure 1.2.1.2 [50] – **Resolution and number of triangles.**

An example of a model in STL format is shown in the following figure:

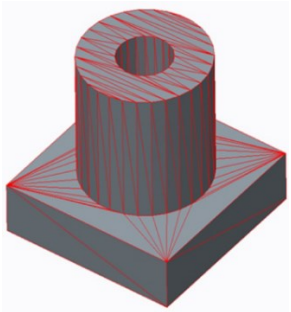

Figure 1.2.1.3 – **Example of an STL file format and its model [51].**

1.2.2 3D slicing

Once obtained the model in STL format, the slicing operation must be carried out to define the layers of the 3D model. The accuracy of the additively manufactured parts is determined by the thickness assigned to the individual layer. In fact, the lower the thickness, the greater the precision that is obtained. So, when the layer thickness is not very thin, the surface resolution could be low. This phenomenon is called ‘‘stair stepping effect’’, which is directly related to the layer thickness.

Also, the deposition rate or productivity is highly relevant to the sliced layer thickness [51].

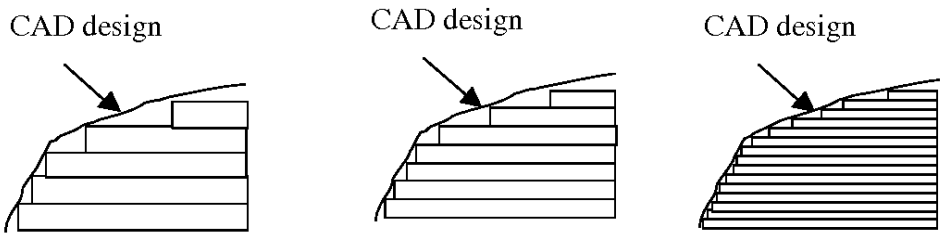

Figure 1.2.2.1 – **Effect of Layer Thickness on Stair-Stepping [52].**

Depending on the level of precision that is required, the slicing can be ‘‘uniform’’ or ‘‘adaptive’’. In the first case, the entire 3D model is divided into layers with the same thickness; in the second case, instead, the thickness of the layers is not constant, but varies in an adaptive way and an algorithm is used which, based on the geometry of the piece, uses the appropriate thickness. This second approach is less used than the first because it requires some modifications to the common machines used. However, it is a way to increase the precision of the surfaces to be produced.

Before slicing, it is important to understand how to orient the part, as different results may be obtained depending on the direction chosen (figure 1.2.2.2). However, this choice has to be taken considering also the mechanical properties, as they also change with the orientation of the part.

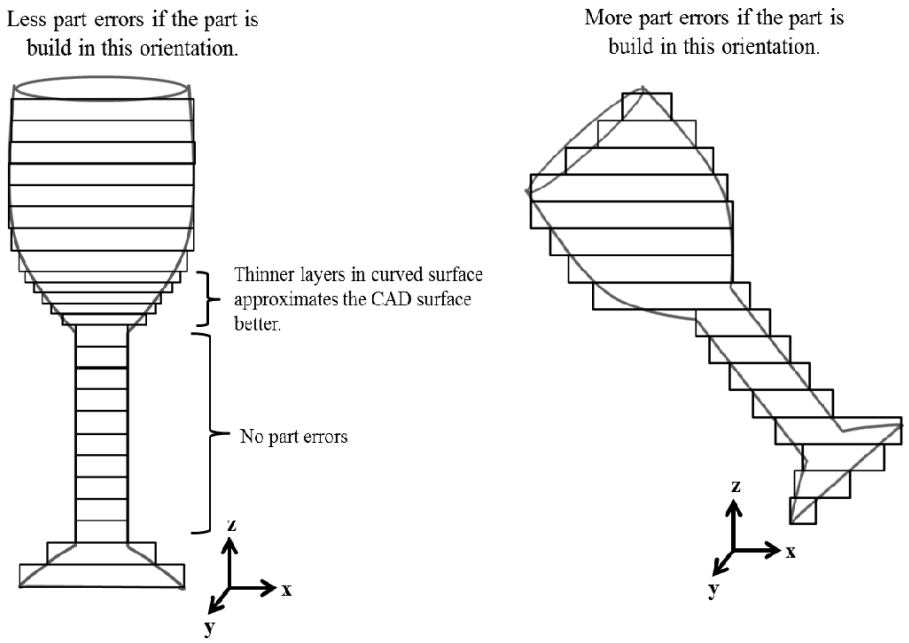

Figure 1.2.2.2 – **Effect of build orientation and layer thickness on staircase errors [53].**

1.2.3 Post Heat-treatment

After the piece was produced, a series of operations are carried out in the post-processing phase. These include the separation from the construction platform by EDM (Electrical Discharge Machine), the removal of the supports and the cleaning of the part realized. In addition, finishing operations to improve surface quality and heat treatments can be carried out. The latter are generally performed before cutting the part to improve the mechanical properties, but given the nature of the additive process, they aim to relax the residual stresses that are created during the building phase. These stresses can cause deformations that are closely related to the thermal gradient generated. Depending on the material used, different gradients are present, resulting in various stresses and deformations. For this reason, the heat treatments applied vary from case to case. As concerns Inconel 718, the temperature during the post heat-treatment has the trend shown in graph 1.2.3.1:

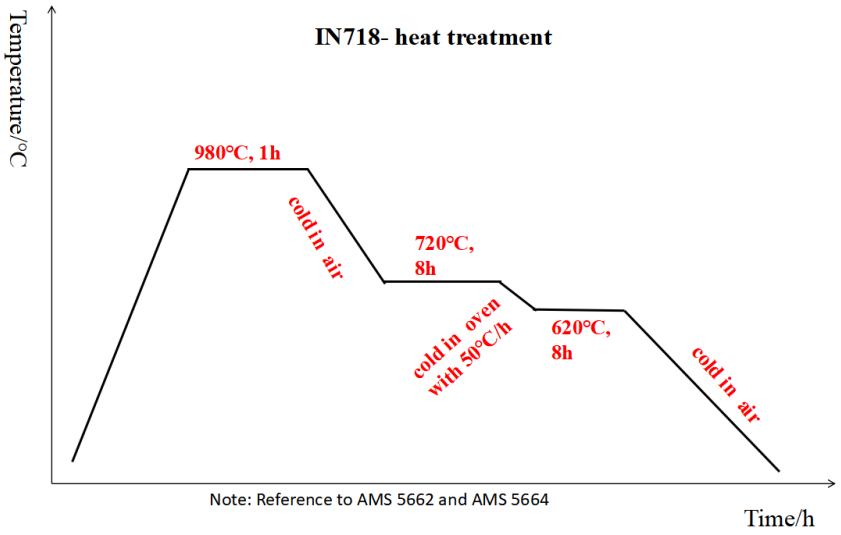

Figure 1.2.3.1 – **Temperature-time graph.**

1.3 Types of Additive Manufacturing technology

AM methods can be classified essentially on the basis of the nature and aggregate state of the raw material and the binding mechanism between the layers of joined material [4].

The American Society for Testing and Materials (ASTM) has classified additive manufacturing technologies using seven high-level process categories. Although there are new additive manufacturing technologies, they belong to one of the seven defined categories shown below:

Additive manufacturing process categories

1. Binder jetting – in which a liquid bonding agent is selectively deposited to join powder materials.

2. Directed energy deposition – in which focused thermal energy is used to fuse materials by melting as they are being deposited.

3. Material extrusion – in which material is selectively dispensed through a nozzle or orifice.

4. Material jetting – in which droplets of build material are selectively deposited.

5. Powder bed fusion – in which thermal energy selectively fuses regions of a powder bed.

6. Sheet lamination – in which sheets of material are bonded to form an object.

7. Vat photopolymerization – in which liquid photopolymer in a vat is selectively cured by light-activated polymerization [5].

Among the various techniques, those using metals in powder form (Powder Additive Manufacturing), which are divided into Laser Directed Energy Deposition (L-DED) and Powder Bed Fusion (PBF), are more relevant at the industrial level. The difference between these two techniques is that with the DED the powder is sprayed by one or more nozzles and simultaneously subjected to the laser beam, while with the PBF the powder is first deposited on a platform and then it meets the energy beam. The powder bed techniques can be further divided into LPBF (Laser Powder Bed Fusion) and EBM (Electron Beam Melting). All these processes are described in the following paragraphs.

1.3.1 Directed Energy Deposition

Unlike powder bed technology, a DED machine deposits the material only where it is needed directly on the desired surface on which the solidification process takes place. Depending on the material and type of heat source used, there are different typologies of DED processes, which have a similar operating system. The material can be in the form of powder or wire and for the generation of heat there can be an electron beam or a laser source. This last one represents the most common variant and goes by the name of Laser Directed Energy Deposition. In this case the material is in the form of

powder, which passes through a tube and meets the laser thanks to which the fusion takes place. Deposition can be performed from any angle with multi-axis machines. After each passage of the deposition head, a track of material is created, and in this way the layers are overlaid. This process is used not only to create new parts, but also to repair components that need material addition. This type of use is encouraged by the fact that DED machines have a larger working chamber than other additive techniques. To generate the relative motion between the piece and the beam, there is a handling system. The movement could be associated with the part or the laser, other times to both. Also in this case, as in the powder bed technology, the use of an inert gas is provided by a nozzle. It serves to create a protective atmosphere and directs the material along the same path as the laser beam. The microstructural characteristics obtained with L-DED are comparable with those of powder bed techniques, however a lower resolution of the parts is achieved.

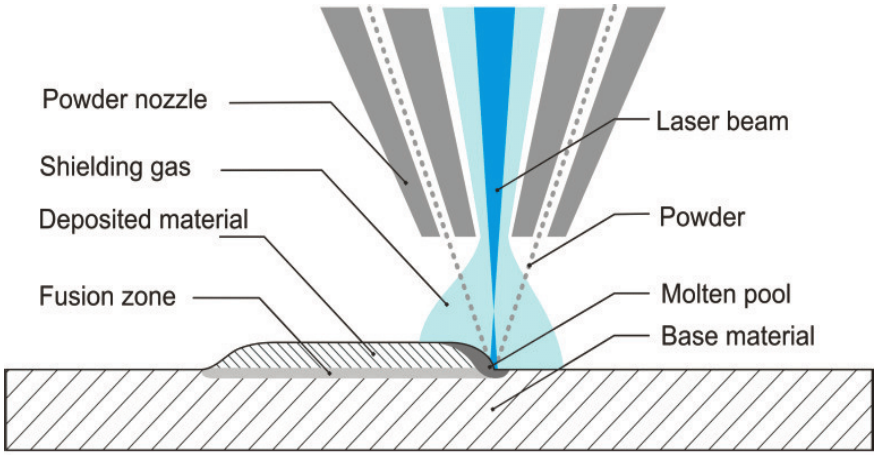

Figure 1.3.1.1 - **Laser metal deposition [30].**

1.3.2 Laser Powder Bed Fusion

As for the LPBF (or SLM) process, it provides for a system that includes a laser, a pointing and focusing system, a powder supply, a powder recoater and a build plate. The powder, contained in a special container, is deposited on the construction platform by the feeding system and then the recoater distributes it. This creates a layer of powder typically 20-60 μm thick on which the laser beam will act selectively, following the geometry of the part. The interaction with the laser causes the melting of the material, which after solidification will form the first solid layer. Note that the laser penetration is deeper than the thickness of a layer, in order to ensure a better union between the layers (figure 1.3.2.1). In this way, it is also possible to obtain parts with a higher density and lower porosity.

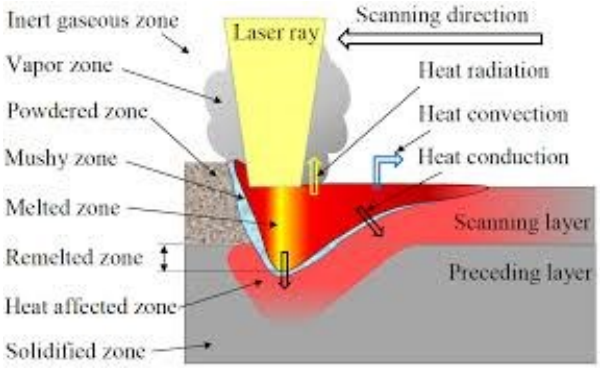

Figure 1.3.2.1 [38] - **Laser source heat.**

Once the first layer of powder is melted, the construction platform lowers, the platform of the chamber in which the powder is contained moves up and the recoater distributes the next layer of powder. This process is repeated until the part is completed. The LPBF process is generally performed in a chamber where inert gas is injected. This solution allows to reduce the value of the oxygen present so as to avoid both the oxidation of the material, and the reaction of some materials such as aluminium and titanium, which are very reactive with oxygen.

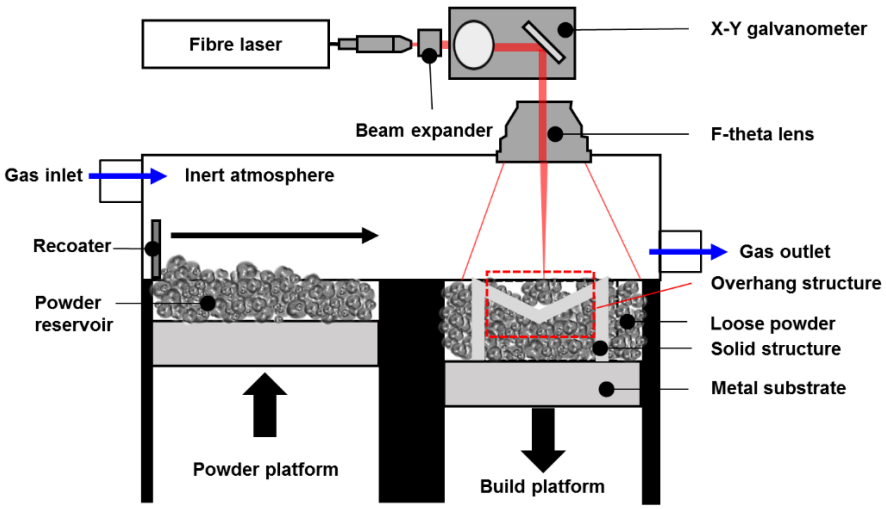

Figure 1.3.2.2- **Schematic of a typical LPBF machine. The build chamber is purged with a flowing inert atmosphere. The blue arrows indicate the gas flow direction [6].**

LPBF technology allows to obtain parts with a good resolution, in fact it is possible to build pieces that do not need further processing and are ready to use. Compared to DED machining, the dimensions of the parts are more limited.

This study refers to the PBF, in particular to Selective Laser Melting (SLM), which involves the selective melting of the metal.

1.3.3 Electron Beam Melting

The Electron Beam Melting (EBM) process was introduced by Arcam AB (a GE Additive company), which released the first production model in 2002. It has as input the CAD model and uses .STL data (triangulated model) of the part to be fabricated. The .STL model of the part is sliced into different layers and passed into the system.

This process is very similar to LPBF, but differs in some aspects. In this case, in fact, a high power electron beam is used as the heat source, which generates the energy necessary to have a high melting capacity, increasing also the productivity. The latter can be further increased by producing, as in the LPBF, more parts during the same job, occupying the working chamber as much as possible.

Due to the higher energy density compared to SLM technology, with EBM it is generally possible to have a higher layer thickness (from 50 μm to 200 μm); with an excessively high thickness of each layer of powder and with the typical particle size of the process, the distribution of the powder remains in the range 45 - 150 μm, which is a larger particle size distribution than that used in the SLM [24].

As mentioned above, in this way the productivity is high, but when a part grows at a high production rate, the surface quality is lower. The EBM process typically results in lower resolutions and higher surface roughness with respect to SLM. The surface roughness of an EBM part is always around 30 - 50 μm in Ra [42].

Another important difference is that the electron beam, thanks to its high scanning rate (up to 8000 m/s), allows a general preheating of the powder (depending from the processed material, even up to 1100°C) before melting, which is a central point to reduce the thermal stresses of the component that is growing [43].
In addition, preheating also reduces the powder diffusion inside the chamber due to the impact with the electron beam and the repulsion generated by the electrostatic force.

The equipment consists of an electron beam head with a tungsten filament, a powder container, spreader, and a build table [40].

The build plate has a size of typically 200 mm x 200 mm in x-y direction. Figure 1.3.3.1 shows the typical system of an EBM process:

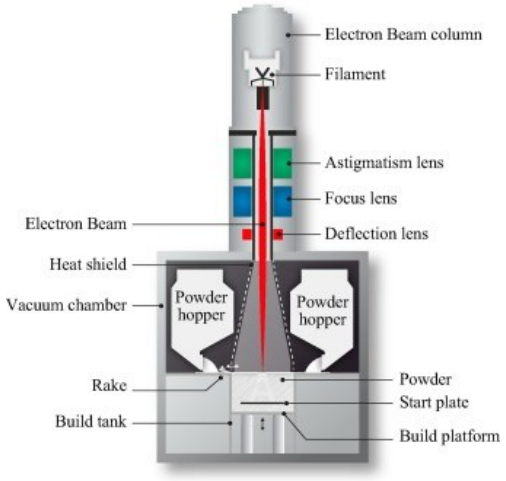

Figure 1.3.3.1 [24] - **EMB system.**

The electron beam is produced by an electron gun that takes electrons from the tungsten filament under vacuum. Subsequently, the electron beam is accelerated with a voltage of 60 kV. The spot can reach a minimum size of about 100 μm, a value that allows to obtain a good resolution even for the most precise details.

Two magnetic fields are present, of which the first one organizes the electron beam in the desired shape and the second deflects the beam to the target position in x-y plane on the build plate. The kinetic energy of the electrons is transferred to thermal energy, fusing the metal particles together. The electron beam scans the metal bed in accordance to the slice data generated from the input CAD file and solidification occurs by cooling [40]. Due to the high scanning speed that can be achieved, the scanning strategy adopted plays a key role. The patterns to be followed may be different, but regardless of the type chosen, they are all distinct in two phases including preheating and melting. Analogous to the SLM process the build plate is lowered afterwards and metal powder is delivered.

The availability of high energy electron beams ensures complete melting of the powder particles. The parts are fabricated in a vacuum chamber (around 1 x 10^{-3} Pa) during the EBM process, which assures impurity free parts unaffected by oxygen and other chemical species available in the atmosphere. The residual stresses are also minimized due to vacuum processing [24].

Helium gas is leaked into the chamber increasing working pressures to 1 x 10^{-2} Pa and is used to reduce electrostatic charging of the powder particles and assist cool down after the build cycle [41].

Once the parts from the machine are obtained, they are cleaned to remove excess powder. This is usually done by a blast of high pressure airstream containing silicon micro-beads [40]. Similar to SLM, the powder can be recycled in the EBM process.

The materials used in the EBM process are only metallic materials. This is due to the fact that conductive materials are needed as electrical charges are used. With other materials there would be no interaction between the electron beam and dust. For this reason, it is technically impossible to produce ceramic or polymer parts.

1.3.4 Position of the part

Now that the processes of the main techniques of additive manufacturing have been described, some considerations can be made. The process steps that are followed using the DED or PBF technique are generally the same, however, different precautions can be taken. In particular with powder bed techniques, before starting printing, it is very important to consider the orientation of the part on the x-y plane for reasons related to the process itself. In fact, in this case the blade of the recoater interfaces with the part and when contact occurs this can be dangerous. To avoid problems due to impact, such as deformation or breakage, it is advisable to position the part so that there are no sides parallel to the blade. For this reason, an inclination of at least 5 degrees has to be imposed. The following figure shows how to improve the position of the piece with respect to the recoater:

Figure 1.3.4.1 – **Part orientation.**

However, this is not the only aspect for which the orientation of the part is important. More generally, for all types of additive technology, it is closely related to building time, mechanical properties and surface quality.

In particular when the shortest side is in the z direction then the layers to be made and therefore the time of realization of the part decrease. As far as the mechanical properties are concerned, they change between the x, y and z directions, so the functionality of the part must be considered.

So, from what it's already said, it can be seen how important it is that the piece is positioned in an optimal way with respect to all directions. This is not an easy job

because it is necessary to find the right compromise between several factors. Remember, in fact, that the orientation of the part also has a contribution to the ‘‘stair-stepping effect’’ described in paragraph 1.2.2.

In addition, as we will see in the next chapter, the orientation of the piece also affects the number of supports needed to sustain an inclined part with respect to the plane of the platform x-y.

Chapter 2: Support structures

In this chapter the reasons why the introduction of support structures is essential for the success of the designed part are explained. In particular, the situations in which their use is necessary are described.
At the end of the chapter, the types of available supports and the geometries of the parts for which each type is best suited are reported.

2.1 Significance of support structures

As previously mentioned, this study focuses on the role of support. Their main task is to support the part during construction because it is not always able to support itself. There are several cases in which the use of supports is necessary, depending on the geometry of the piece and its placement on the construction platform.

The situations in which the supports must be provided are indicated on the following points:

- when the model has an overhang or a bridge which is not supported by anything below.

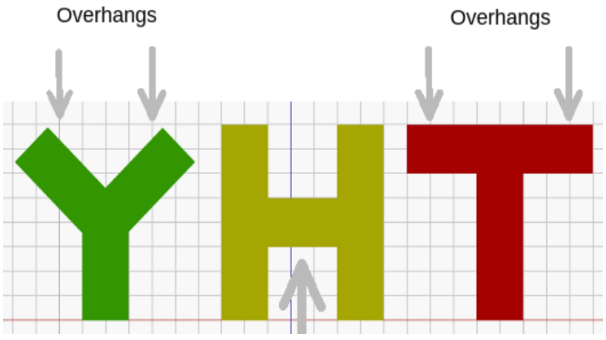

Figure 2.1.1- **Overhangs and bridges illustrated with the classic example of letters Y, H and T [7].**

- Beyond a specified angle, the part is no more able to support itself. The value of this angle may differ with the material, but generally the limit is considered 45 degrees.

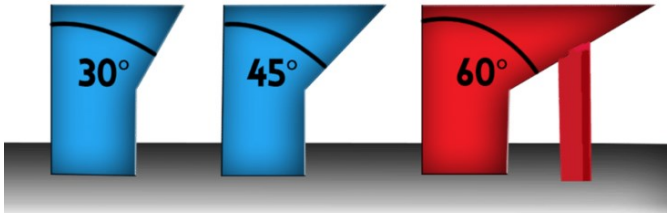

Figure 2.1.2- **Overhangs at an angle of more than 45 degrees from the vertical require 3D printing support structures [7].**

- Lateral holes cause a severe overhang to form at the top. This means that, if too large, a lateral hole will be a bit squished at the top and therefore smaller. Holes of less than 6 mm diameter are ideal.

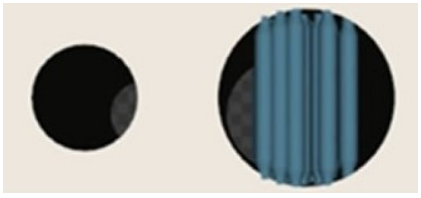

*Figure 2.1.3 [8]-***Different sizes of hole diameter.**

- When the piece is placed on the building platform, it is important to ensure that there is no dangerous contact with the blade. To obtain this, it is necessary to avoid that the direction of growth is opposite to that of the recoater movement. This is in fact the worst case that could compromise the realization of the piece. If it is impossible to find a solution then the parts must be equipped with support structures.

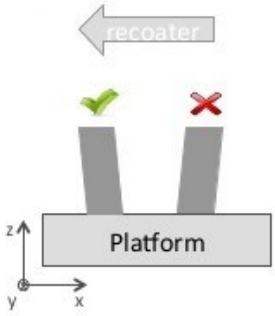

Figure 2.1.4 **– Direction of growth.**

- The construction of thin walls could be problematic as well. In fact, there are cases where these need to be supported in order to be built. Moreover, note that circular walls have fewer problems than flat walls.

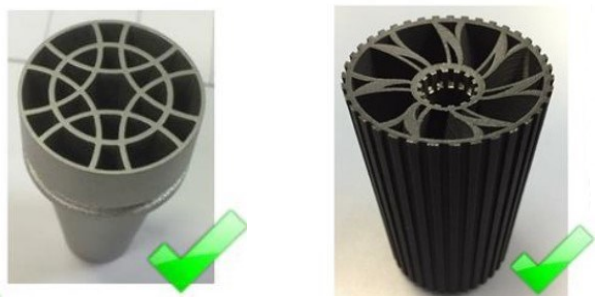

Figure 2.1.5 – **Thin walls.**

In addition to the cases shown above, there are other reasons why supports can be used, including heat dissipation.

Some printing operations may include high thermal gradients, especially metal processes. Therefore, shape distortions and residual stresses may occur due to this excessive heat accumulation. In this case, the support structures play the role of both a heat diffuser and rigidity enhancer [9].

The areas that are most in danger of deforming are mainly cantilevered ones because the conduction of heat towards the central area of the component is limited and in addition the powder has a much lower coefficient of heat conduction than the solid material. For this reason, the protruding parts are subject to severe overheating, which cause residual stresses. In an experimental study conducted by Chivel and Smurov [31], the temperatures reached and the problems caused by undercuts or overhangs of some components were evaluated. The authors argue that the instability between the melted material of the undercut area and the underlying powder is caused by the fact that the denser material above tends to flow down and mix with the less dense one, because it is linked to the Rayleigh-Taylor phenomena. For all the reasons described above, there are really many geometries and dimensions that can be used to support the components manufactured SLM.

Residual stress is due to the rapid heating and cooling that result from the laser powder bed fusion process. Heat flows from the hot weld pool to the solid metal below and then the molten metal cools and solidifies.
When a new layer of metal cools and solidifies, it contracts. The new metal is constrained by the solid structure underneath and therefore its contraction creates shear forces between the layers.

With the use of supports, adding more material, the laser induced heat energy can be dissipated more effectively. For this reason, when optimizing the shape of the part and especially of the supports, it is necessary to consider how the dissipation capacity changes in relation to the quantity of material used.

The supports that are used for additive manufacturing can be found in two forms depending on the material of which they are composed: the same as the built piece or another type of material. […] In this respect, supports made of different materials present an effective way to remove from the part. By using other material supports, it is easy to distinguish support from part, to use a weaker material for support that can be removed easily or to apply a material that can be removed chemically without affecting the part.
However, for the powder-bed processes supports have to be made using the same material as the part due to difficulties associated with using multiple materials such as mixing and recycling problems [10].
The amount of material used represents a cost item, therefore it should be minimized. In this sense, the supports represent costs and waste of material, since they will have to be removed. However, the optimization of the shape of the supports is not only carried out to minimize costs, but also to facilitate their removal.
This operation takes place once the piece has been extracted in the post-processing step, in which the trapped powder is also recovered. Delicate parts increase the difficulty to remove supports because the removal process can easily cause small pieces of the part to break off. In fact, the removal operation sometimes is simple, while other times is a complicated procedure that require and highly skilled operators, safety equipment and controlled environments. Surface finishing is usually required after support removal.

2.2 Types of support structures: purpose-use

When the supports have to be inserted, it is possible to choose between different types, which have different characteristics and functions.
The choice may be a critical step, but software programs used in this field, such as Materialise Magics, are provided with an automatic support generation module. The generated supports can be modified by the user, who can also choose to create them himself.

Among all types of supports, block supports are the most used in the SLM. However, the amount of material used in traditional supports in some cases, for delicate parts, may be excessive because it increases the difficulty of removal. In these situations, other types of supports are used that differ in shape and parameters, as well as in the contact area. In general, each type of support has a specific function and therefore it is better suited to a given geometry. As a result of research, carried out by comparing scientific papers, the different types of supports were classified in the following table:

TYPE OF SUPPORT	FUNCTIONALITY	GEOMETRY PART
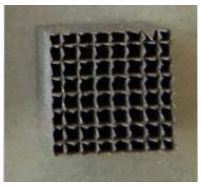 **Block**	It is unsuitable for recovering the raw loose powder which are trapped inside the support structures during the build [11]. Grid pattern is great to achieve sturdy supports. It is resilient against vibration; however, it does increase print time and generally exhibits more contact with the support areas. This may lead to more difficult post processing [12].	For large surface areas [12].
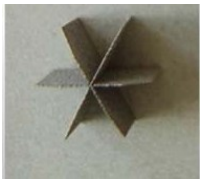 **Point**	To reduce contact area.	For very small surfaces and downfacing points [13].
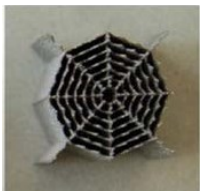 **Web**	The web supports are designed to support overhanging. The webs of the supports are used to reduce the contact area of the part surface and let the unexposed powder to be easily removed [14].	For circular areas [15].

TYPE OF SUPPORT	FUNCTIONALITY	GEOMETRY PART
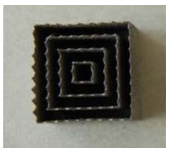 **Contour**	For easy removal [13].	Down-facing surfaces. Complex geometry.
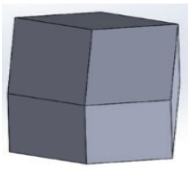 **Volume**	Volume supports provide more stability to fragile parts to prevent parts from breaking.	For large overhangs.
 **Line**	It still makes for great, easy-to-remove supports, but it doesn't usually "pop off" in one piece [12].	For narrow down-facing areas. For thin surfaces or edges [13].
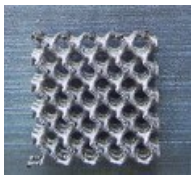 **Lattice**	The material resists impact and stress like a simple structure, but less material is used. The shape of the cells determines the overall strength. Another advantage of cell structure is heat dissipation. It is dissipated more quickly and evenly thanks to the regularity of the lattice structure and hollow cross sections.	Use for flat, angular or very steep overhang. Interesting for small, thin parts [13].
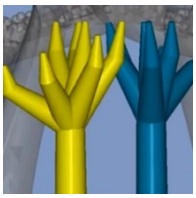 **Tree**	Tree-type supports are almost exactly what they sound like. They start from a couple of 'trunks' near the base of your print, and branch out to support overhangs in your model as height increases.3D printing these supports can save on material and print time. It only touches the overhang at certain points.it is only suitable for non-flat overhangs like nose tip, fingertip or arches. It does not provide enough stability for flat overhangs [14].	Use for angular or very steep overhang. Interesting for small, thin parts [13].
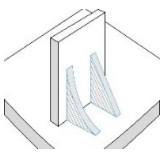 **Gussets**	The bellows support structures are placed between a horizontal and a vertical surface of the piece, so that the support rests on the part and not on the construction platform.	For overhanging parts.
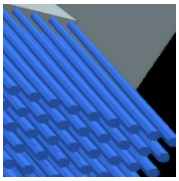 **Cone**	Choosing cones offers more stability [13]. To save material.	For small, thin parts [13].

Table 2.1.1- **Types of support structures.**

As can be seen from the information given in the table 2.1.1 each support generally is suitable for a certain situation. Note that there are other factors to consider, besides the geometry, when choosing the type of support, such as the orientation of the part to be built.

Paying particular attention to block support, the main parameters on which it is possible to act are hatch distance, fragmentation interval, separation width and tooth height.

These supports are made with a grid of x and y lines separated at a certain distance (x hatching and y hatching). Hatching can be chosen depending on the surface area. When creating block supports, it is convenient to fragment the block. Fragmentation will leave a small gap in the hatching of the block support at each chosen distance, so the removal of block supports will become a lot easier [15]. The separation width is the distance between each identified block. The teeth are located between the proper support and the supported part and the dimensions that characterize them have to be defined. They also represent a way to simplify the removal phase of the supports. All these parameters can be changed manually by the user using the software. Varying these distances, the grid is more or less dense, consequently the amount of material needed and the quality of the built part change.

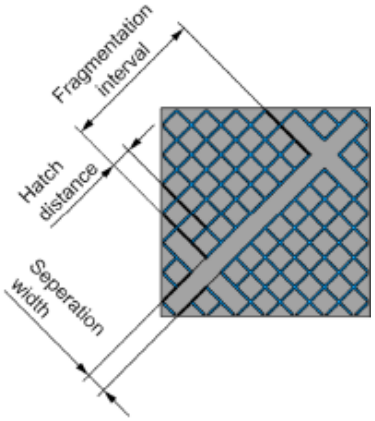

Figure 2.2.1 [10] – **Hatch distance, fragmentation interval and separation width.**

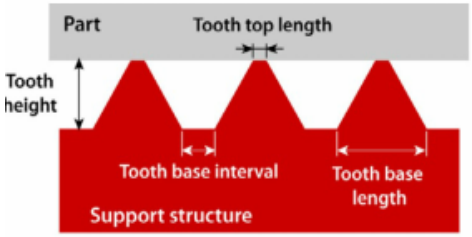

Figure 2.2.2 [15] - **Tooth parameters.**

Chapter 3: Parameters and machine's sub-systems

Before printing, it is necessary to set process parameters that have to be chosen in an appropriate way according to the application and optimized in order to obtain the characteristics that are desired. For this reason, due to their importance, the fundamental process parameters that need to be carefully set before starting the process are considered. Once selected, they are controlled by the systems with which the machine is equipped. These systems are inserted to perform various functions and are generally installed according to a modular approach.

3.1 Process parameters

The parameters to be defined concern various aspects that define the entire process. Every time a variation is made, there is an influence on the quality of the part regarding the structural aspect and the way in which heat is generated and distributed.

3.1.1 Power and speed

For the process, the values of power and speed at which the machine works must be defined. The optimization of these parameters is very important in order to have a homogeneous construction of the part and avoid the formation of defects and porosity.

The scanning speed is the velocity at which the laser beam moves and it is measured in mm/s. It can be seen in the following figure:

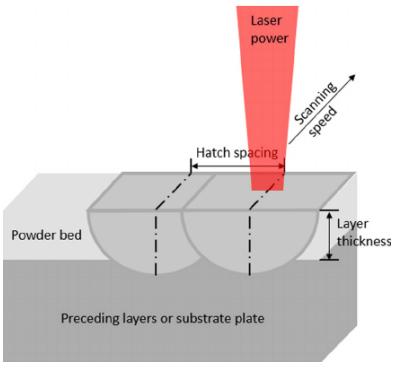

Figure 3.1.1.1- **SLM process parameters: laser power, scanning speed, hatch spacing and layer thickness [20].**

Build rate is the result of this speed (s) multiplied by the hatching distance (h) and layer thickness (t).

$$B = s \cdot h \cdot t$$

This factor represents the volume of material produced per hour, normally expressed in cm^3/h. In order to have a high productivity, this value should be increased.

As can be seen, the degree of construction (B) is directly proportional to the layer thickness. During the process parameters setting phase, it is necessary to consider that although an increase of the layer thickness determines an increase of the productivity, at the same time it involves a reduction of the part resolution, a very restrictive condition in some specific uses.

Another way to increase productivity is to have a higher laser beam speed, but if this is too high, it means that will remain less time in the same spot. This leads to a decrease of the energy transferred to the powder and therefore poor melting and formation of defects such as porosity. However, if the speed is too low the laser remains on the same spot more time and transmits too much energy that will evaporate the powder, causing also in this case pores.
Low laser power and high scanning speeds reduce energy penetration and generate intolerable porosity and “balling” or “bead up” phenomena [21].
In this way, wave effect distortions or micro-residues of material are created which can block the recoater during powder rearrangement operations.
On the other hand, too high beam powers can more easily generate porosity at melt pools called “keyholes” [21].

For these reasons the scanning speed must be chosen carefully, remembering that it is closely related to the power, in fact if one of them varies the energy varies as well.

Note that the power indicates the amount of energy transferred over time, whereas speed influences the time spent in the same point; so, the two values define the amount of energy transferred along the path of the laser beam (measured in J/mm). In addition to this value, which represents the Linear Energy Density (LED), the Surface Energy Density (SED) and the Volume Energy Density (VED) can also be calculated, which

represent the energy transferred on an area (J/mm^2) and on a volume (J/mm^3) respectively.

$$LED = \frac{P}{s} \quad \left[\frac{J}{mm}\right];$$

$$SED = \frac{P}{s \cdot h} \quad \left[\frac{J}{mm^2}\right];$$

$$VED = \frac{P}{s \cdot t \cdot h} \quad \left[\frac{J}{mm^3}\right];$$

where

P = laser power [J/s]

s = scanning speed [mm/s]

t = layer thickness [mm]

h = hatch distance [mm]

The energy densities, for the same process parameters, depend on the type of material and its thermal properties such as melting temperature and thermal conductivity.

The choice of the described parameters therefore influences not only the realization of the part, but also the quality of the surface, which can have different levels of roughness. In fact, for the same material, the roughness of the surface changes in relation to the energy absorbed. In particular, when the phenomenon of "balling" occurs, the formation of a continuous and homogeneous surface is hindered.
A decrease in scan speed or an increase in laser power, which will provide a higher energy density, can improve the surface quality in the horizontal plane while a contradictory effect can be obtained in the vertical plane [22]. Finishing operations can be carried out to improve the surface.

3.1.2 Scanning strategy

As regards scanning, in addition to speed, various strategies can be defined concerning the path that the laser follows during the formation of the layers. The scanning strategy is an important variable that has a significant influence on the thermal history during the SLM process. It influences part density, microstructure evolution, residual stress and mechanical properties.

The software used for the additive processes allows the user to almost freely define these paths, which require a large number of parameters to be set. The following figure shows the main patterns used, which are distinguished by the direction or the way in which the defined track is traversed:

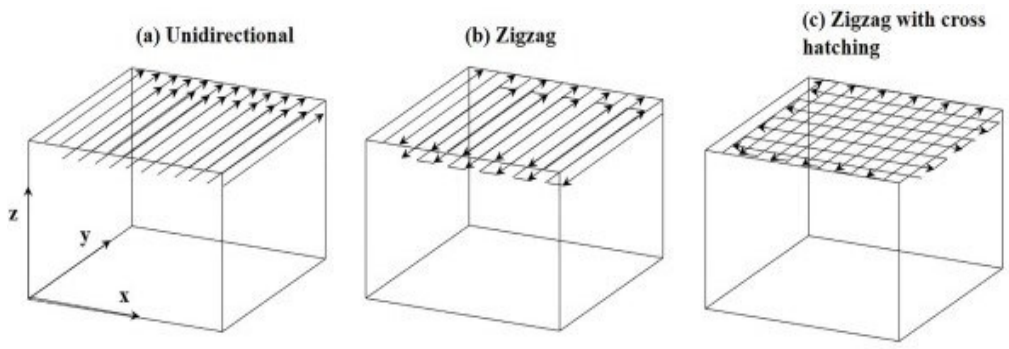

Figure 3.1.2.1- **Schematic of typical scan patterns. (a) unidirectional scan with the same orientation in successive layers, (b) zigzag scan with same orientation in successive layers and (c) zigzag with 90° rotations in alternate layers [23].**

The first type of strategy (a) consists of scanning unidirectionally along the y-axis for all levels without changing direction. The second is a zigzag type and also in this case the direction between the following levels is the same. Finally, a pattern is reported in which the direction to be followed in the next level is rotated by 90°, passing from the direction of the x axis to that of the y axis.

In addition to those described above, there are other ways to move the laser; for example, switching between layers, the hatch angle, that is the scanning direction, can be changed after a rotation:

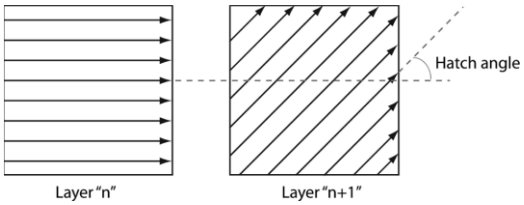

Figure 3.1.2.2 [24] – **Hatch angle.**

Variation of the hatch angle affects the density, surface finish and mechanical properties of the part. When the angle of rotation changes, the number of layers after which the direction of the scan lines is equal to that of the first layer also changes. The number of levels required is equal to N and is related not only to the mechanical properties, but also to anisotropy: as N increases, the mechanical characteristics improve and those of anisotropy decrease.

Another type of scan involves changing direction on the same layer by creating a grid pattern. This scanning method is called "island scanning" or "chessboard strategy" because well-defined areas are identified and it is illustrated in the figure 3.1.2.3. The hatch angle between the islands can be set to different values depending on the properties that have to be given to the part.

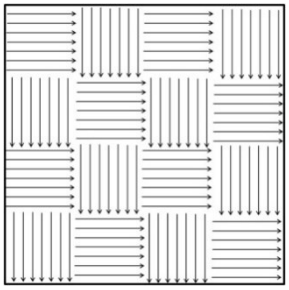

Figure 3.1.2.3 [25]- **Chessboard strategy.**

The areas that define the islands can be melted with a stochastic order or using a chessboard logic according to which the layer is divided into black and white sectors that are melted in sequence.

Each strategy involves specific characteristics, so it is necessary to evaluate advantages and disadvantages according to the application. In general, to have parts with a higher density and isotropy, it is necessary to make sure that the passes of the laser beams overlap to a certain extent. This overlap is also useful because the powder hit by the

laser beam does not absorb energy evenly: the central part of the circle has more energy than the outer areas. For this reason, the external zones may not be fused correctly and therefore the tracks must be close to each other.

Therefore, even if it is better to have the highest possible hatching distance for productivity, at the same time it is necessary to ensure the correct melting of the powder. Note that the track distance refers to the distance between the centres of adjacent tracks.

3.2 Machine technology systems

Among the main equipment of the machine there are the laser with all the optical system, the gas flow regulation system and the one that regulates the temperature. Before describing these systems in more detail, the machine used to produce the parts analysed is presented. The general characteristics and uses for which it is suitable are described.

3.2.1 Print Sharp 250

The machine used for the work done is the Print Sharp 250, a machine for additive manufacturing made by Prima Industrie SpA. It is the medium volume machine developed for Powder Bed Fusion applications, used for the industrial production of complex components.

Figure 3.2.1.1- **Print Sharp 250.**

Building volume is 250 x 250 x 300 mm, suitable dimensions for the fabrication of medium size components. For energy source the machine is equipped with an IR single-mode fiber optic laser with a power of 500 W.

A reliable and compact scanning head allows for different scanning strategies and high processing speeds, moreover the optimized gas flow minimizes the consumption of nitrogen or argon. To keep clean the working area, the machine is equipped with a filter for gas recirculation.

Intelligent control and operating software are used to set machine functions and orient parts quickly.

The materials that can be processed with the Print Sharp 250 are: stainless steel, maraging steel, high temperature nickel base alloy (Inconel), titanium alloy, cobalt chromium alloy, aluminium alloy, high strength steel, copper alloy.

A table containing more specific characteristics is given in the appendix.

3.2.2 Laser and optical system

Lasers in the metal powder bed system are typically fiber lasers with wavelengths in the 1.06 - 1.08 μm range and powers on the order of magnitude of 100s of Watts (200-500 W). Unpolarized IR lasers are the industry standard for SLM machines. Wavelength and to a lesser extent polarization can have a significant impact on absorptivity [26].

In SLM systems, a laser beam is generated with a continuous and high quality emission to obtain a small beam. In this way, details such as thin walls are produced with great precision. The generated laser passes through optical elements until it reaches above the working chamber. Here there is a galvanometric system that is used for focusing and controlling the movement of the laser beam in the working chamber through the rotation of mirrors.

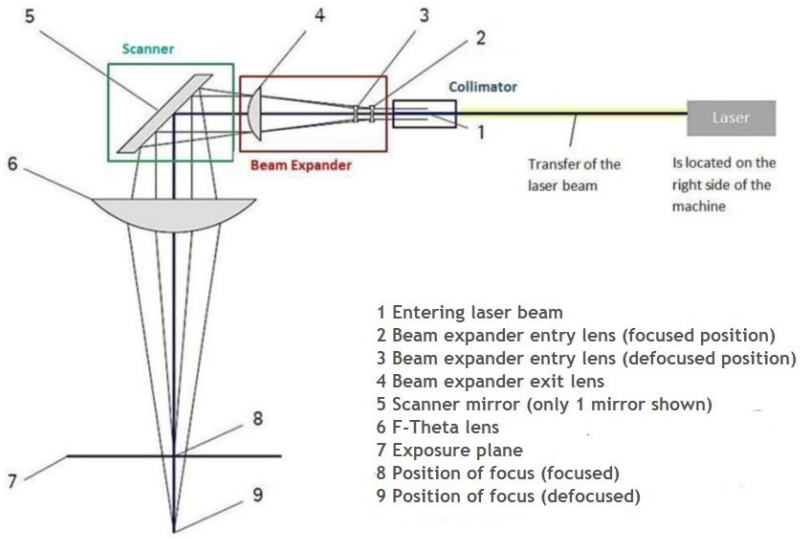

Figure 3.2.2.1 – **Optical system.**

Using the same galvos and optics as the scanning laser ensures that the area probed by the sensor is coincident with the focal point of the laser and presumably the heat affected zone. However, the reflective profile of the mirrors and distortion of the f-theta (or any other) lens limits the ability to probe process signatures with wavelengths relatively close to that of the scanning laser [26].

Previously, the laser has been described as a circle that hits the powder bed, generating localized melting, but this circle has a beam that determines the area that is affected: if the radius increases, the interested area also increases. Variation in the size of the laser spot produces different results using the same powder.

3.2.3 Gas flow

The process parameters also include the choice and regulation of the gas used to obtain a protective atmosphere inside the building chamber.

The method of delivery of the inert gas flow across the build platform can significantly influence the quality and reproducibility of components across the build area. This gas flow is primarily used to maintain the required inert atmosphere during processing. However, it also serves a secondary function by removing any process by-products such as vaporised powder (condensate) from the path of the laser, which may affect

the laser beam properties (energy, spot diameter, or intensity profile) at the powder bed [27].

The SLM process is executed inside the closed chamber where the inert atmosphere is maintained so that the oxygen so that the oxygen is below a certain value depending on the material; for example, less than 0.1% for materials such as aluminium and titanium. Based on the reactivity of the powder, nitrogen or argon is used as a gas to protect heated parts from oxidation and other problems that may affect mechanical properties. In addition, some machines provide the possibility to pre-heat the platform or the entire construction chamber to reduce the thermal gradient and the cooling rate.

The machine can be equipped with a gas recycling system, which once used can be filtered and returned to the building chamber. After the filter there is a collector of impurities that have been separated from the gas collected at the end of the process. This process is shown in the following figure:

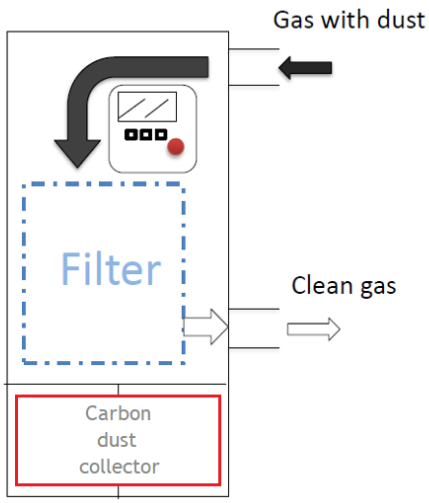

Figure 3.2.3.1 – **Gas filter and recycle system.**

3.2.4 Pre-heating

As mentioned above, 3D printers can include a pre-heating system for the building platform. In fact, during the process the heating and cooling rates can generate high thermal gradients in the component. In this way, deformations are created that are proportional to the thermal gradient through the thermal expansion coefficient α:

$$\varepsilon = \alpha \cdot \Delta T$$

Since the component is not free to deform, both normal and tangential stresses are generated. In fact, in SLM processes the part is bound to the baseplate, which has a lower temperature. This temperature difference contributes to the generation of internal stresses. These stresses can be calculated by determining the force needed to prevent the deformation that the piece would have if it were free to move. Note that if the platform and component materials are the same, the residual stresses are lower than if different materials are used, because in the first case the thermal expansion coefficient is the same. Large thermal gradients are also generated on the single layer due to the scanning strategy which causes a non-uniform temperature distribution. In SLM processes between two successive levels there are two mechanisms that may cause residual thermal stresses:

1) induced stresses in the solid substrate just underneath the present layer being melted;

2) stresses due to the cool-down phase of the melted top layers.

This first phenomenon, referred to as the Temperature Gradient Mechanism (TGM), derives from large thermal gradients in the solid material just underneath the laser spot (figure 3.2.4.1) [28]. Due to the high temperature in the upper layers of the solid part, these upper layers will expand, but the colder underlying solidified layers will limit this expansion. This induces compressive stresses (σ_{comp}) in the upper layers of the substrate that can exceed the yield strength of the material and reach the plastic field. When this situation occurs, the compressive stresses in the material cause plastic

deformation (ε_{pl}) of the upper layers. The state of compression is converted into residual tensile stress (σ_{tens}) when these plastically altered layers cool down and those residual stresses may induce cracking of the part.
In the second phenomenon, the melted top layers tend to shrink due to the thermal contraction. This deformation is again prohibited by the underlying layers, thus introducing tensile stresses in the top layer, and compressive stresses below [28].

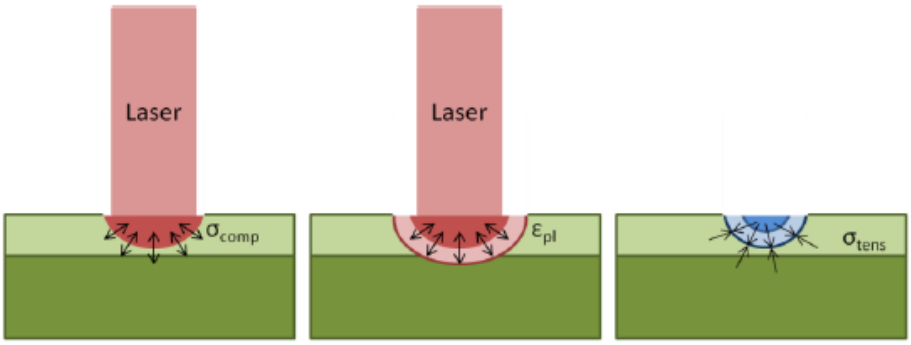

Figure 3.2.4.1 – **Temperature Gradient Mechanism in SLM [28].**

For the reasons just discussed, the platform is pre-heated in order to reduce the thermal gradient between the workpiece and the baseplate and the local thermal gradients.

Generally, parts built with a higher density are more inclined to crack because they accumulate more residual stress. Instead, when there is a certain degree of porosity, the tensional state is reduced because the pores cannot contain internal stresses. However, to obtain more precise parts an appropriate density is required and a technique to improve this property is laser re-melting. This operation provides that the most recent layer before adding new layers is re-melted and this may also improve the part microstructure and surface finish.

In conclusion, in order to set up the process, factors relating to both the component and the machine used must be carefully considered. The machine is equipped with tools and accessories that execute specific operations and that must be set, calibrated and coordinated with each other in order to have a good realization of the products. The process parameters would also include the choice of supports for which the quantity, type and relative characteristic quantities must be indicated. As already anticipated in paragraph 2.2, the introduction of support structures requires the

definition of additional parameters such as hatch distance, fragmentation interval, separation width and tooth height. In general, the values to be set are chosen according to the piece to be produced and the heat to be dissipated. In the present work the influence of block supports parameters is analysed and it will be discussed in the part dedicated to experimental phase.

Chapter 4: Material

The first part of the chapter presents the material used in this work, its chemical composition, properties and applications. Afterwards, articles are cited that report studies carried out on the same or similar material and that contribute to defining the state of the art.

4.1 Inconel 718

The material considered in this study is Inconel 718, a high-strength, corrosion-resistant nickel chromium material. This type of alloy is characterized by good tensile strength, creep, fatigue and failure resistance at temperatures up to 980 °C (1290 °F). The resistance to high temperatures is due to the formation of an oxide layer that performs a protective function. The following table shows the chemical composition:

	min (%)	max (%)		min (%)	max (%)
Ni	50	55	**Co**	-	1
Cr	17	21	**Cu**	-	0,3
Nb	4,75	5,50	**C**	-	0,08
Mo	2,80	3,30	**Si/Mn**	-	0,35
Ti	0,65	1,15	**P**	-	0,015
Al	0,20	0,80	**S**	-	0,015

Table 4.1.1- **Chemical composition of IN718 [16].**

This material lends itself to many high temperature applications such as parts for nuclear reactors, in the petrochemical sector, in the chemical and power industry, gas turbine engine components, such as discs, blades etc.

The phase composition of Inconel 718 mainly consists of a γ matrix with the precipitates of γ', γ", δ and, additionally, some carbides. These precipitates, particularly γ", provide the desired mechanical properties to Inconel 718.

The γ' phase is a solid composition coherent with the matrix that morphologically may appear spherical, block, globular or cuboidal, depending on the temperature and duration of treatments.
This phase is stable at high temperatures and this leads to improvements in the mechanical characteristics of the alloy. With the increase of the percentage of γ' the mechanical resistance increases, but at the same time the workability decreases. For this reason, the volume percentage doesn't exceed 40%.
The γ'' phase is the one that most confers strength to Inconel 718 and it is a metastable compound of Ni3Nb that has a circular shape. For prolonged heat treatments or high temperature heat treatments it evolves in the δ phase, since it is a metastable phase [18].

These characteristics of IN718 make this alloy not easy to work with traditional machines, however it is suitable for additive manufacturing processes, ensuring that the parts produced have the properties required for the applications.

The mechanical properties considered for the analysed material are the ones detected from finished components (as build) produced by Prima Industrie SpA.

	Inconel 718
Accuracy	Small part: ±40-60 µm
	Big part: ±0.2%
Thinnest wall	0.3-0.4 mm
Layer thickness	40 µm
Roughness	Original: Ra 17 µm, Rz 32 µm
	After Shot blasting: Ra 4-6.5 µm, Rz 20-50 µm
	After polishing: Rz < 0.5 µm
Build speed	13 cm^3/h
Density	8.1 g/cm3
Tensile stength	1060±50 MPa, (XY)
	980±50 MPa, (Z)
Yield strength	780±50 MPa, (XY)
	634±50 MPa, (Z)
Young modulus	160±20 GPa, (XY)
	130±20 GPa, (Z)
Elongation	27±5% (XY)
	31±5% (Z)
Hardness	30 HRC

Table 4.1.2- Properties of IN718.

Note that the build speed depends on the process parameters that are chosen during the setting of the machine mentioned in Chapter 3.

4.2 Literature review on the experimentation of support structures

Although the use of AM technologies with Inconel 718 allows to overcome some design limits of many components with complex geometry, to date there are not many studies and characterizations for this material.

Research on materials used as supports began more than twenty years ago, focusing mainly on computational support generation techniques related to stereolithography (SLA) and Fused Deposition Modelling (FDM) [10].

Before starting the present work, a research on the study of supports in Additive Manufacturing processes was carried out. A summary of the articles that have shown greater pertinence to the objectives of the thesis work is given below.

- Tatiana Mushurova and others carried out a study on the influence of supports on the deformation and residual stress of a part in IN718. Two samples are used: one was produced on a lattice support structure (S), another one on the base plate (B).

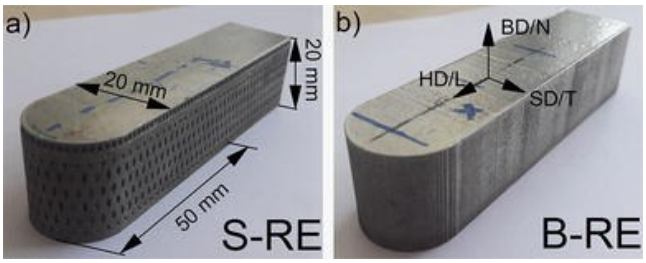

Figure 4.2.1 [19]-**Sample on support structure a), bulk b).**

The samples were investigated in two conditions: as-built on the base plate (AB) and in released condition (RE), removed from base plate by wire erosion [19].

The results include:

residual stress of top surface for the transversal stress component

Samples in AB condition show an increase of stress toward tip region, but the stress gradient along the length is more pronounced for B-AB. The removal from the base plate does not significantly change the residual stress values for B-RE in comparison to B-AB. For the thin sample S-RE, the stress gradient remains similar to S-AB, but the overall stress values decrease by about 200 MPa [19].

Residual stress of the longitudinal component of the top surface

The B-AB sample has higher residual stress values than S-AB. The gradient along the length decreases for both samples after removal from the base plate. […] The sample on support S-RE shows an overall decrease of stress values (redistribution) [19]. In conclusion, the sample with support structure shows a lower level of von Mises stress in both conditions (AB and RE) in comparison to the bulk sample.

Although the sample on the support structure showed lower stress values than the bulk one, if one wants to reduce the residual stress value and avoid severe distortions after the separation of the part, heat treatments have to be performed after production.

Distortion of the top surface

The difference between the conditions AB and RE characterizes the distortion of the samples due to removal from the baseplate. In the case of B sample, only the tip region shows a significant decrease in height after releasing, while the rest of the sample looks undistorted. For S sample, some stripe-like distortion with small amplitude can be seen in the middle of sample. […] The support structure gives more compliance to the sample and results in higher distortion, with stripe-like pattern correlated with period of the support structure [19]. For sample S there are some effects of removal from the base plate only near the tip, where the sample bends downwards.
The tip region shows a larger distorted area in comparison to the bulk sample [19].

- An experimental study on the analysis of block supports parameters on a part with a protrusion was conducted by O. Poyraz and others in two sets of experiments. In this case IN625 was used, a nickel-chromium alloy very similar to IN718. A first set of experiments examine the impact of the support dimensions such as hatch distance of a block, while the second set of experiments focuses mainly on the effects of part-support contact in the form of teeth dimensions. […] Dimensional inspection was conducted by a height gage in order to see the part distortions in the upward direction to check the effectiveness of the created supports.

For the first set of experiments the hatch distance is the first remarkable factor causing a lift for the overhanging geometry and it further enhances a separation after it reaches to a certain value of 1 mm [10]. The tests conducted revealed that a lower hatch distance implies less distortion and the best results between the values examined were achieved with a 0,5 mm hatch distance. The specimens, which have fragmented islands comprising more cells, show less deformation. In the 2nd set of experiments, both the top length and Z offset value reductions, respectively the width of the tooth at the point of contact and the depth of the tooth, influence the distortion results [10]. Note that hatching parameters have greater influence on the support structures comparing to tooth parameters. The results show that the influence of the Z offset value is inversely proportional to the value of the top length. In particular, with values lower than the top length, increased Z offset values show major deformation. Both sets of experiments have shown that support structures built with greater hatch distance and fragmentation interval are more easily detached from the part.

From the results of the second set of tests, the micrographs also show that top length with lower values for the tooth structures of the supports lead to weaker support attachments, but the adverse effect is lower than the hatch distance [10].

Regarding the microstructure of the specimens, precipitates were identified near the supports.

In this study, the grain formation at the connections between the support structures and the part was also analysed to understand if the geometric characteristics of a support structure have any influence on the grains, but no relation was found.

From some micrographs, it is evident that the self-detaching of the support structures from the part can lead to irregularities on the surface quality as well as some porosity formation [10].

- Kaifei Zhang, Guang Fu and others studied the effect of the geometric design of the supports on components produced by SLM. The raw material used was titanium alloy powder atomized with Ti-6Al-4V gas. In this research, an unconventional block support structure whose interspaces are fully or partially filled by solid cuboids for better heat dissipation was used to anchor the designed specimens with some overhanging structures.

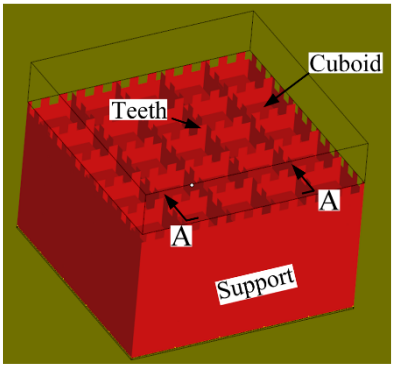

Figure 4.2.2 - **Block support structure with cuboids for heat dissipation [32].**

It was found that solid pieces or cuboids as support structures can reduce the deformation. Although the inserted solid piece can decrease the deformation of part, this contact-less support is still not be sufficient to anchor the overhang. Therefore, it is proposed to insert solid cuboids to the conventional block support. The results showed that the maximum amount of deformation came down with the reduction of the gap between the overhang and the solid part. In addition, it is demonstrated that the deformation magnitudes of the specimens with solid pieces have decreased comparing to that of the specimen without solid piece. The distance between every two adjacent walls of support and the gap between the cuboids and the overhang, respectively, most influence the part's deformation and surface quality. As the gap between the cuboids and the overhang decreases, the bottom surface of part has a better quality. Absolutely, the gap between the cuboids and the overhang cannot be too small to form a non-assembly mechanical structure [32].

- Kai Zeng in his dissertation reported the experiments that were conducted to investigate thresholds for support structure density with parts with dimensions 40 x 5 x 2 mm made of TI64. The first experiment was designed to see the influence of support structure height and large hatch space. The results show that with the overlarge

hatch space, the powder, rather than support structure, is underneath the part in large areas when the laser scans the first several layers. The strength of the powder and the reduced thermal conductivity results in an accumulation of defects in the first few layers.

Figure 4.2.3 [33] – **Defects due to the overlarge hatch space.**

The other samples in the experiment show that the height of the support structure and the types of support do not affect the building of the part. Subsequent experiments were carried out considering uniform, non-uniform supports and supports with non-uniform wall thicknesses. In the first case the main problem was support structure cracking where the support structure attached to the base plate. In the second case, instead, all the parts are built successfully, although a few of them showed evidence of crack initiation. With non-uniform support walls, three different t/l (thickness / support spacing) ratios were used. The experimental results showed that all parts were built successfully. In addition, samples with different dimensions (20 x 20 x 2 mm) have been produced for which the uniform hatch spacing support structures showed obvious defects: it was observed from the experiment that cracking starts growing from corners.

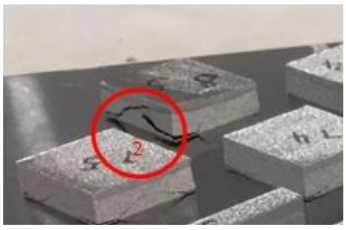

Figure 4.2.4 [33] – **Support cracking.**

In this case it is suggested to put dense support structures around the corner, while the rest of the area could be supported less densely. The non-uniform support structure experiment indicates that loose support structures far away from the corners would have no negative effects on a part [33].

Chapter 5: Experimental procedure

This chapter contains all the experiments performed to carry out the study of the support structures. Initially, the characteristics of the source material used with the 3D printer to produce the parts are reported. It is then explained the setting of the different experiments executed for the analysis on the influence of the geometric parameters of the supports and the process parameters on the quality of the generated supports.

5.1 State of the material

The material used for the production of the samples analysed is Inconel 718 in the form of powder composed of spheroidal particles. It was produced using the atomised gas technique (with Argon) by the Oerlikon company.

The chemical composition for the material used is given in table 5.1.1:

	Weight Percent (nominal)							
	Ni	**Cr**	**Fe**	**Nb+Ta**	**Mo**	**Al**	**Ti**	**Other**
MetcoAdd 718C	Balance	18	18	5	3	0,6	1	<5

Table 5.1.1 [54] - **Chemical composition [54].**

The characteristics of the powder are contained in table 5.1.2:

	Nominal Range [µm]	**D90 [µm]**	**D50 [µm]**	**D10 [µm]**	**Hall Flow [s/50 g]**
MetcoAdd 718C	-45 +15	46	30	18	<18

Table 5.1.2 [54] - **Powder specifications [54]**.

5.2 Design of Experiment

Design of Experiment (DoE) is a method used to determine the correlation between process parameters and process output. The purpose is to optimize the result by varying the input factors. In powder bed processes there are many parameters to set before starting to make parts. As seen in paragraph 3, they can be divided into process and machine parameters.

The objective of the experiments carried out in this work is actually to identify the influence of some parameters. In particular, the geometric dimensions of the support structures are analysed, which are made for different samples with varying power and scanning speed.

The following paragraphs describe the experiments and the steps taken to carry them out.

5.2.1 The first Design of Experiment

The first experiment was set up with the aim of evaluating the variation of three different parameters of the block supports: the hatch distance, the fragmentation interval and the separation width. The supports were created to sustain a protrusion and evaluate their effectiveness and removability. In particular, for each combination of parameters a sample was considered for a total of nine. All parts have the same shape and dimensions as shown in figure 5.2.1.1 and were made using Materialise Magics.

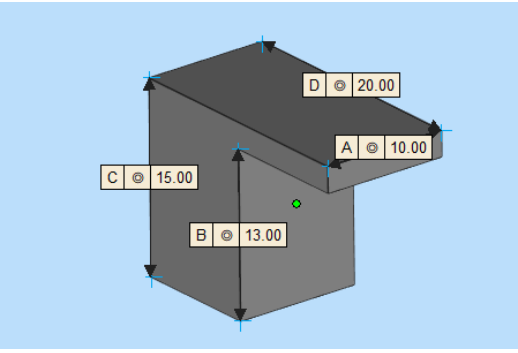

Figure 5.2.1.1 – **Part dimensions.**

The following table shows the values of the parameters for each sample, which are also present on the upper surface of the parts to distinguish them from each other after printing.

Sample number	Hatch distance [mm]	Fragmentation interval [mm]	Separation width [mm]
1	0,5	2,5 (x5)	0,5
2	0,5	3 (x6)	0,5
3	0,5	3,5 (x7)	0,5
4	0,75	3,75 (x5)	0,75
5	0,75	4,5 (x6)	0,75
6	0,75	5,25 (x7)	0,75
7	1	5 (x5)	1
8	1	6 (x6)	1
9	1	7 (x7)	1

Table 5.2.1.1- **Supports parameters for the first DoE.**

The quality of the support structures depends not only on the geometric characteristics chosen, but also on the process parameters such as power and scanning speed. To evaluate their impact, the Volumetric Energy Density (VED) was calculated on the nine supports:

$$VED = \frac{P}{s \cdot t \cdot h} \quad \left[\frac{J}{mm^3}\right]$$

Where

P = laser power [J/s]

s = scanning speed [mm/s]

t = layer thickness [mm]

h = hatch distance [mm]

For privacy reasons, the values of power and scanning speed are given in percentages.

Sample number	Power	Scanning Speed	Layer thickness [mm]	Hatch distance [mm]	Volume Energy Density [J/mm³]
1	26%	75%	0,04	0,5	5,417
2	26%	75%	0,04	0,5	5,417
3	26%	75%	0,04	0,5	5,417
4	26%	75%	0,04	0,75	3,611
5	26%	75%	0,04	0,75	3,611
6	26%	75%	0,04	0,75	3,611
7	26%	75%	0,04	1	2,708
8	26%	75%	0,04	1	2,708
9	26%	75%	0,04	1	2,708

Table 5.2.1.2 – **VED values.**

The supports have been made using the same software, which allows to import the model of the building platform of the printer used (figure 5.2.1.2). Thanks to this option, the best disposition of the parties can be identified at a preliminary stage. In this case, with the Print Sharp 250 the working volume is 250 x 250 x 350 mm and the samples were disposed by placing them against the recoater with a short side and with an inclination of 5° to avoid the problems caused by the possible impact of the blade.

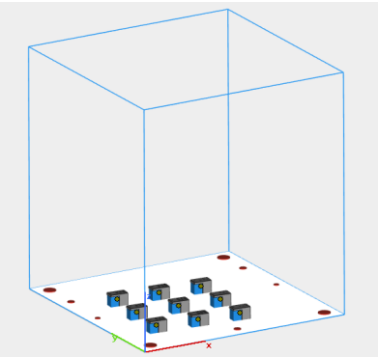

Figure 5.2.1.2 - **Building platform.**

Note that in this first set of samples the distance of the supports from the vertical wall of the part was considered equal to 0.5 mm, as shown in the following figure, as well

as the offset on the x-y plane (that is the distance between the edge of the part and the edge of the support) is also equal to 0.5 mm. With these distances, the actual area under which the block support is built is 92.12 mm^2.

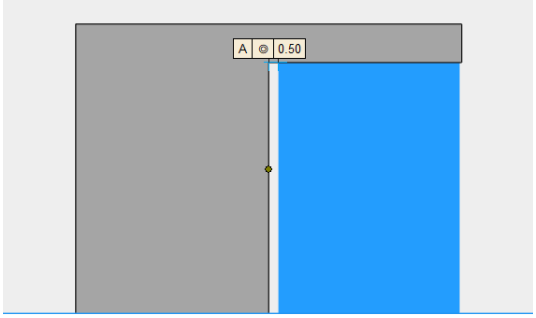

Figure 5.2.1.3 - **Distance from the vertical wall.**

In figure 5.2.1.4 the samples are shown from the lower view so as to notice the difference between the supports passing from one sample to another.

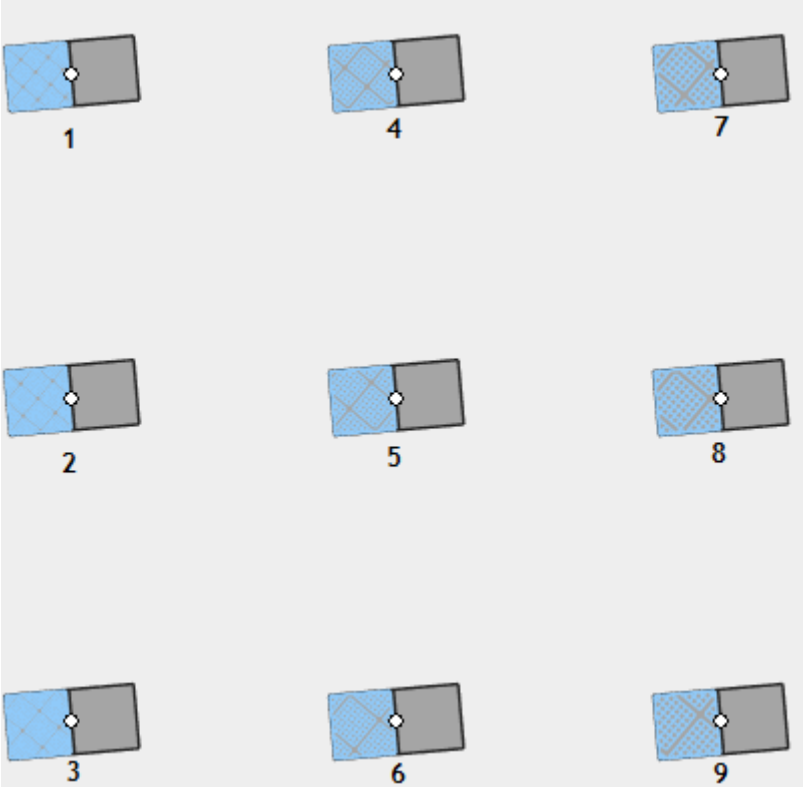

Figure 5.2.1.4 - Lower view.

After the supports were made there was the slicing phase, which involves the division into layers of both the part and the support structures.

Slicing was also performed with a Materialise Magics function, which allows to set the thickness of the layers (figure 5.2.1.5).

This operation is carried out separately for the part and for the supports, in fact at the end of the slicing the output files have two different formats:

- ".cli" for the part;
- ".slc" for the supports

In both cases, the layer thickness was set at 20 micrometres, value that will be considered during printing.

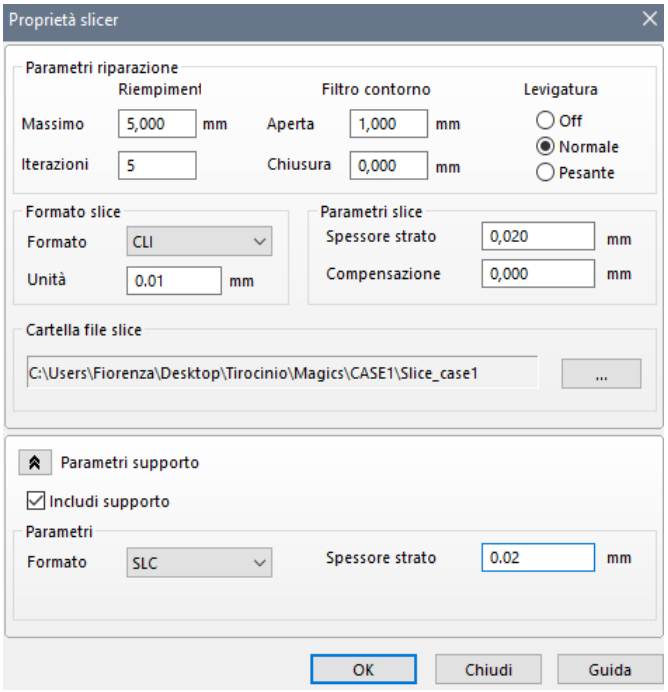

Figure 5.2.1.5 - **Slicer properties.**

Once the files in the formats indicated above are obtained, those in the ".cli" format are opened with the post processor software. This software is used to set the machine parameters that are used during printing. At the end of this phase the files are saved in the ".epi" format and can be inserted in the machine together with the ".slc" files.

Before starting printing, the chamber was preheated to prevent the formation of thermal stress. The temperature used for the Inconel 718 is 60°C.
At this stage, also the injection of the inert gas (Nitrogen) is initiated to create a protective environment.

For productivity reasons, the samples were produced, during the same job, together with other parts on the same platform. The figure below shows the building chamber during the printing phase:

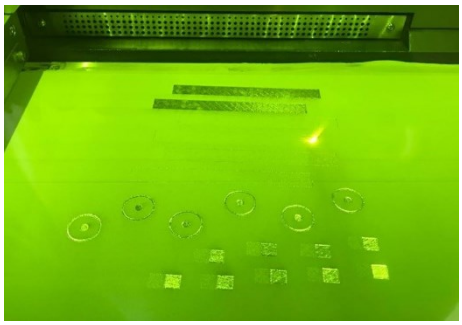

Figure 5.2.1.6 - **Printing phase.**

At the end of the job, the platform was extracted and the realized samples looked as shown in the following figure:

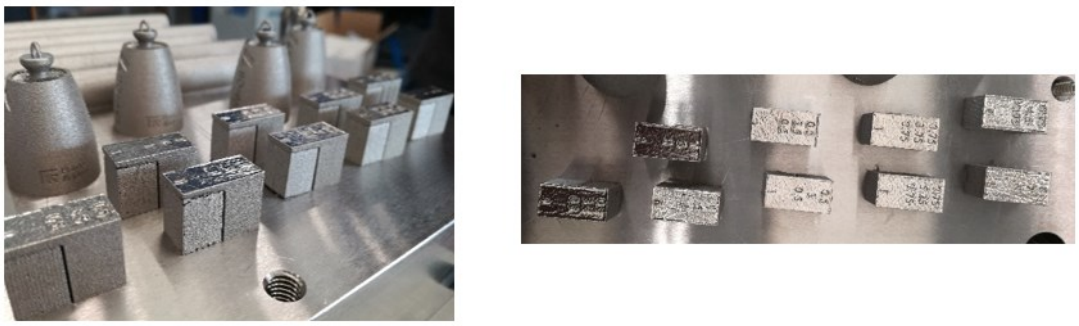

Figure 5.2.1.7 - **Samples after printing process.**

Once taken out of the machine, the samples were separated from the platform by the wire cut EDM (Electrical Discharge Machining).

5.2.2 The second Design of Experiment

The second Design of Experiment was performed on nine samples with different geometry and dimensions than the first. In this case, a bridge structure supported by block supports was created. Given the simplicity of the geometry used, it was possible to create the 3D CAD model directly using the Materialise Magics software.

Note that one dimension that needs attention is the height of the part. In fact, two cases with different heights have been realized, identifying supports 5 mm and 15 mm high. So having made nine samples for each case, eighteen samples were printed in total for this DoE. The steps for setting up the work are the same for both cases and are now reviewed.

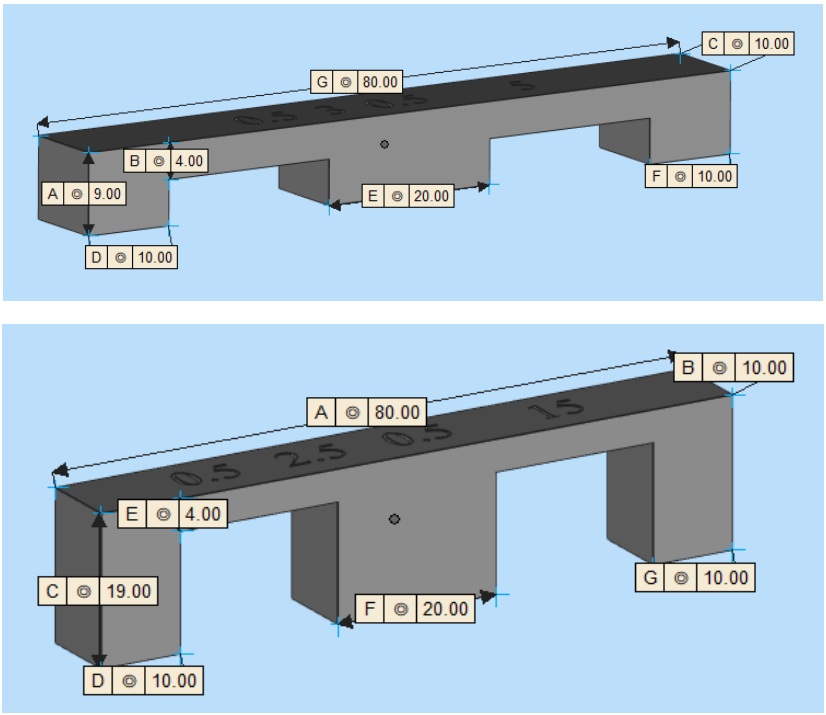

Figure 5.2.2.1 – **Part dimensions.**

The geometric parameters of the supporting structures are the same as for the first DoE. The following table shows the values associated with the supports produced for the eighteen samples:

Sample number	Hatch distance [mm]	Fragmentation interval [mm]	Separation width [mm]
1, 10	0,5	2,5 (x5)	0,5
2, 11	0,5	3 (x6)	0,5
3, 12	0,5	3,5 (x7)	0,5
4, 13	0,75	3,75 (x5)	0,75
5, 14	0,75	4,5 (x6)	0,75
6, 15	0,75	5,25 (x7)	0,75
7, 16	1	5(x5)	1
8, 17	1	6(x6)	1
9, 18	1	7(x7)	1

Table 5.2.2.1 – **Supports parameters for the second DoE.**

Therefore, the supports were realized, always using Materialise Magics, only under the surfaces that are between the solid parts.

The offset on the x-y plane is 0,1 mm and 0,5 mm from the vertical wall of the part, so the actual supported area on the entire sample has a value of 372,4 mm^2.

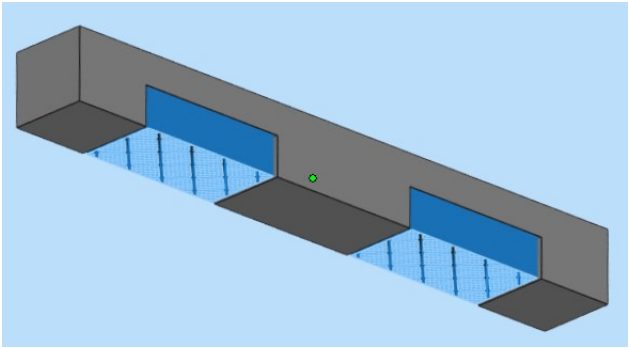

Figure 5.2.2.2 – **Supported sample.**

This operation was carried out for each sample and, once all the necessary support structures were obtained, the parts were placed on the platform model used for the Print Sharp 250.

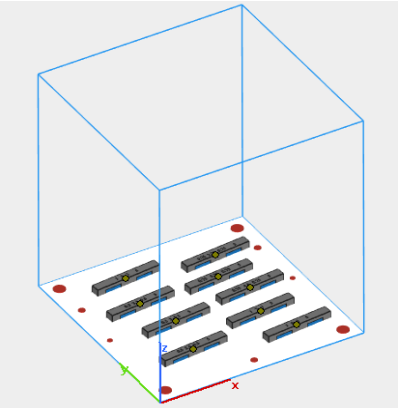

Figure 5.2.2.3 – **Samples on the building platform.**

Also in this case, labels were created on the upper surfaces to distinguish between the samples. However, even from the lower view it is possible to appreciate the difference between the block supports created.

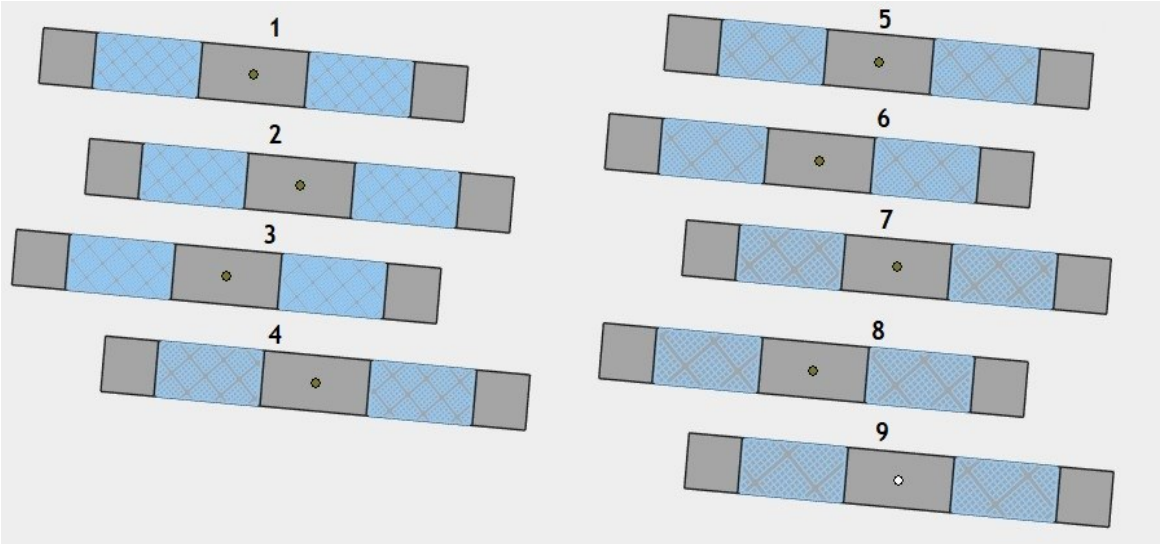

Figure 5.2.2.4 – **Lower view.**

As can be seen, no side of the test pieces is parallel to the blade of the recoater, as they are rotated by 5 degrees with respect to the direction of motion to prevent the impact from creating problems.

Once all the samples and supports were completed, slicing was performed using the dedicated function in Materialise Magics. As with the first DoE, layers thickness was set at 20 micrometres for both parts and supports.

With the slicing, the files were obtained in the formats .cli for the parts and .slc for the support structures. The files in the .cli format were then converted to the .epi format in order to have all the information in the machine language.

At this point all the eighteen samples were placed on the same building platform, so that they could all be made in a single job.

The next image shows the printing step:

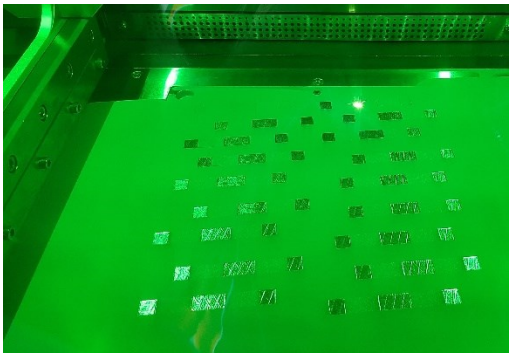

Figure 5.2.2.5 - **Printing phase.**

In the figures below it is possible to see the eighteen samples created on the same platform at the end of the printing process:

Figure 5.2.2.6 – **Samples on the building platform.**

As regards the Volumetric Energy Density (VED) of support structures, this assumes a certain value for the laser power and scanning speed chosen and also in this case was calculated.

Sample number	Power	Scanning Speed	Layer thickness [mm]	Hatch distance [mm]	Volume Energy Density [J/mm³]
1, 10	22%	75%	0,04	0,5	4,583
2, 11	22%	75%	0,04	0,5	4,583
3, 12	22%	75%	0,04	0,5	4,583
4, 13	22%	75%	0,04	0,75	3,056
5, 14	22%	75%	0,04	0,75	3,056
6, 15	22%	75%	0,04	0,75	3,056
7, 16	22%	75%	0,04	1	2,292
8, 17	22%	75%	0,04	1	2,292
9, 18	22%	75%	0,04	1	2,292

Table 5.2.2.2 – **VED values.**

5.2.3 The third Design of Experiment

With this third Design of Experiment the objective is to evaluate the influence of laser power and scanning speed. As already mentioned, these two process parameters are fundamental and are the main terms to be used for the calculation of Volumetric Energy Density (VED).

In this regard, samples were printed by varying the two study quantities one by one with respect to the values used in the second DoE.

In total, four cases are distinguished, two for the variation of the laser power and two for the variation of the scanning speed.

	Power	Scanning Speed
Case 1	16%	75%
Case 2	28%	75%
Case 3	22%	62,5%
Case 4	22%	87,5%

Table 5.2.3.1 – **Process parameters.**

The samples used to carry out this study have the same geometrical characteristics as those used in the second DoE, with a height of 15 mm, as they showed better results than those with a height of 5 mm. So a total of 36 samples were printed.

For all the parts the VED was calculated with the new parameters and the values obtained are the following:

Sample number	Power	Scanning Speed	Layer thickness [mm]	Hatch distance [mm]	Volume Energy Density [J/mm³]
19	16%	75%	0,04	0,5	3,333
20	16%	75%	0,04	0,5	3,333
21	16%	75%	0,04	0,5	3,333
22	16%	75%	0,04	0,75	2,222
23	16%	75%	0,04	0,75	2,222
24	16%	75%	0,04	0,75	2,222
25	16%	75%	0,04	1	1,667
26	16%	75%	0,04	1	1,667
27	16%	75%	0,04	1	1,667

Table 5.2.3.2 – **VED values for CASE 1.**

Sample number	Power	Scanning Speed	Layer thickness [mm]	Hatch distance [mm]	Volume Energy Density [J/mm³]
28	28%	75%	0,04	0,5	5,833
29	28%	75%	0,04	0,5	5,833
30	28%	75%	0,04	0,5	5,833
31	28%	75%	0,04	0,75	3,889
32	28%	75%	0,04	0,75	3,889
33	28%	75%	0,04	0,75	3,889
34	28%	75%	0,04	1	2,917
35	28%	75%	0,04	1	2,917
36	28%	75%	0,04	1	2,917

Table 5.2.3.3 – **VED values CASE 2.**

Sample number	Power	Scanning Speed	Layer thickness [mm]	Hatch distance [mm]	Volume Energy Density [J/mm³]
37	22%	62,5%	0,04	0,5	5,500
38	22%	62,5%	0,04	0,5	5,500
39	22%	62,5%	0,04	0,5	5,500
40	22%	62,5%	0,04	0,75	3,667
41	22%	62,5%	0,04	0,75	3,667
42	22%	62,5%	0,04	0,75	3,667
43	22%	62,5%	0,04	1	2,750
44	22%	62,5%	0,04	1	2,750
45	22%	62,5%	0,04	1	2,750

Table 5.2.3.4 – **VED values CASE 3.**

Sample number	Power	Scanning Speed	Layer thickness [mm]	Hatch distance [mm]	Volume Energy Density [J/mm^3]
46	22%	87,5%	0,04	0,5	3,929
47	22%	87,5%	0,04	0,5	3,929
48	22%	87,5%	0,04	0,5	3,929
49	22%	87,5%	0,04	0,75	2,619
50	22%	87,5%	0,04	0,75	2,619
51	22%	87,5%	0,04	0,75	2,619
52	22%	87,5%	0,04	1	1,964
53	22%	87,5%	0,04	1	1,964
54	22%	87,5%	0,04	1	1,964

Table 5.2.3.5 – **VED values CASE 4.**

Chapter 6: Results and discussions

This chapter explains the results of all the experiments carried out. After the most important information has been reported, it will be discussed and analysed with the aim of drawing conclusions. All the parts produced for the three DoE presented in the previous chapter were inspected and measured with appropriate precision instruments in order to obtain graphs and tables so as to easily understand what was recorded. Therefore, the results of each of the tests will be presented separately in the following paragraphs.

6.1 First DoE

Once the samples were separated from the building platform by EDM, they were subjected to a visual analysis aimed at evaluating which are the parameters that allowed to generate the best supports. Figure 6.1.1 shows the samples from the underside, from which the difference between the dimensions of the created supports can be seen:

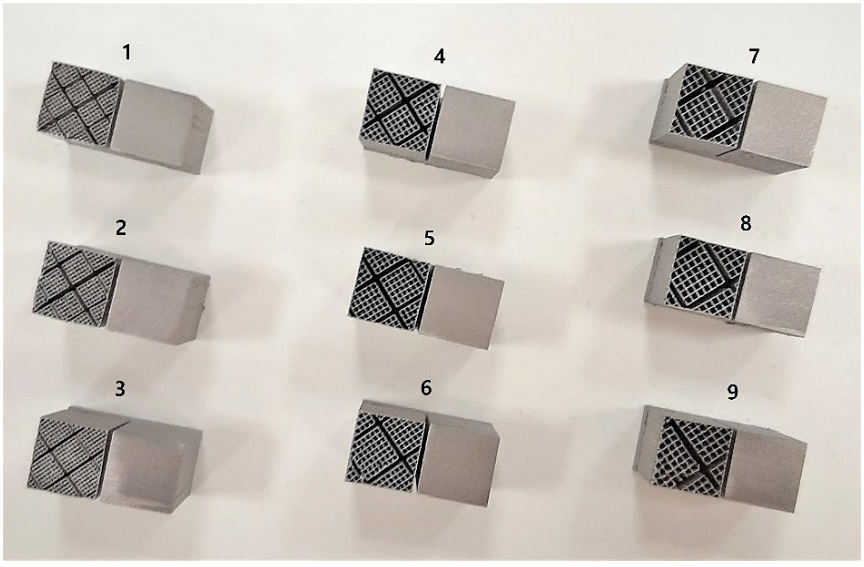

Figure 6.1.1 – **Support structures with different parameters.**

After the inspection some evaluations can be made considering the relationship between the geometric parameters and the quality of the support.

As regards the hatch distance, as this size decreases, better supports are obtained. Comparing three samples with the three hatch distance values considered, the difference between them can be clearly seen (figure 6.1.2).

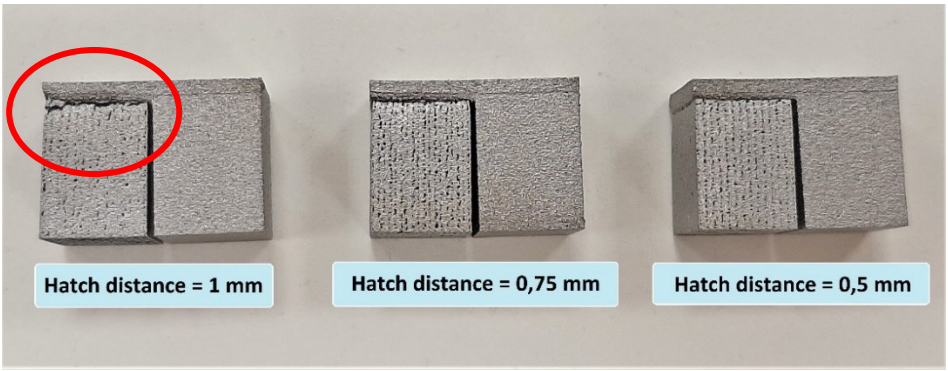

Figure 6.1.2 – **Samples with different hatch distance values.**

As it can be noticed from the image, increasing the hatch distance creates an ever more evident detachment, which reaches the worst case when the value is equal to 1 mm. When the part is detached, the use of the supports is not exploited, since their purpose is exactly to support the part and dissipate heat to avoid deformation.

The other distance that exercised a considerable influence is the fragmentation interval, that is the dimension that defines the size of each block created. In this case the relation with the quality is inverse because this time it is with the increase of such dimension that the realization of the supports is better.
Note that this evaluation must be done with the same hatch distance and separation width (always equal to the hatch distance).

For this reason, the samples are shown in groups of three in the following figures, in which they are ordered from left to right from best to worst.

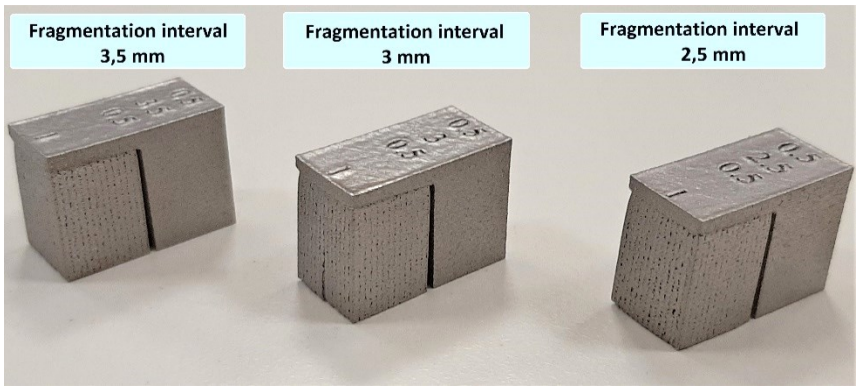

Figure 6.1.3 – **First group of samples.**

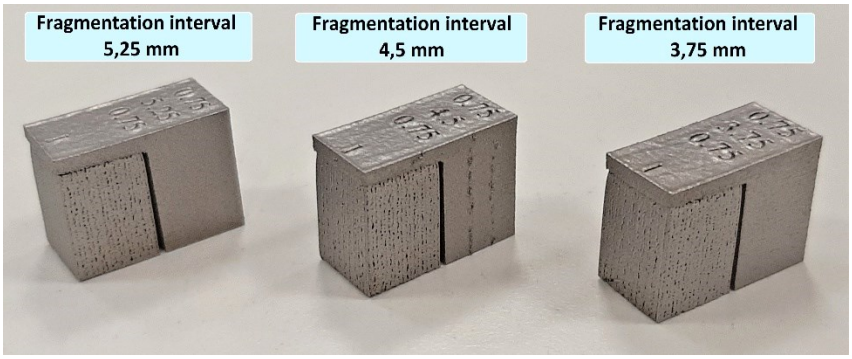

Figure 6.1.4 – **Second group of samples.**

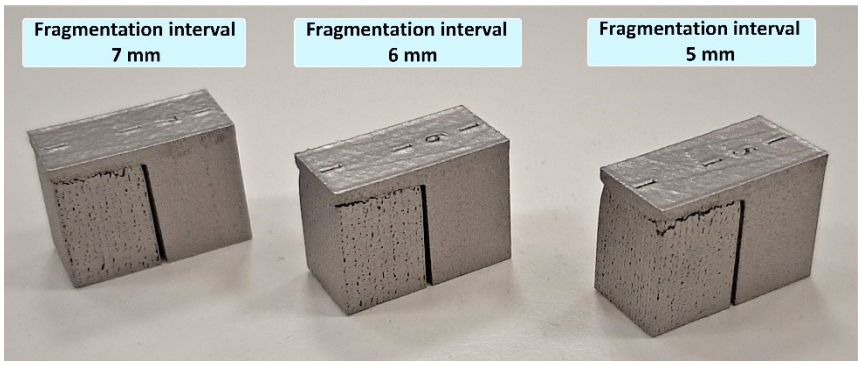

Figure 6.1.5 – **Third group pf samples.**

From what has been said so far, the conclusion is that the sample with the best supports is number 3, while the one with the worst supports is number 7.

Sample number	Hatch distance [mm]	Fragmentation interval [mm]	Separation width [mm]	
3	0,5	3,5	0,5	✓
7	1	5	1	✗

Table 6.1.1 - **Better and worse parameters.**

Another aspect that was analysed is deformation, so relations were found with both the hatch distance and the fragmentation interval.

For this purpose, the following four dimensions were measured with the digital caliper:

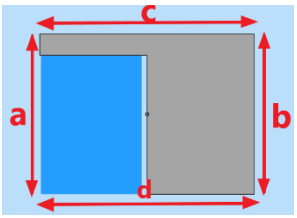

Figure 6.1.6.

a) height of the part from the side with the support
b) height
c) upper total width
d) lower total width

The data obtained were used to create graphs. The resulting graph for height measurements *a* and *b* is the following:

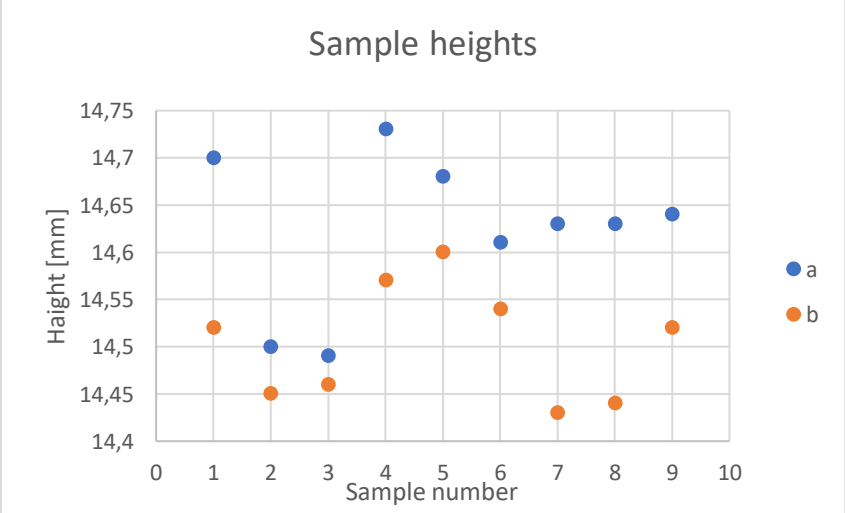

Figure 6.1.7 - **Measurements of dimensions a) and b).**

Before commenting on the graph, note that the deviation from the nominal size of 15 mm is probably due to the separation procedure from the plate by using EDM. For this reason, in order to assess the extent of the deformation, it is better to focus the analysis on lifting the supported area with respect to the unsupported area.

Made this premise, the most representative information that emerges from the graph is that increasing the fragmentation interval, with the same hatch distance, decreases the difference between the two heights, the value of which is highlighted by this graph:

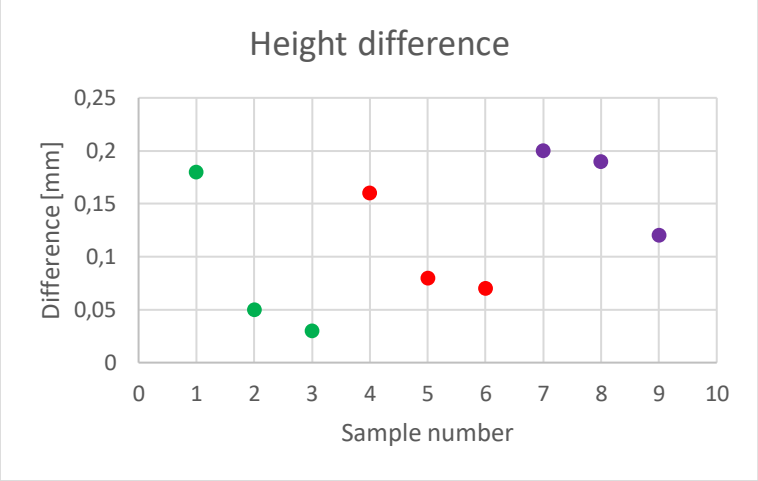

Figure 6.1.8 - **Difference between a) and b).**

This means that having a higher fragmentation interval results in less lifting of the supported area and therefore in better results. The trend of the points also shows that if instead the hatch distance increases, the difference is larger.

This result is coherent with what was found with the visual inspection and confirms samples 3 and 7 respectively as the best and the worst case.

As regards the width, the visual analysis shows a certain deformation at the base of each sample. In particular, the distance of the support from the vertical wall seems to increase from the top to the bottom. This deformation gives origin to a positive difference between the measure *d* and the measure *c*, which for each sample assumes the values contained in the graph:

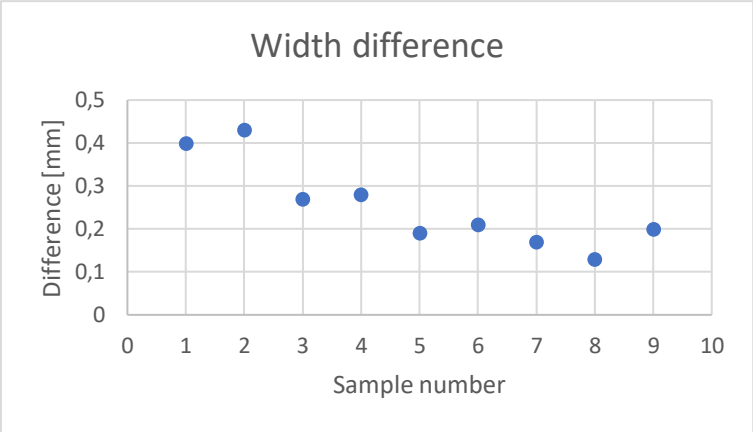

Figure 6.1.9 - **Difference between d and c.**

Even if the gap between the two dimensions is minimal, it is possible to recognize a certain decreasing trend as the hatch distance and the fragmentation interval increase. Thus, from this point of view, the set of parameters that has so far been identified as the worst, shows this advantage.

6.2 Second DoE

The eighteen samples produced for the second Design of Experiment were visually inspected.

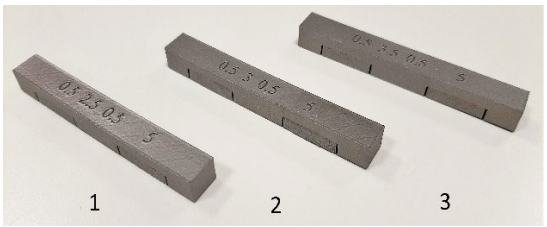

Figure 6.2.1.

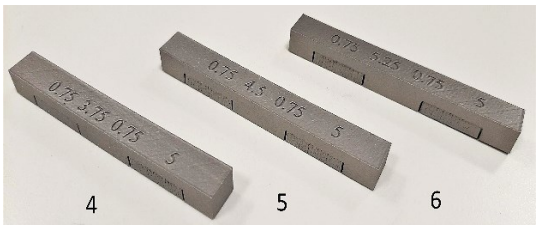

Figure 6.2.2.

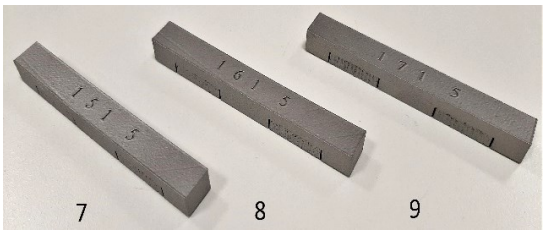

Figure 6.2.3.

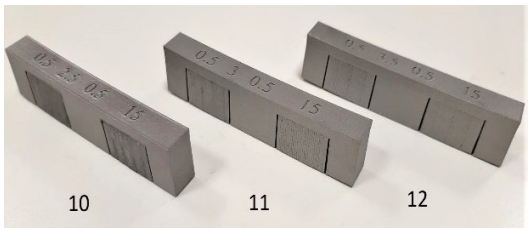

Figure 6.2.4.

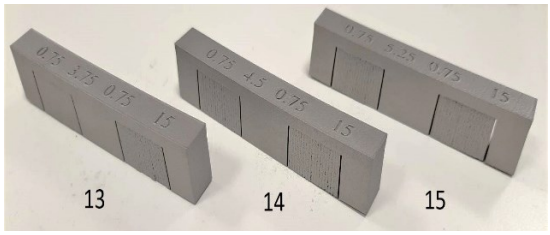

Figure 6.2.5.

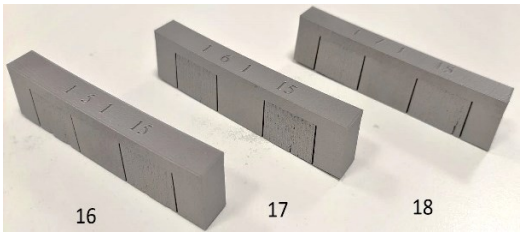

Figure 6.2.6.

The following images show the 18 parts obtained turned, so as to give emphasis to the different supports made for each set of parameters.

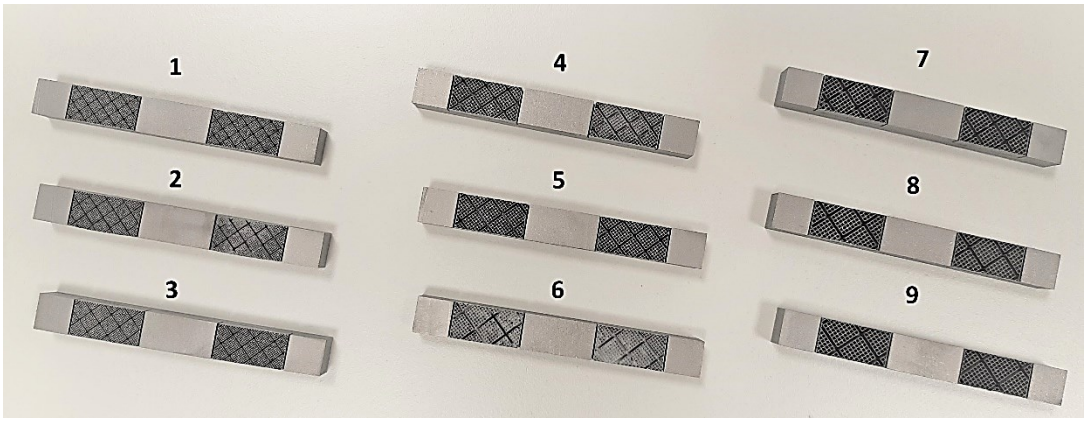

Figure 6.2.7 - **Lower view.**

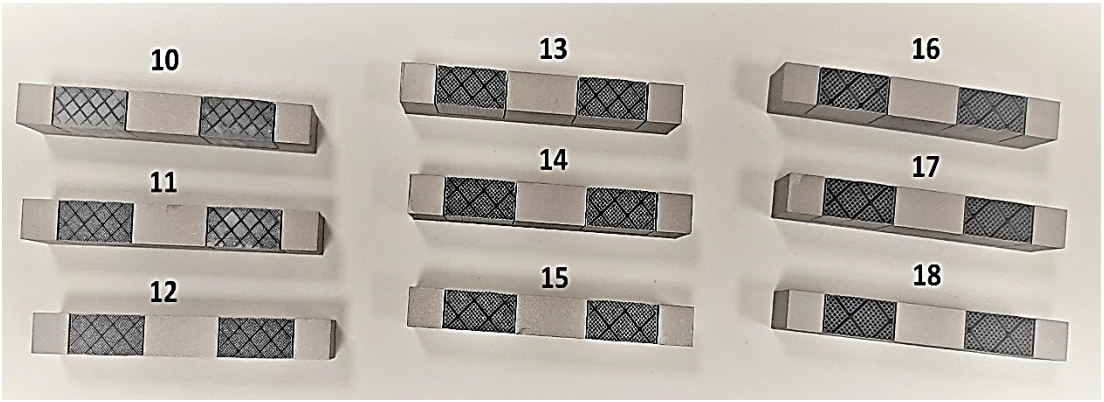

Figure 6.2.8- **Lower view.**

No particular problems emerge from the visual analysis; however, some observations can be made according to which samples 7, 8, 9 and 18 have supporting structures that show signs of detachment.

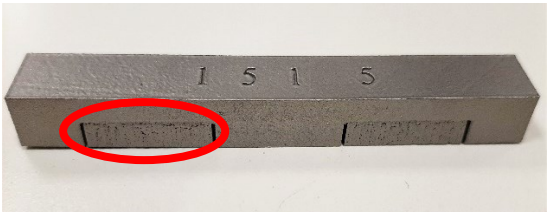

Figure 6.2.9 – **Sample 7.**

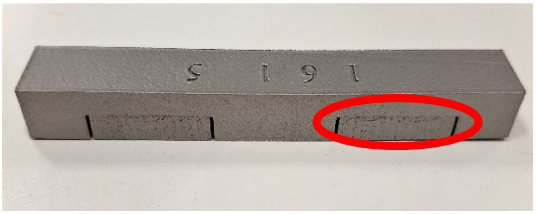

Figure 6.2.10 – **Sample 8.**

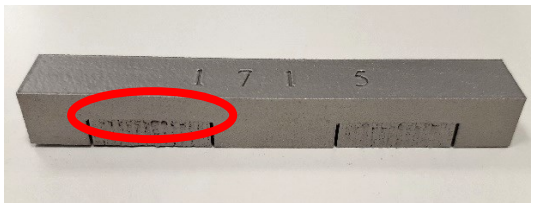

Figure 6.2.11 – **Sample 9.**

Figure 6.2.12 – **Sample 18.**

Furthermore, by analysing samples 2, 13, 14, 15 and 16 before separating them from the platform, it was possible to notice that the supports were not perfectly attached to the base. During the printing phase, when the first layers were fused, the areas of the supports of the samples indicated were not perfectly melted, but after a few layers the process stabilized.

From the observations made, it is concluded that supports with a height of 15 mm show fewer defects than those with a height of 5 mm. For the same height, instead, there is worsening as the hatch distance, separation width and fragmentation interval increase. As a result, the worst set of parameters is this:

Hatch distance [mm]	Fragmentation interval [mm]	Separation width [mm]
1	5(x5)	1
1	6(x6)	1
1	7(x7)	1

Table 6.2.1 - **Worst set of parameters.**

Before being separated from the platform with the digital caliper, some measures were taken, in order to evaluate the difference between the supported and unsupported areas. The measures that were taken are those shown in figure 6.2.13. The most representative of all is the height, which has been taken at certain specific points.

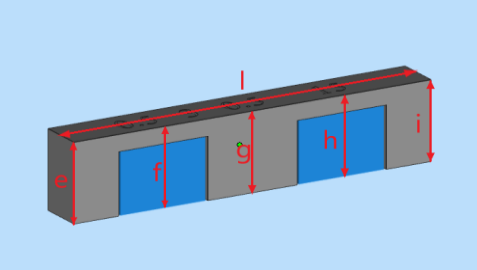

e), g), i): height of the part

f), h): height of the part in the supported areas

l): total width

Figure 6.2.13.

The values reported by the measurement have been graphed in order to easily identify the trend of the quantities:

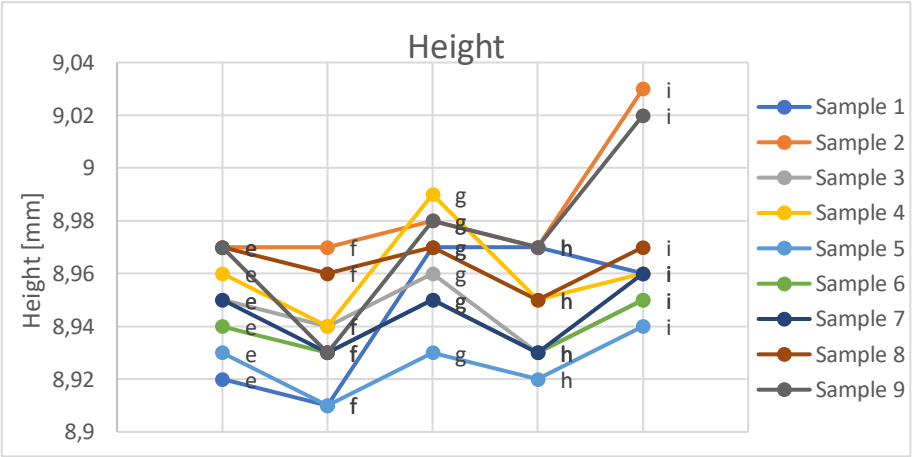

Figure 6.2.14 – **e), f), g), h), i) for the samples with a height of 9 mm.**

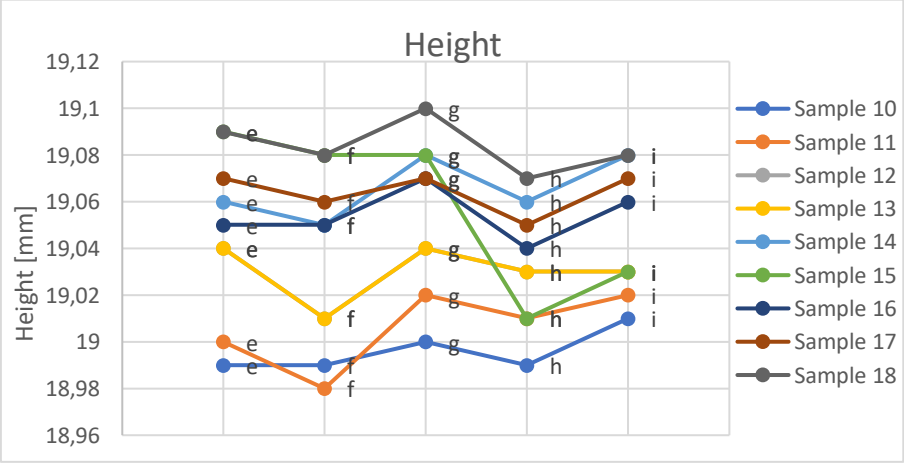

Figure 6.2.15 – **e), f), g), h), i) for the samples with a height of 19 mm.**

As it can be seen from the graphs for all measures, specific trends are evident.

In particular, both the 9 mm high and the 19 mm high parts reach lower heights in correspondence with the supported areas. The lowering of the part in these areas can be explained by the fact that less material is used for the realization of the supports compared to the part. So, when the first layer of powder belonging to the part is deposited, it does not find a flat surface, but the blocks of the supporting structure, which are less stable and dissipate less heat than the full solid part. This makes it more probable that deformation will occur than in unsupported areas.

As regards the total width, from the measures shown in the following graphs, there are no particular trends to be related to the geometric parameters of the support structures.

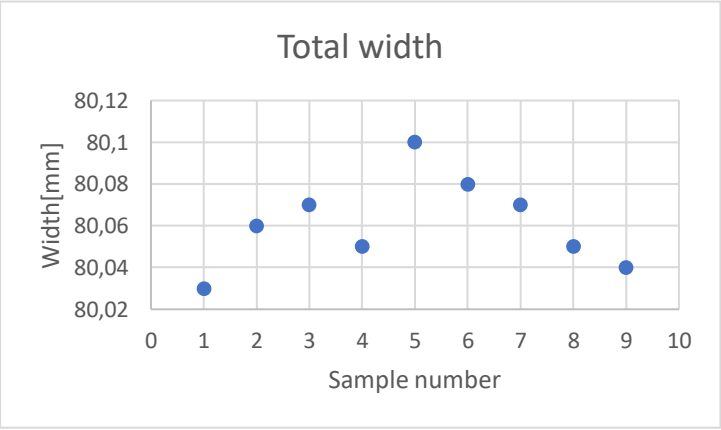

Figure 6.2.16 – **l) for the samples with height of 9 mm.**

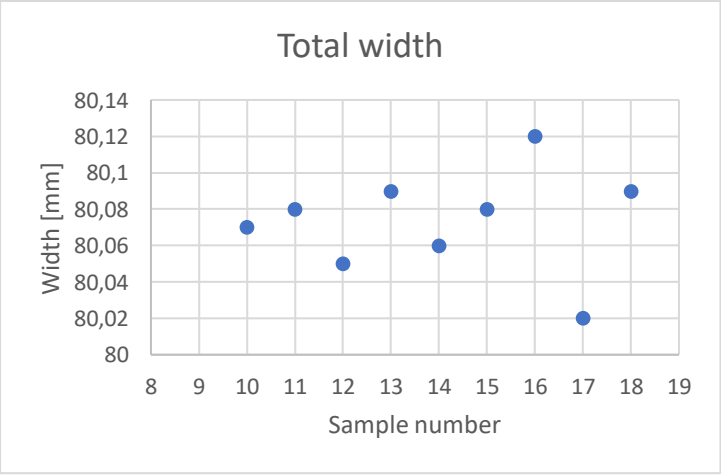

Figure 6.2.17 – **l) for the samples with height of 19 mm.**

6.3 Third DoE

In this paragraph the results of the third DoE are reported and discussed, for which four cases have been distinguished. As anticipated in paragraph 5.2.3, a total of 36 samples were printed in groups of 9 in each case. The following paragraphs illustrate the four cases, which are analysed separately.

6.3.1 First case

The parameters used for the first case require a 6% reduction in power compared to the second DoE, while the scanning speed remains unchanged.

	Power	Scanning Speed
Case 1	16%	75%

Table 6.3.1.1 -**Process parameters.**

After printing and extracting the platform, the samples result as shown in the following images:

Figure 6.3.1.1.

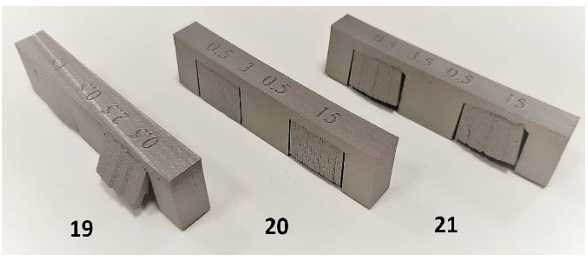

Figure 6.3.1.2.

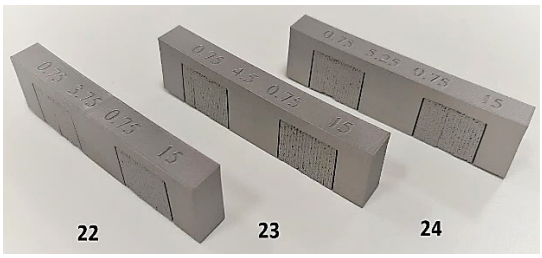

Figure 6.3.1.3.

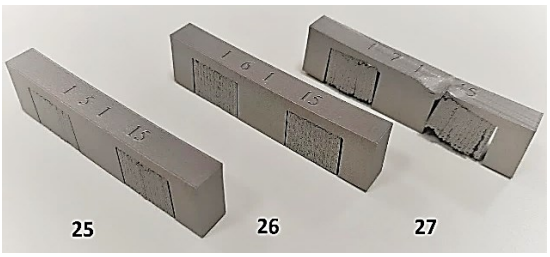

Figure 6.3.1.4

It can be seen that some of the supports realized are detached because the power value set was not enough to completely melt the powder and then the growth, layer after layer, was not occurred correctly. The worst cases are shown in the following figures:

Figure 6.3.1.5.

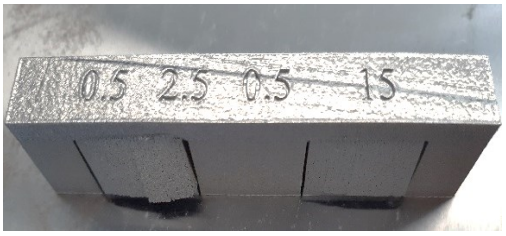

Figure 6.3.1.6.

Figure 6.3.1.7.

Figure 6.3.1.8.

Figure 6.3.1.9.

In general, it can be observed that, for the power value used, the support structures that show the greatest problems are those with the geometric parameters of the first three samples (19, 20 and 21) and the last three (25, 26 and 27). On the other hand, those relating to the three intermediate parameters (table 6.3.1.2) can be considered successful because there were no significant detachments.

Sample number	Hatch distance [mm]	Fragmentation interval [mm]	Separation width [mm]
22	0,75	3,75 (x5)	0,75
23	0,75	4,5 (x6)	0,75
24	0,75	5,25 (x7)	0,75

Table 6.3.1.2 – **Geometrical parameters of support structures.**

This distinction between media with different parameter sets is also evident by looking at the samples from below (figure 6.3.1.10), where it is clearly seen how some "blocks" are separated.

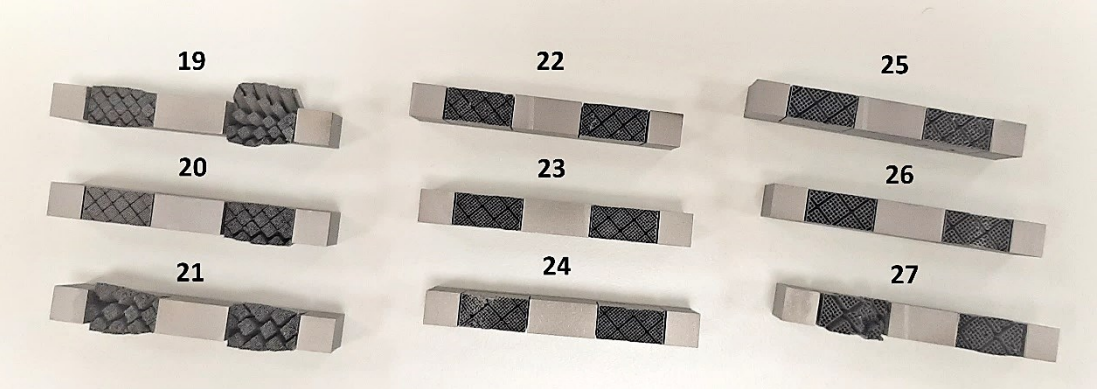

Figure 6.3.1.10 - **Lower view.**

On all the samples produced for the 4 case studies, measurements of height and width were taken in the same positions as for the second DoE.

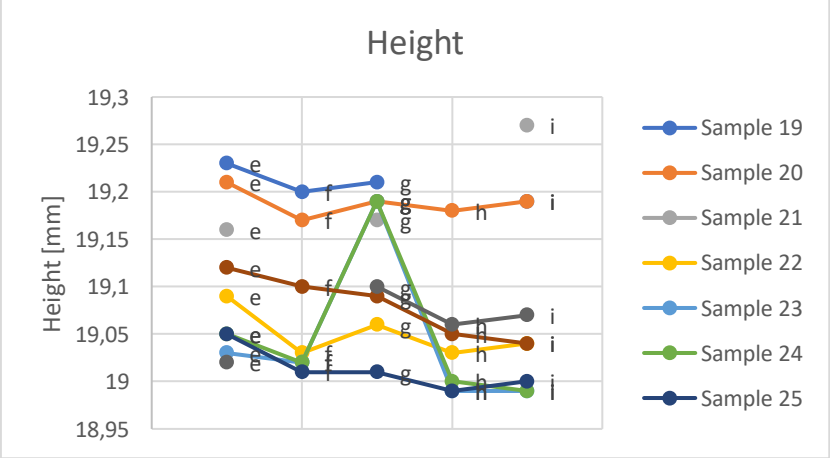

Figure 6.3.1.11 – **Heights in e), f), g), h), i).**

Note that due to the detachment of the supports, it was not possible to position the caliper at certain points to take the measurement.

Compared to the second DoE, with 16% power, all parts have a slightly greater height, in fact the range in which all measures fall is shifted up from 18,98-19,1 mm to 18,99-19,27 mm. Despite this small difference, the trend remained unchanged, showing a lowering in correspondence of the supported areas.

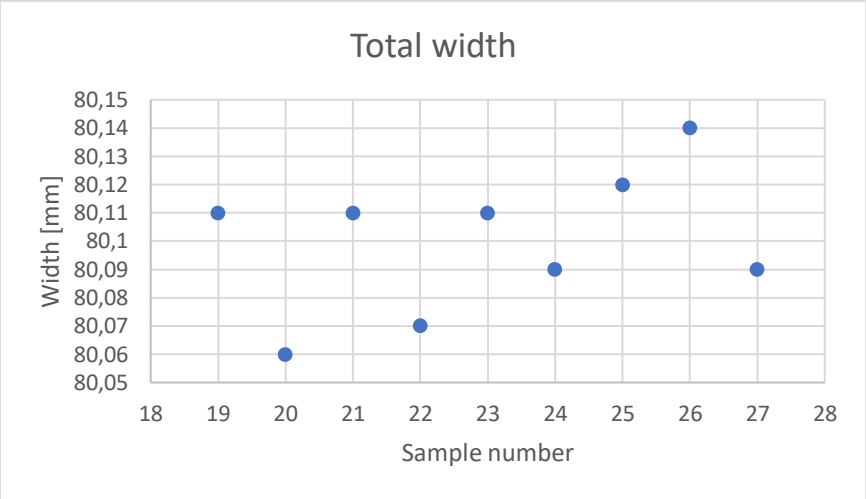

Figure 6.3.1.12 – **Total width of samples.**

Also this time, for the total width, no tendency correlated to the geometric parameters of the supports is observed.

6.3.2 Second case

In the second case of the third DoE, the power of the laser beam is changed. In particular, the power of the laser beam is increased by 6% compared to the initial power, while the scanning speed is the same.

	Power	Scanning Speed
Case 2	28%	75%

Table 6.3.2.1 – **Process parameters.**

As power increases, so does the Volumetric Energy Density (VED), since the laser remains at the same point for longer, transferring more heat.

The following figures show the parts during the building phase and after completing the printing process:

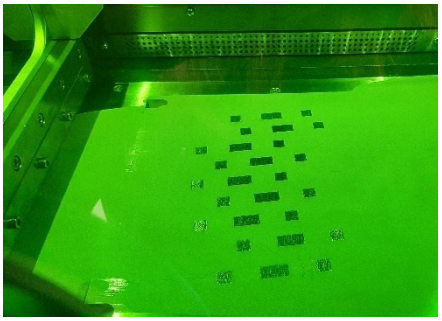

Figure 6.3.2.1- **Printing phase.**

Figure 6.3.2.2 – **Samples after building.**

After the platform had been extracted, the separation by EDM was carried out, after which the nine samples result like this:

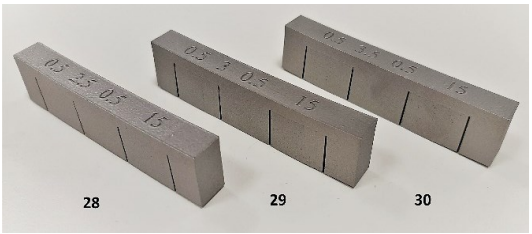

Figure 6.3.2.3.

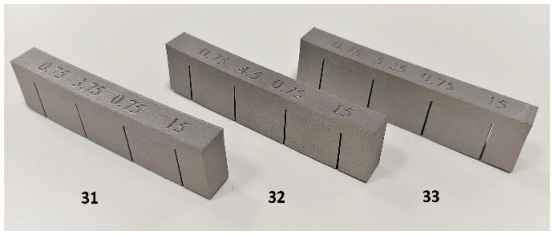

Figure 6.3.2.4.

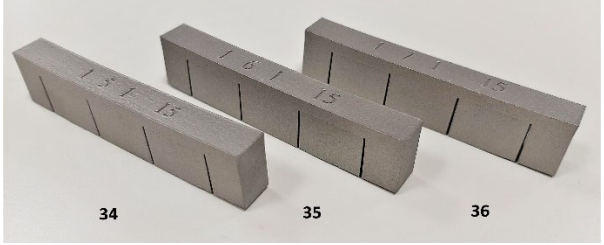

Figure 6.3.2.5.

With the process parameters used in this second case, the defects of the support structures are reduced and concern samples 28, 34, 35 and 36.

Figure 6.3.2.6.

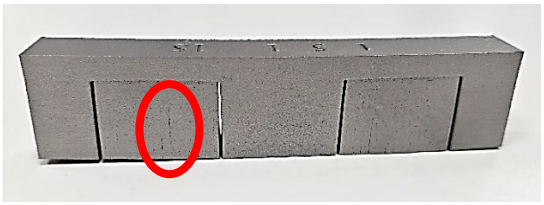

Figure 6.3.2.7.

Figure 6.3.2.8.

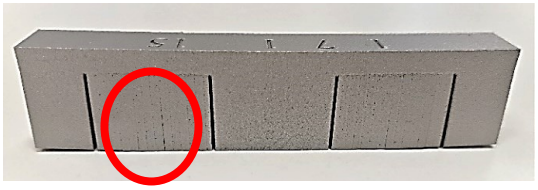

Figure 6.3.2.9.

This result is consistent with that found for the first case, since sample number 28 has the smallest geometric parameters, while the others belong to the final group of hatch distance, fragmentation interval and separation width. So the optimal parameters are in the middle.

It should also be noted that at 28% power, the deformation of the parts after separation from the building platform is particularly evident. This phenomenon is due to the internal stresses developed during the process, which are distributed in the part after eliminating contact with the surface of the plate. A solution to this problem is post-treatment, which has the function of relaxing the tensions generated inside the piece and which is carried out before separation, but this is outside the scope of this work.

In order to have a clearer view of the support structures created for each sample, the following image shows the lower view:

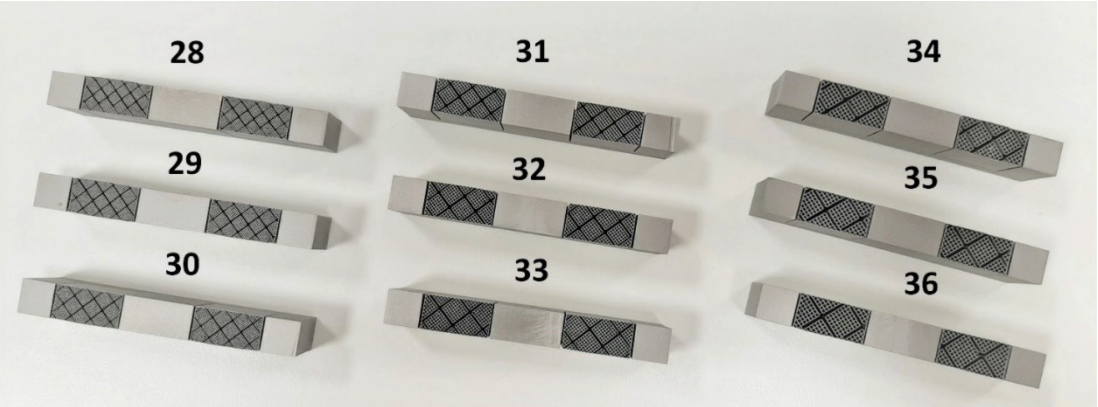

Figure 6.3.2.10 - **Lower view.**

The dimensions *e, f, g, h* and *i* taken with the digital caliper have, in this case, the trend shown in the graph below:

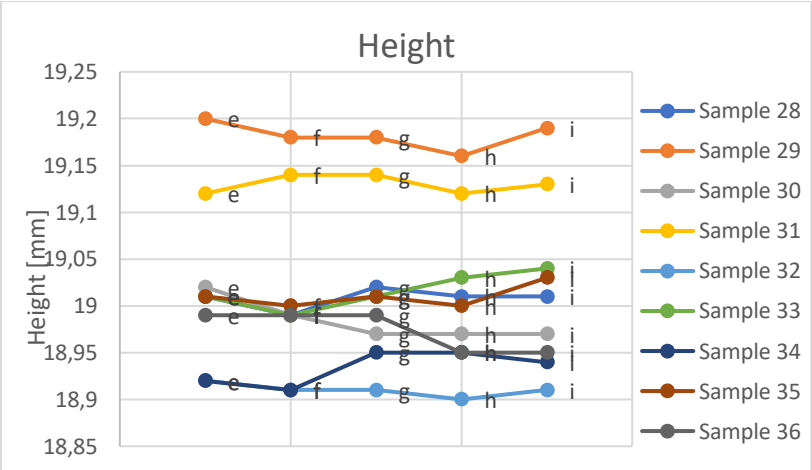

Figure 6.3.2.11 – **Heights in e), f), g), h), i).**

As it can be seen, the trend observed so far is not repeated. In fact, the curves obtained are flatter, showing a smaller difference between the heights of the supported areas and those of the solid parts.

This behaviour is coherent with the increase in power, because greater heat transfer means that the support structures melt more and the growth in the building direction is amplified compared to cases where less power is used. From this point of view, the height reached by the supports has led to greater uniformity of the parts.

The width *l*, on the other hand, shows a random trend with small deviations from the nominal size:

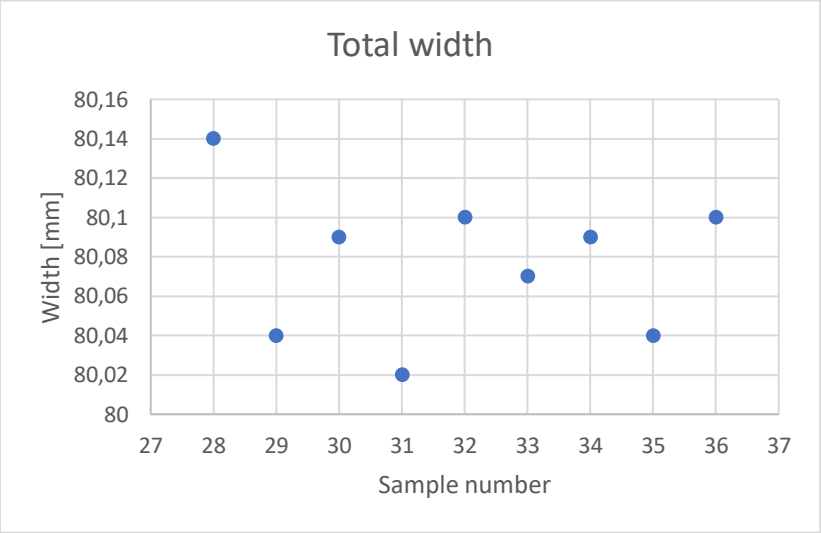

Figure 6.2.3.12 – **Total width of samples.**

6.3.3 Third case

This is the first of the two cases in which the power remains unchanged with respect to the second DoE, while the scanning speed is modified by reducing it by 12,5%.

	Power	Scanning Speed
Case 3	22%	62,5%

Table 6.3.3.1 – **Process parameters.**

Decreasing the scanning speed increases the Volumetric Energy Density, as well as for the second case where a higher laser beam power was used. In fact, by reducing the speed, the same area is hit for more time by the laser beam.

The parts on the building platform after the printing phase were extracted and inspected visually.

Figure 6.3.3.1 – **Part on the building platform.**

Other observations can be made after separation from the plate:

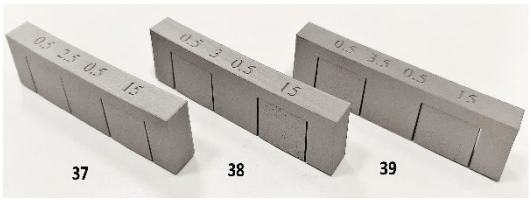

Figure 6.3.3.2.

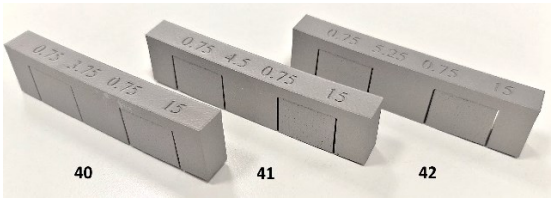

Figure 6.3.3.3.

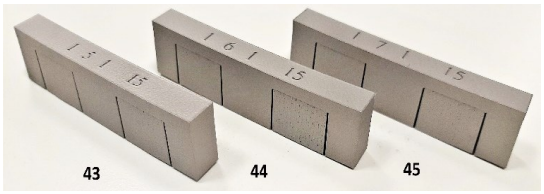

Figure 6.3.3.4.

The image below shows the lower view:

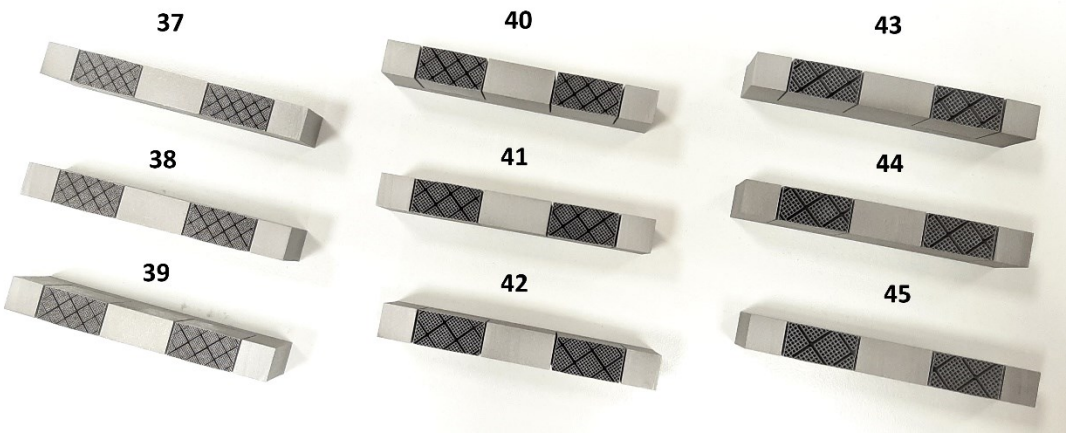

Figure 6.3.3.5 - **Lower view.**

In general, no particular problems emerged with regard to the separation of the supports from the part, so in this case it is not recognized a specific trend related to the different sets of geometric parameters used. However, for sample number 39, there is a crack on the support after separation from the plate. This is due to the residual stresses generated during the process.

Figure 6.3.3.6.

As regards the trend of the heights *e, f, g, h* and *i*, this time it shows the tendency, for the majority of the samples, to assume higher values in correspondence of the supports (*f* and *h*).

This is justified by the increase in VED, which, as already mentioned, favours the melting and growth of support structures.

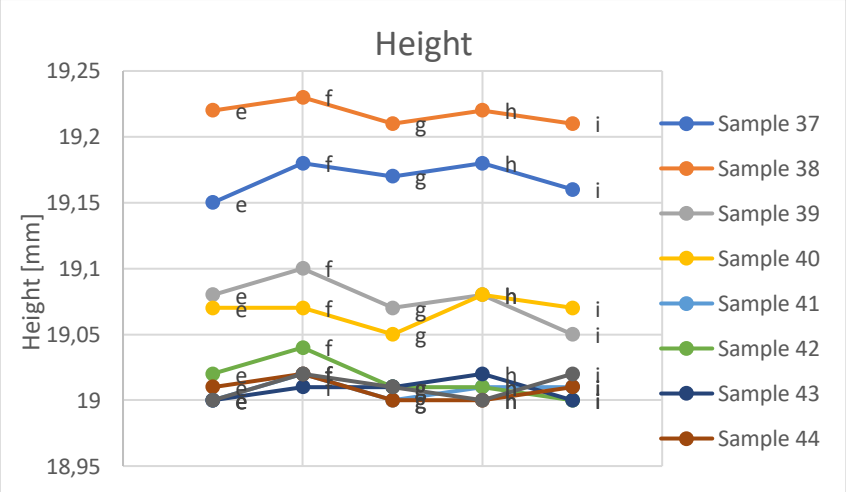

Figure 6.3.3.7 – **Heights in e), f), g), h), i).**

It can be observed that the increase in height of the supported areas was also registered for case 2, but without having a reversal in the trend of the curves. From this it can be deduced that, for this study, the decrease in scanning speed had a greater influence than the increase in power.

The following graph shows the total width measurements, which increase as the hatch distance and fragmentation interval increase.

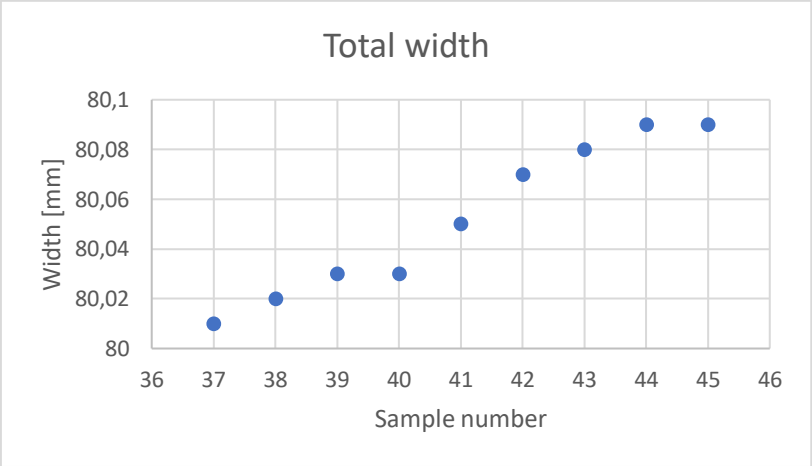

Figure 6.3.3.8 – **Total width of samples.**

6.3.4 Fourth case

The fourth and last case involves using the starting power and increasing the scanning speed by 12,5%.

	Power	Scanning Speed
Case 4	22%	87,5%

Table 6.3.4.1 – **Process parameters.**

The increase of the speed at which the scanning is done leads to a lower transfer of energy, reaching lower values of the VED. Therefore, this case is comparable with the first one, in which the power used is 16%.

The samples were printed without encountering the problems that occurred in the first case.

The following two images show the parts during the building phase and at the end of the process:

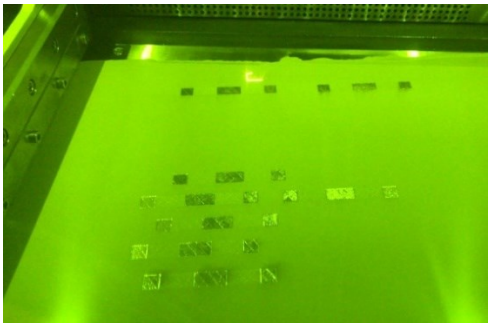

Figure 6.3.4.1 – Printing phase.

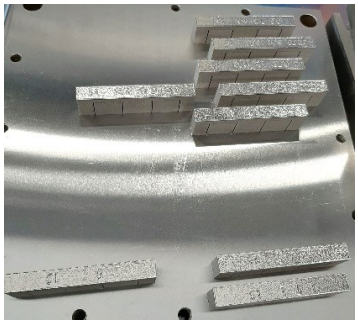

Figure 6.3.4.2 – **Samples on the platform.**

Subsequently the parts were separated from the building platform and analysed:

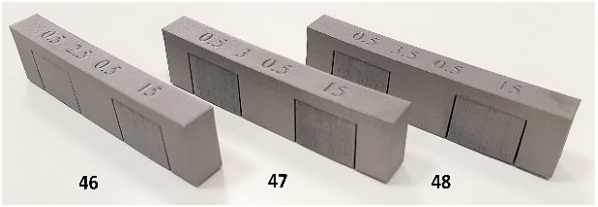

Figure 6.3.4.3.

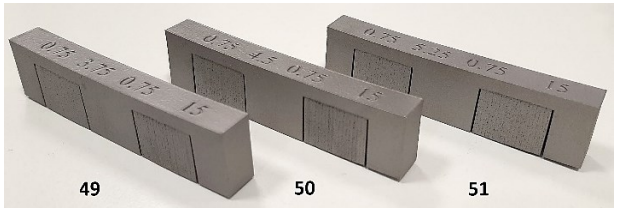

Figure 6.3.4.4.

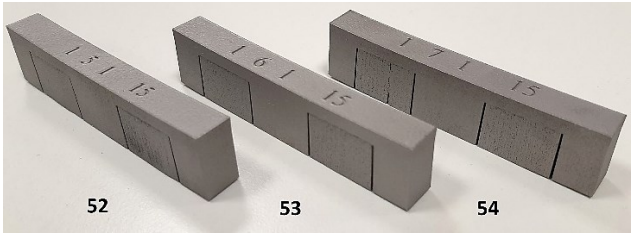

Figure 6.3.4.5.

The parts were turned to evaluate the difference of the supports from the bottom side:

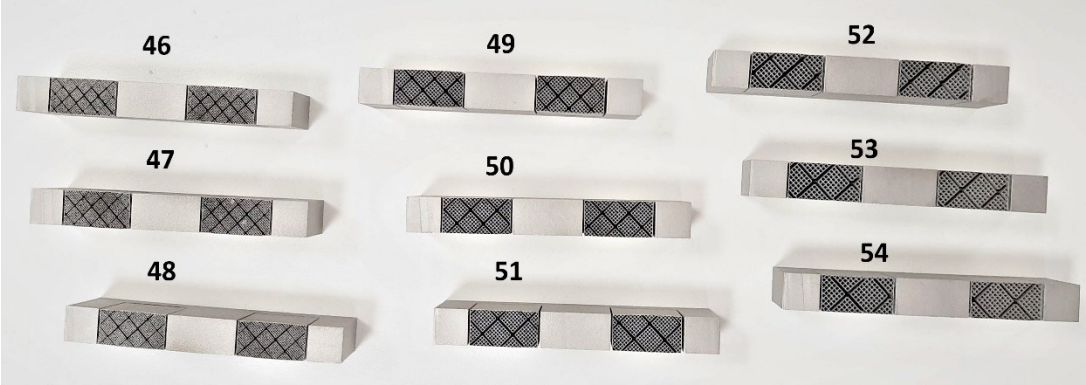

Figure 6.3.4.6 - **Lower view.**

Although there are no important detachments as in case 1, also this time not all the supports are perfectly attached to the part. In particular, this is observed for the samples 47, 52, 53 and 54.

With regard to the formation of cracks after separation, the supports produced with the central parameter set also prove to be the best in this respect. The images show some of the most obvious defects found on samples 53 and 54.

Figure 6.3.4.7.

Figure 6.3.4.8.

These observations reinforce the conclusion in paragraph 6.3.1 that better results are achieved for intermediate hatch distance and width fragmentation values.

With the graph in figure 6.3.4.9 it is possible to observe how the trend initially recorded recurs, in which the supported areas tend to have lower heights.

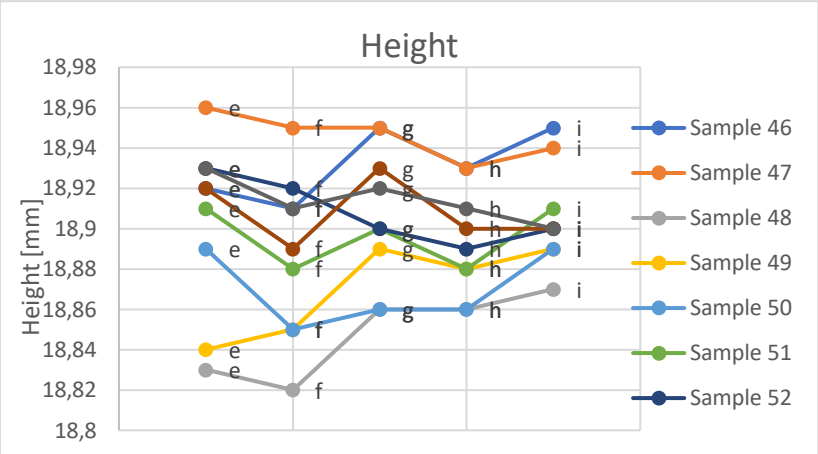

Figure 6.3.4.9 – **Heights in e), f), g), h), i).**

This result confirms that with a change in energy density the support structures grow differently depending on how the powder is melted. With a lower scanning speed, therefore, at the end of the melting of all the layers, the underlying supports cause a slight depression of the part they support.

The total width also this time shows a trend for which it grows together with the geometric parameters used for the support structures. As a result, larger measurements are recorded as the hatch distance and fragmentation interval increase.

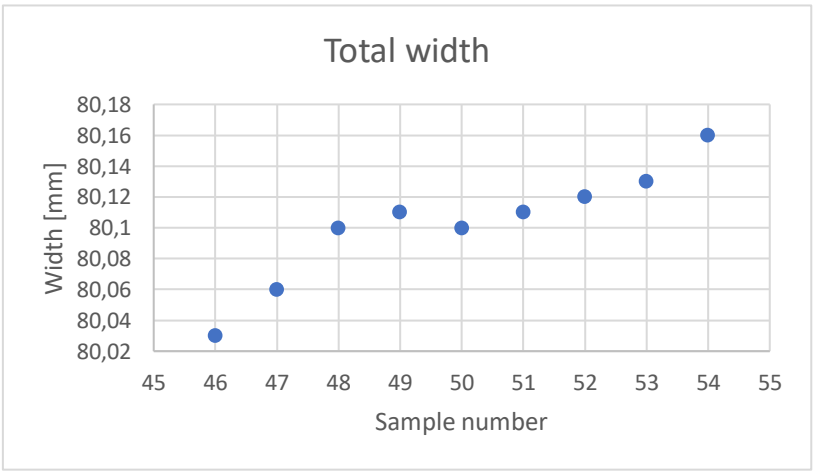

Figure 6.3.4.10 – **Total width of samples.**

6.4 Removability

The removal of support structures is an activity that takes place in the post-processing phase and that could have a considerable time duration. This depends on how easily they can be removed. For this reason, it is important to assess removability. Another factor on which this operation acts is the cost, which increases with the time and the other resources exploited.

To have an idea of the degree of removability of each support, it is useful to create levels in which to classify them. The levels identified are listed in table 6.4.1.

In this respect, a distinction is made between the case of manual removal and the case in which machining such as EDM is required. The latter case is identified with level 0 because it represents the extreme situation.

For the parts produced for this work it was not necessary to use special machining and therefore level 0 was never reached, since all the supports were removed manually.

0	**extremely hard to remove**
1	**very hard to remove**
2	**hard to remove**
3	**average**
4	**easy to remove**
5	**very easy to remove**

Table 6.4.1 - **Levels of removability.**

Removal was done for all supports of the samples realized and was analysed with the same approach. In particular, the analysis is valid for the same shape and sizes of the samples, for this reason the results obtained are presented separately.

6.4.1 Removal of supports from overhanging parts

To complete the removal work, tools were employed to facilitate the operation. In particular, a screwdriver and a hammer were used to hit the supports at the points of connection with the protruding area of the part.

Evaluating the difficulty used for each sample, the following classification was made:

Sample number	Level of removability					
	0	1	2	3	4	5
1		X				
2		X				
3		X				
4				X		
5			X			
6			X			
7					X	
8				X		
9				X		

Table 6.4.1.1 – **Removability.**

The most important information that can be deduced from the reported data is that by increasing the hatch distance the difficulty of removal decreases.

Concerning the fragmentation interval, it can be said that indicatively, with the same hatch distance, when it is greater the difficulty tends to increase, but there are no substantial differences.

The support that was removed most easily by applying a minimal effort is the number 7.

Sample number	Hatch distance [mm]	Fragmentation interval [mm]	Separation width [mm]
7	1	5 (x5)	1

Table 6.4.1.2 – **Geometrical parameters.**

In fact, unlike all the others, after being hit, it entirely detached from the part without breaking into many parts. Figure 6.4.1.1 shows the part with the relative separate support.

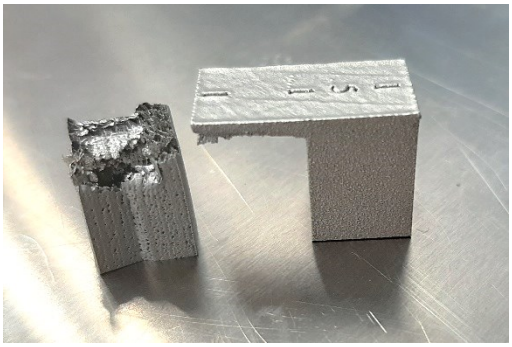

Figure 6.4.1.1 – **Sample number 7.**

Note that sample number 7 is the same which in the analysis of the results of the first Design of Experiment was identified as the one with the worst support realized. In fact, the detachment created between the part and the underlying support during the building phase has certainly advantaged the removal operation. In general, the relation between removability and hatch distance and between removability and fragmentation interval is correlated to the quality of the support structures. In conclusion, there is a lower level of removability if the quality of the support obtained is higher.

Once the supports were removed, the parts obtained have this aspect:

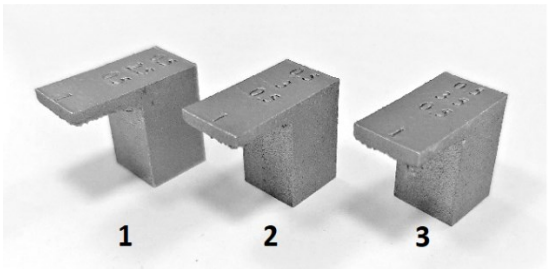

Figure 6.4.1.2

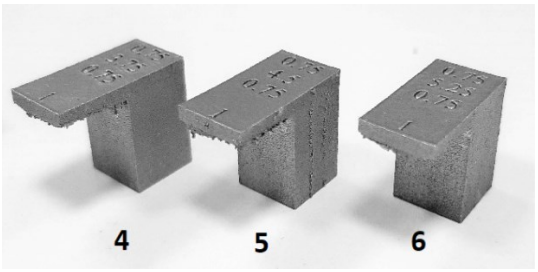

Figure 6.4.1.3

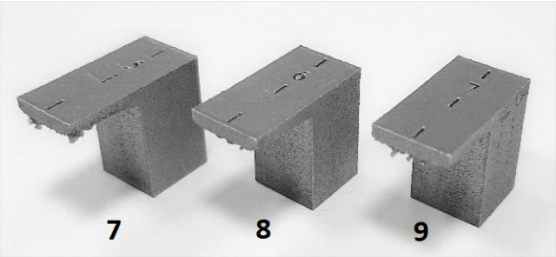

Figure 6.4.1.4

6.4.2 Removal of supports from the bridge structures

This paragraph illustrates the levels of removability with which the supports for the bridge structures built for the second and third DoE have been classified. Since different process parameters were used for the experiments, they are divided. Also this time, for all the following cases, a screwdriver and a hammer were used as tools for the removal.

2° Design of Experiment

For this experiment, a distinction must be made between parts with different heights. In particular, a difference was found in the removal of the support structures, which showed higher levels of removability in the case of parts with a higher height.

The table below assigns removability levels to the first nine samples produced:

Sample number	Level of removability					
	0	1	2	3	4	5
1		X				
2		X				
3		X				
4			X			
5			X			
6			X			
7				X		
8				X		
9				X		

Table 6.4.2.1 – **Removability.**

After removing all the supports from the parts, the nine samples appear as shown in the following figures:

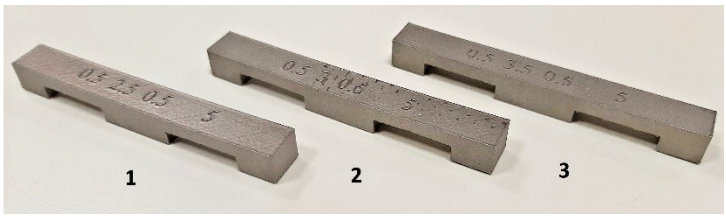

Figure 6.4.2.1.

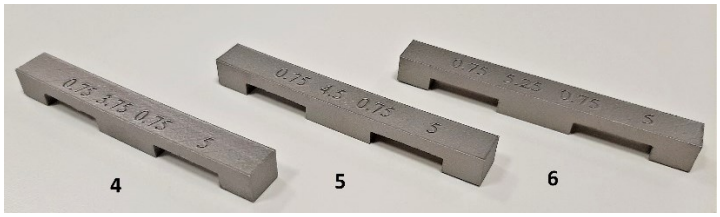

Figure 6.4.2.2.

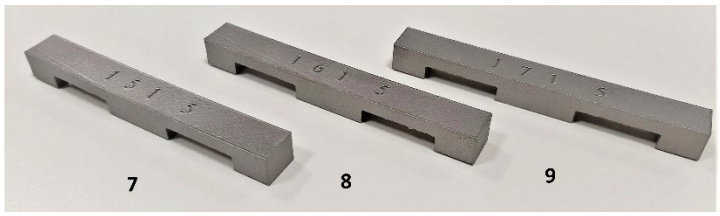

Figure 6.4.2.3.

With regard to 15 mm high supports, the levels of removability assigned are these:

Sample number	Level of removability					
	0	1	2	3	4	5
10			X			
11			X			
12			X			
13				X		
14				X		
15				X		
16				X		
17					X	
18					X	

Table 6.4.2.2 – **Removability.**

The following figures show the last nine parts after the removal operation:

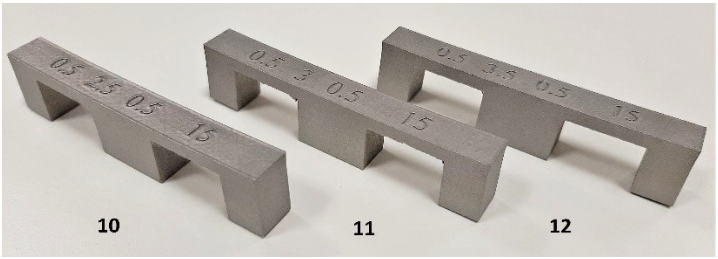

Figure 6.4.2.4.

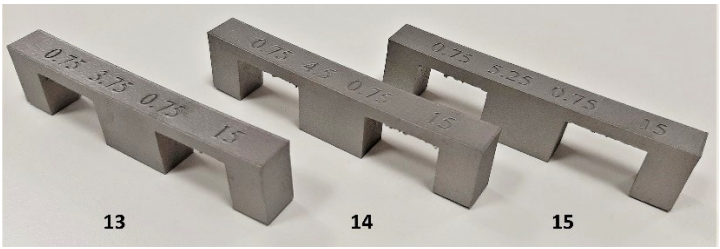

Figure 6.4.2.5

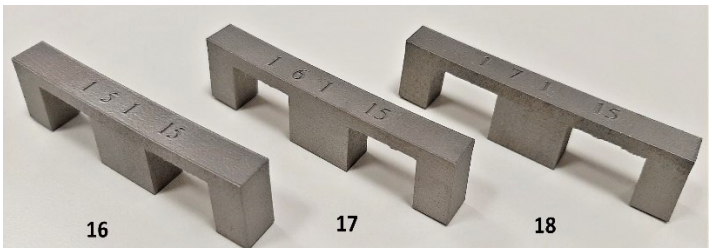

Figure 6.4.2.6.

As the two 6.4.2.1 and 6.4.2.2 tables show, for supports with a height of 5 mm the starting level of removability is lower.

For both sets of samples, the same behaviour as for the parts of the first DoE is observed. This trend shows that, with the same height, as the geometric parameters increase, the removal of supports is easier. In fact, the blocks become less dense and, consequently, less compact. When, on the other hand, hatch distance, fragmentation interval and separation widths are smaller, the support structure is more resistant, as it has more points of contact with the supporting part.

Therefore, as for the parts with protrusion, the removability is correlated to the quality of the realized support. If the block structure is successful, in fact, there are no signs

of detachment from the side and this makes the removal operation more difficult, which requires a greater effort.

3° Design of Experiment: case 1

The supports generated with the parameters of the first case are those with the greatest defects, as some of them are not attached to the building platform or to the part. This has made removal easier and with less effort. The supporting structures that showed a slight difficulty were those for samples 22, 23 and 24.

Sample number	Level of removability					
	0	1	2	3	4	5
19					X	
20					X	
21					X	
22				X		
23				X		
24				X		
25					X	
26					X	
27					X	

Table 6.4.2.3 – **Removability.**

This result shows that the supports with worse characteristics make the removal easier and faster. Therefore, in this case there is no direct proportionality between removability and the values of the geometric parameters used.

After removing all the supports, the bridge structure of the parts produced is evident:

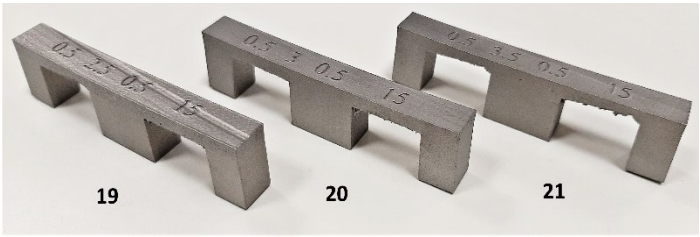

Figure 6.4.2.7.

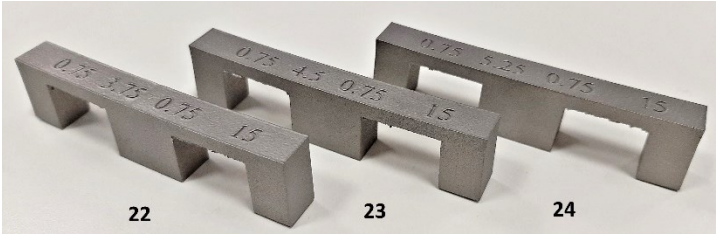

Figure 6.4.2.8.

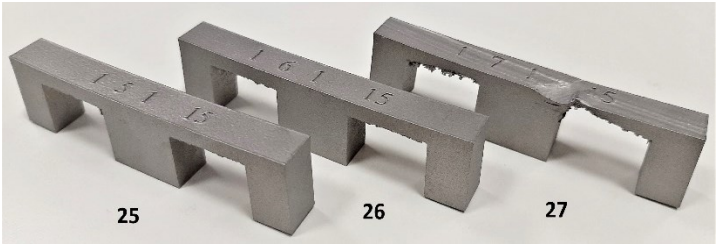

Figure 6.4.2.9.

3° Design of Experiment: case 2

The supports of the second case were realized with a power increase of 6% for which the melting of the powder is more complete. In this way the supports produced are more resistant, showing a substantial difference from those used for case 1. Specifically, a particularly significant effort and a longer time were required for the first three samples (28, 29 and 30).

Sample number	Level of removability					
	0	1	2	3	4	5
28		X				
29		X				
30		X				
31				X		
32			X			
33				X		
34					X	
35					X	
36					X	

Table 6.4.2.4 – **Removability.**

Going forward with hatch distance, fragmentation interval and separation width there are tendentially higher levels of removability, as the less dense structure of the blocks facilitated removal.

The figures below show the parts without supports:

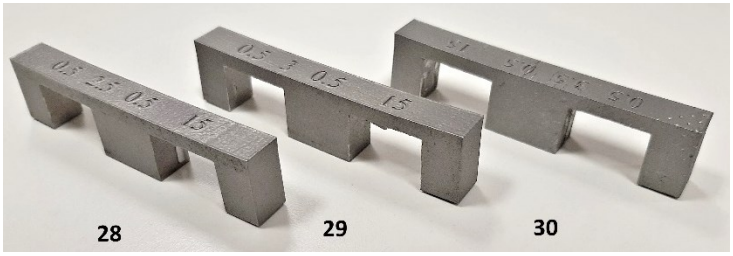

Figure 6.4.2.10.

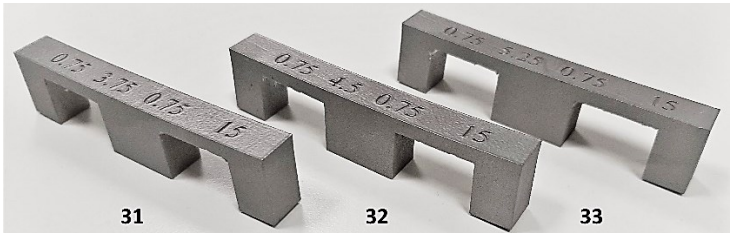

Figure 6.4.2.11.

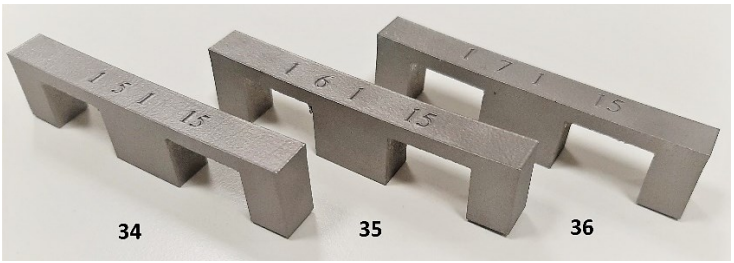

Figure 6.4.2.12.

3° Design of Experiment: case 3

In terms of removability, the third case does not differ so much from the second. This similarity is justified by the reduction of the scanning speed, which, as already mentioned, increases the energy density.

The marked levels are approximately the same as in the previous case:

Sample number	Level of removability					
	0	1	2	3	4	5
37		X				
38		X				
39		X				
40				X		
41				X		
42				X		
43					X	
44					X	
45					X	

Table 6.4.2.5 – **Removability.**

Also this time the first three supports are those that have been removed with greater difficulty. The difference with the following ones is very evident, as both the effort and the time required for the operation are much lower.

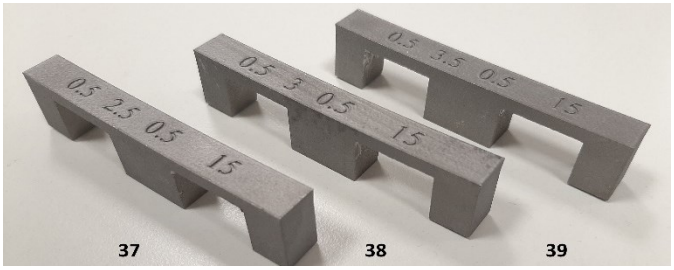

Figure 6.4.2.13.

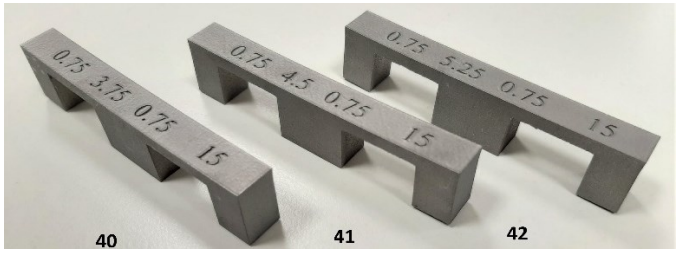

Figure 6.4.2.14.

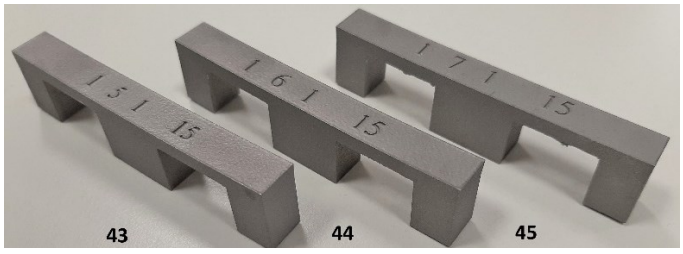

Figure 6.4.2.15.

3° Design of Experiment: case 4

In the fourth and last case, the support structures were removed from the parts produced with an increase in scanning speed. However, there were no substantial differences from the second DoE, where the standard parameters were used.

Sample number	Level of removability					
	0	1	2	3	4	5
46			X			
47			X			
48			X			
49				X		
50				X		
51				X		
52					X	
53					X	
54					X	

Table 6.4.2.6 – **Removability.**

Although once again the first three levels are lower, unlike case 3, they have a higher level. This result is consistent with the fact that, with a decrease in VED, less resistant supports are obtained.

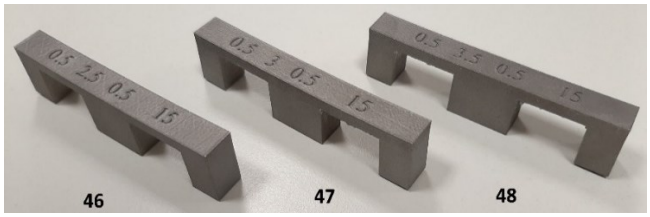

Figure 6.4.2.16.

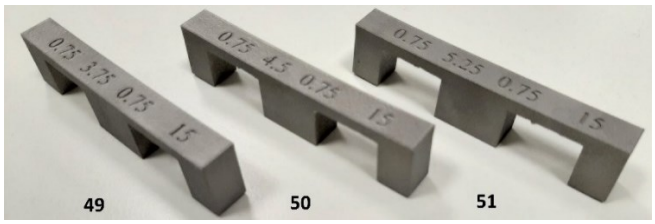

Figure 6.4.2.17.

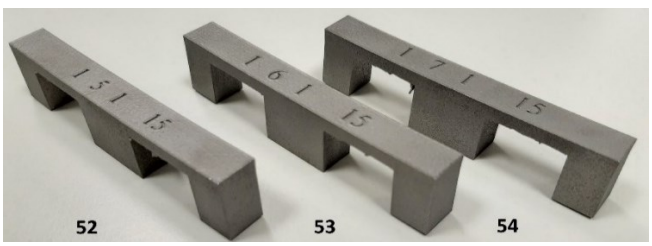

Figure 6.4.2.18.

Chapter 7: Case study

In this work, the evaluation of the built parts focuses mainly on the realization of the support structures. In this chapter a case study is reported in which the results obtained from the experiments carried out on the samples are applied. In addition, the optimization of the support structures is evaluated together with other aspects before determining the final solution.

7.1 Evaluation criteria

The case study concerns a bracket used in the automotive sector made with the powder bed process (SLM) by Prima Additive (a division of Prima Industrie Group). This part has a geometry for which, in the modelling phase of the process, it is necessary to provide support structures.

Although the supports have fundamental functions in the realization of the piece, it is not correct to think of applying all the possible optimizations. Before a user decides to use additive technology for the realization of his object of interest, it is necessary to find the right compromise between:

- resistance of the supports;
- volume of material used for the support structures;
- removal of supports in the post-process phase;
- part orientation;
- cost.

These evaluation factors constitute the KIPs (Key Performance Indicators) through which the quality of the process is analysed. They are closely related to each other, in fact, depending on the orientation of the piece on the platform, and therefore based on the direction of growth of the part, the amount of supports needed changes. With the quantity the volume also varies and it represents the most relevant quantity. The volume determines the amount of powder required and consequently the cost of

production of the part. Although cost is a key factor, it is not enough on its own to determine the selection of support structures. As already explained, they have specific functions because they support the part during the layers overlapping and represent a means for the heat dissipation that otherwise would cause greater distortions inside the component that accumulates thermal stresses. For this reason, it is essential to ensure first of all that the support structures carry out the functions for which they were inserted and secondly to balance the functionality with the cost that they entail. The terms to evaluate to ensure that there are good supports are the volume and resistance. In general, with the same number of supports, if the volume is greater, then the stability of the structures and therefore their strength will also increase. The same can be said for the dissipation capacity, which increases with volume because there is more material to which the heat generated by the process can be transmitted. Last but not least, removability is important because the removal phase is fundamental and is also an influential item of the total process costs. In general, as the supports volume increases, their removal will be more difficult and expensive.

Note that the KIPs values depend on the material, since the properties that determine both strength and thermal characteristics change depending on it.

Optimization of the volume used for the support structures is useful not only to have a cost advantage, but also to reduce material waste since they are parts to be removed at the end of the process. As mentioned above, the amount of support structures also varies according to the orientation of the structure. In fact, the quantity of the bottom surfaces that need supports varies considerably depending on it. Ideally the optimal solution would be to find an orientation with which it is possible to avoid the supports, but due to the geometry of the part, it is often only possible to reduce the quantity of the necessary support structures. This is because additive manufacturing is a technology which is used for the possibility of creating geometrically complex parts. These parts therefore easily have particular shapes which have to be supported even if the component changes orientation relative to the platform.

7.2 Implementation

The CAD model of the part used as a case study was imported on Materialise Magics in STL format and positioned inside the model of the building platform used for the Print Sharp 250, then through the section dedicated to the supports the geometric parameters were set.

Note that before the choice of the supports, the model was optimized topologically. This reduces the volume of the surfaces needed to be supported and consequently the cost.

The following images show the two models before and after optimization:

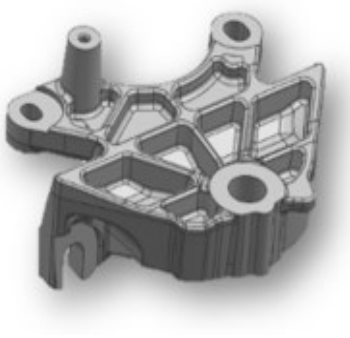

Figure 7.2.1 – **3D model before optimization.**

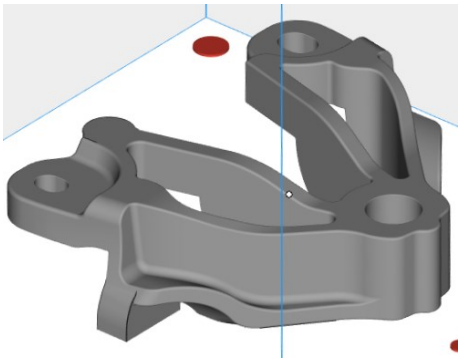

Figure 7.2.2 –**3D model after optimization.**

In order to highlight the difference between the initial model and the optimised model, the volume obtained in both cases is reported:

	Initial model mm^3	Optimized model mm^3
Volume of the part	2755000	239216,264

Table 7.2.1 – **Volume of the part before and after the optimization.**

As regards the orientation, the bracket is positioned with an inclination of 5 degrees with respect to the direction of motion of the blade (x), as can be seen from the top view:

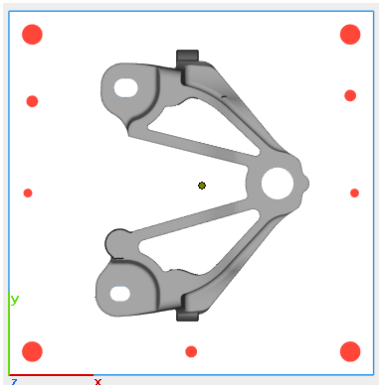

Figure 7.2.3 – **Top view.**

This orientation allows to use less material, in fact if the part is inclined with respect to the plane of the platform, would need a greater number of layers and therefore more powder. In addition, the volume of supports would also increase.

For example, for an inclination of 50 degrees, the volume associated with the support structures is 165,491 cm^3.

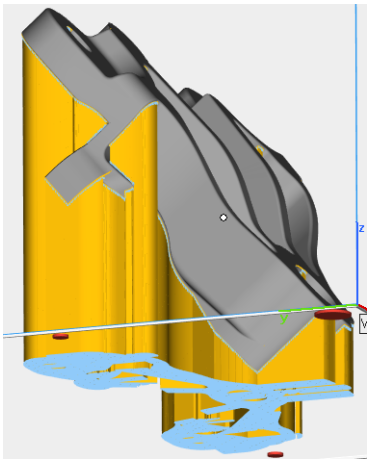

Figure 7.2.4 - **Supports generated for an inclination of 50 degrees.**

The only disadvantage of the solution adopted is that the heat is not dissipated in height and this requires a post-stress relief treatment.

The part has multiple zones that need to be supported and for each of them there are different needs. In the following figure, the areas of interest are highlighted:

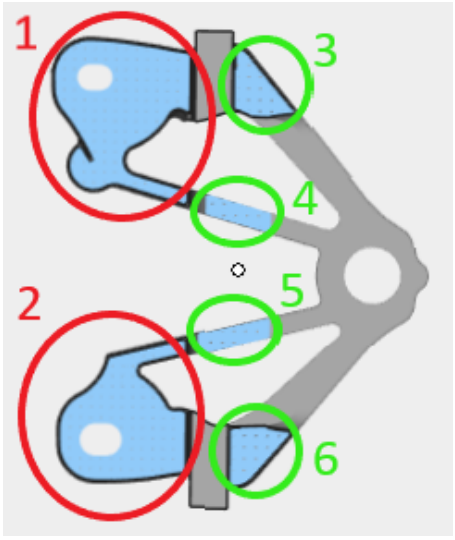

Figure 7.2.5 – **Areas to be supported.**

The circles have different colours depending on the parameters chosen for the generated supports.

In particular, the areas highlighted by the red circles require very strong supports for which, in addition to the blocks, there is also the solid contour. Resistance in this case is essential, even if it is at the expense of removability. In fact, this time, the possibility of using EDM for the removal of supports is considered.
The areas circled in green, on the other hand, can be sustained by supports that are slightly weaker than the first ones and that can be removed more easily. An observation has to be made for supports 3 and 6, which are reinforced by solid contours.

The data considered for this part are those used for the experimental tests, balancing the properties conferred by the geometric parameters with those obtained with the process parameters.

The parameters used for the supports highlighted in red are those relating to sample number 30 in case 2 of the third DoE:

- laser power: 28%
- scanning speed: 75%
- hatch distance: 0,5 mm
- fragmentation interval: 3,5 mm
- separation width: 0,5 mm

The choice fell on this solution after having made some considerations. The need for resistant supports initially restricted the field to cases 2 and 3 of the third Design of Experiment, as these are the cases in which, thanks to the higher energy density, the most compact supports have been made. Among the two cases, the second was then selected because, from the measurements made, it emerged that using a reduced scanning speed (case 3) the supported areas exceeded the height of the parts. This, for the piece considered here, is a phenomenon to be avoided as it could facilitate the lifting of the part. Among the geometric parameters of case 2, those used for sample number 30 were chosen, as they are close to the set of parameters identified as the best. Moreover, the evaluations of the first DoE show that the best case is for the sample that has supports with the smallest hatch distance and the highest fragmentation interval at the same time. As already mentioned, giving this robustness results in a low level of removability, which in this case would be equal to 1. However, the presence of solid contours makes removal more difficult.

The green circled supports are made with the parameters of sample number 13 of the second DoE:

- laser power: 22%
- scanning speed: 75%
- hatch distance: 0,75 mm
- fragmentation interval: 3,75 mm
- separation width: 0,75 mm

In this case, the process parameters used at the beginning were selected and not those that confer the highest density, so intermediate energy density values are reached. The alternatives to this option were cases 1 and 4 of the third DoE, but these were excluded to avoid having too weak supports. In fact, in both cases the values of the VED are lower than those reached with the second DoE. This solution allows to have more choice regarding the geometric parameters for two reasons:

1. It is the case in which there are more samples with supports made without particular defects;
2. the six samples have different levels of removability.

For all the supports, note that the side of the blocks is positioned parallel to the blade, since it has been empirically demonstrated that it is the orientation with which the best results are obtained.

The following image shows in detail the two types of supports made with the selected parameters:

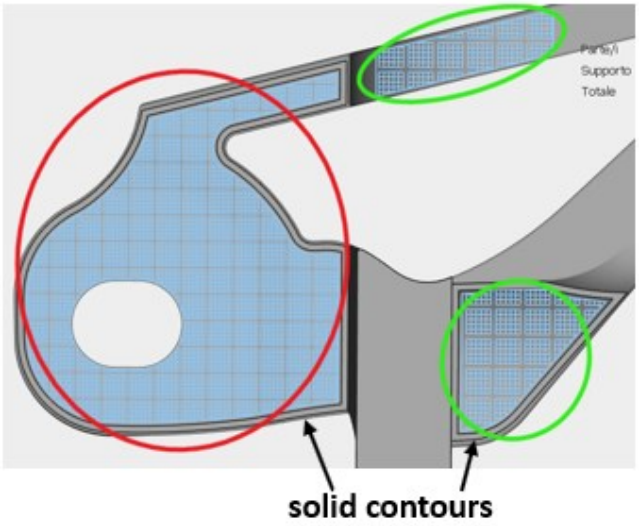

Figure 7.2.6 – **Supports in detail.**

As concerns the costs of the realization of the part with supports, a comparison can be made between the case in which the supports are generated with the chosen geometric

parameters (A) and the case in which the geometric parameters for which there is the densest pattern are used (B).

	Case A	Case B
Volume of the supports	73,433 cm^3	76,236 cm^3

Table 7.2.2 – **Volume of support structures.**

	Case B – Case A
Cost difference	0,45 %

Table 7.2.3 – **Cost difference.**

The total cost includes all the items that contribute to the realization of the piece which concern:

- material
- gas
- electrical energy
- process cost

Process cost is obtained by applying the following formula:

$$Process\ cost\ [€] =$$

$$(process\ hours + \ set\ up/unloading\ hours) \cdot machine\ cost\ per\ hour$$

The cost difference coming from the optimization of the supports in terms of geometric and process parameters has a small impact in the overall cost benefits for the part produced by AM; however, this impact can be significantly more important in applications where less and weaker supports volume is required. In addition, the total cost calculated above does not take into account the removal cost, which is lower with the optimized supports. Finally, it is evident that the process of minimizing supports

or printing without them is highly dependent from the design of the part, the printing orientation and the research on process parameters that can provide at the same time adequate mechanical properties.

Conclusions

The objective of this work was to examine the block support structures, used in SLM process, realized under different conditions. In particular, geometric parameters such as hatch distance, fragmentation interval and separation width, and process parameters such as laser beam power and scanning speed were varied. In the first experiment, using standard process parameters, supports were generated for a protruding part. It showed that the best support is the one related to sample number 3 and has the smallest hatch distance (0,5 mm, equal to the separation width) and the largest fragmentation interval (3,5 mm) at the same time. In general, with the same hatch distance, there are better results as the fragmentation interval increases. Consequently, the worst sample is 7, which has the support with hatch distance and separation width equal to 1 mm and fragmentation interval equal to 5 mm. The difference in height between the part and the supported area has the same correlation with the geometric parameters, since, at the same hatch distance, it decreases as the fragmentation interval increases, confirming samples 3 and 7 as the best and the worst respectively. In the second experiment, bridge structures with different heights (9 mm and 19 mm) were supported. The supports with a greater height generated less defects and in general for both cases a different trend was recorded compared to the first experiment. The difference between the supports is in groups of three and the worst group is the one created with the last set of parameters, with a hatch distance of 1 mm. For both structures a lower height is reached in the supported areas than in the unsupported ones, showing a deflection of the part. The third and final experiment was performed on samples with a bridge structure with a height of 19 mm. This time, changing the process parameters showed that as the power increases and the scanning speed decreases, the energy density increases, resulting in stronger support structures; while as the power decreases and the scanning speed increases, the supports are weaker. Comparing the four cases by pairs, the decrease in scanning speed in case 3 (-12,5%) had a greater influence on sample growth than the increase in power (+6%) in case 2, as the supported areas grew more than the part, reaching greater heights and reversing the trend. Instead, the decrease in power in case 1 (-6%) had more evident effects than the increase in scanning speed (+12,5%) in case 4, because with lower power there were obvious detachments of the blocks realized. For each case, the best set of

geometric parameters has been identified. For cases 1, 2 and 4 it is the intermediate one with a hatch distance of 0,75 mm, while for case 3 no particular trend has been identified. Finally, removability was assessed, a property that contributes to the calculation of the final cost in terms of time and resources used. The removal was performed for all the created supports, assigning to each of them a certain level of removability. In general, this operation showed that for all samples the difficulty of removal decreases with increasing geometric parameters. This trend was not only found in the first case of the third experiment, since for the first and last three samples the removal of the supports was favoured by the presence of important defects, thus reaching higher levels of removability compared to the three samples in the middle.

Appendix

Print Sharp 250

DIMENSIONS (L*W*H)	3500 (L) - 1100 (W) - 2450 (H)
WEIGHT	2000 kg.
POWER SUPPLY	380 V / 50 Hz / 8 kW
LASER IR	Laser Yb (Itterbio) IR single mode
POWER LASER IR	500 W
LASER FOCUS DIAMETER	70 - 100 µm
BEAM WAVELENGTH	1060 - 1080 nm
BUILDING VOLUME	250 * 250 * 330 mm
BEAM DEFLECTION SPEED	8 m/s
POSITIONING SPEED	10 m/s
BUILD RATE *	12 - 30 cm^3/h
* Dependent on process parameters and material used.	
LAYER THICKNESS	0.02 mm - 0.1 mm
LAYER WIDTH	0.1 mm (single line width)
BUILDING PLATFORM Z-AXIS	Travel: 350 mm / Speed: max 6 mm/s / Res: 0.01 mm
HEATING PLATFORM	<= 200°C
MONITORING OF O2 LEVEL	Below 100 ppm (0,01%)
PERMISSIBLE ROOM TEMPERATURES	15 - 30 °C
GAS (Consumption - running / filling)	7 L/min (running)
SYSTEM FILL CONSUMPTION	20 L / min. (up to filling)
CAM SOFTWARE	Materialise Magics
CONTROL AND OTHER SOFTWARE	Eplus control software (EPC)
INDUSTRIAL INTERFACES	Ethernet

Size and power
Laser
Machine and additive process details
Peripheral and auxiliaries - Software

Bibliography and sitography

[1] http://www.factoryofknowledge.net

[2] F. Trevisan *et al.*, "*On the Selective Laser Melting (SLM) of the AlSi10Mg Alloy: Process, Microstructure, and Mechanical Properties*", 2017.

[3] https://www.energygroup.it/additive-manufacturing

[4] D. Herzog, V. Seyda, E. Wycisk, and C. Emmelmann, "*Additive manufacturing of metals*",*Acta Mater.*, vol. 117, pp. 371–392, 2016.

[5] R.Hague, P.Reeves and S.Jones "*Mapping UK Research and Innovation in Additive manufacturing*",2016.

[6] Chu Lun Alex Leung *et al*., "*Laser-matter interactions in additive manufacturing of SS316L and 13-93 bioactive glass revealed by in situ X-ray imaging*",2018.

[7] https://all3dp.com/1/3d-printing-support-structures/

[8] http://additivemanufacturing.com/

[9] J.Jiang , X.Xu *and* Jonathan "*Stringer Support Structures for Additive Manufacturing: A Review*",2018.

[10] O. Poyraz *et al*., "*Investigation of support structures for direct metal laser sintering (dmls) of in625 parts*".

[11] A.Hussein *et al*., "*Advanced lattice support structures for metal additive manufacturing*",2013.

[12] https://all3dp.com/2/cura-support-settings-optimize-your-supports/

[13] https://www.materialise.com/en/software/magics/modules/support-generation-for-sl-module

[14] Jukka-Pekka Järvinen *et al*., "*Characterization of effect of support structures in laser additive manufacturing of stainless steel*",2014.

[15] F. Clignano, "*Design optimization of supports for overhanging structures in aluminium and titanium alloys by selective laser melting*",2014.

[16] https://all3dp.com/2/3d-printing-supports-guide-all-you-need-to-know/

[17] http://www.specialmetals.com/assets/smc/documents/inconel_alloy_718.pdf

[18] V. Flint, G.M. Davidson, R.L. Boring, C.L. Powers, A.P. Pauna, "*Heat Treater's Guide. Practices and Procedure for Nonferrous Alloys, ASM nternational*", 1996.

[19] T. Mishurova *et al*., "*The Influence of the Support Structure on Residual Stress and Distortion in SLM Inconel 718 Parts*",2018.

[20] Chor Yen Yap, Swee Leong Sing *et al*., "*Review of selective laser melting: Materials and applications*", 2015.

[21] H. Gong, D. Christiansen, J. Beuth, J.J. Lewandowski, "*Melt Pool Characterization for Selective Laser Melting of Ti-6Al-4V Pre-alloyed Powder*", 2014.

[22] Sing, S.L., Wiria, F.E.,Yeong, W.Y. "*Selective laser melting of titanium alloy with 50 wt % tantalum: Effect of laser process parameters on part quality*", 2018.

[23] Javed A., Pradeep C., Deepankar P., Brent S., "*Understanding grain evolution in additive manufacturing through modeling*", 2018.

[24] F. Calignano, D. Manfredi *et al*., "*Overview on Additive Manufacturing Technologies*", 2017.

[25] Sing S.L., Wiria F.E., Yeong W.Y. "*Selective laser melting of titanium alloy with 50 wt % tantalum: Microstructure and mechanical properties*", 2015.

[26] Thomas G. Spears and Scott A. Gold "*In-process sensing in selective laser melting (SLM) additive manufacturing*", 2016.

[27] B. Ferrar, L. Mullen, E. Jones, R. Stamp, C.J. Sutcliffe "*Gas flow effects on selective laser melting (SLM) manufacturing performance*", 2011.

[28] K. Kempen, L. Thijs *et al*., "*Lowering thermal gradients in selective laser melting by pre-heating the baseplate*".

[29] L. N. Carter, C. Martin *et al*., "*The influence of the laser scan strategy on grain structure and cracking behaviour in SLM powder-bed fabricated nickel superalloy*",2014.

[30] B. Graf, S. Ammer *et al*., "*Design of experiments for laser metal deposition in maintenance, repair and overhaul applications*",2013.

[31] Chivel Yu., Smurov I. "*Temperature Monitoring and Overhang Layers Problem*",2011.

[32] K. Zhang, G. Fu *et al*., "*Study on the Geometric Design of Supports for Overhanging Structures Fabricated by Selective Laser Melting*", 2018.

[33] Kai Zeng, "*Optimization of support structures for selective laser melting*", 2015.

[34] https://www.rmit.edu.au/news/all-news/2019/may/advanced-manufacturing

[35] https://3dprintingindustry.com/news/3d-printing-automotive-industry-3-132584/

[36] L. Jyothish Kumar and C.G. Krishnadas Nair, "*Current Trends of Additive Manufacturing in the Aerospace Industry*", 2017.

[37] Gibson, I.; Rosen, D.; Stucker, B., "*Introduction and Basic Principles in Additive Manufacturing Technologies*",2015.

[38] Pal, S.; Drstvensek, I. & Brajlih, T. "*Physical Behaviors Of Materials In Selective Laser Melting Process*",2018.

[39] https://www.americanmachinist.com/cad-and-cam/programming-perfection

[40] J. Parthasarathya , B. Starlya, S. Ramana, A. Christensenb, "*Mechanical evaluation of porous titanium (Ti6Al4V) structures with electron beam melting (EBM)*", 2009.

[41] John O. Milewski, "*Additive Manufacturing of Metals*", Springer, volume 258, pp. 157-161, 2017.

[42] J. K. Algardh *et al*., "*Thickness dependency of mechanical properties for thin-walled titanium parts manufactured by electron beam melting (EBM)*", 2016.

[43] J. Wang and H. Tang, "*Review on metals additively manufactured by SEBM*", 2016.

[44] https://sites.google.com/a/ewg.k12.ri.us/medical3dprinting/how-has-3dmedical-printing-evolved-since-it-was-created

[45] https://www.igi-global.com/chapter/history-of-additive-manufacturing/182410

[46] https://blog.trimech.com/a-brief-history-of-additive-manufacturing

[47] Ugur M Dilberoglu, Bahar Gharehpapagh *et al*., "*The role of additive manufacturing in the era of Industry 4.0*", 2017.

[48] https://www.smartechanalysis.com/reports/2019-additive-manufacturing-market-outlook/

[49] https://all3dp.com/what-is-stl-file-format-extension-3d-printing/#pointfour

[50] Julien Gardan "*Additive manufacturing technologies: state of the art and trends*", 2015.

[51] D.Ding, Z. Pan, D. Cuiuri, H. Li and S. van Duin "*Advanced Design for Additive Manufacturing: 3D Slicing and 2D Path Planning*",2016.

[52] Bharath Vasudevarao, D Natarajan, Mark Henderson "*Sensitivity of Rp Surface Finish to Process Parameter Variation*",2000.

[53] Paramita Das "*Optimum Part Build Orientation in Additive Manufacturing for Minimizing Part Errors and Build Time*",2000.

[54] https://www.oerlikon.com/